IN VITRO EVALUATION OF LINEAR PLANT HOST DEFENSE PEPTIDES SHEPHERIN 2, SKH-AMP1, CN-AMP1, AND CR-ACP1 FOR CYTOTOXICITY AND ANTIMICROBIAL ACTIVITIES AGAINST POTATO PATHOGENS

CHRISTIE STEPHEN
Bachelor of Science, University of Lethbridge, 2020

A thesis submitted in partial fulfilment of the requirements for the degree of

MASTER OF SCIENCE

In

AGRICULTURAL BIOTECHNOLOGY

Department of Biological Sciences
University of Lethbridge
LETHBRIDGE, ALBERTA, CANADA

IN VITRO EVALUATION OF LINEAR HOST DEFENSE PEPTIDES: SHEPHERIN 2, SKH-AMP1, CN-AMP1, AND CR-ACP1 FOR CYTOTOXICITY AND FOR ANTIMICROBIAL PROPERTIES AGAINST POTATO PATHOGENS

CHRISTIE STEPHEN

Date of Defence: MAY 1, 2023

Dr. Dmytro Yevtushenko Supervisor	Associate Professor	Ph.D.
Dr. Igor Kovalchuk Thesis Examination Committee Member	Professor	Ph.D.
Dr. Jenny McCune Thesis Examination Committee Member	Assistant Professor	Ph.D.
Dr. Cameron Goater Chair, Thesis Examination Committee	Professor	Ph.D.

Dedication

This thesis is dedicated to my family who supported and cheered me on throughout this entire process.

Abstract

The aim of this study was to evaluate the antimicrobial and cytotoxic activities of four linear plant host defense peptides (HDPs), Shepherin 2, Cr-ACP1, Skh-AMP1, and Cn-AMP1, *in vitro* and to identify potential candidates for transgenic expression in potato plants for enhanced disease resistance. The antimicrobial activities of the HDPs were tested against major potato pathogens: the fungi *Fusarium culmorum* and *Alternaria solani,* and the bacteria *Pectobacterium carotovorum* and *P. atrosepticum*. Shepherin 2 had the strongest antimicrobial activity, inhibiting the germination of 98% *F. culmorum* conidia at 16 µM, and 84% *P. carotovorum* cells at 64 µM. Combination of Shepherin 2 with Cr-ACP1 resulted in inhibition of 89% *P. carotovorum* cells over the expected 70% at 16µM, indicating a synergistic interaction. All HDPs had low cytotoxicities toward plant protoplasts and mammalian cells. The gene encoding Shepherin 2 was introduced into potato plants for future evaluation of its activity *in planta.*

Acknowledgements

I would like to express my gratitude to my supervisor, Dr. Dmytro Yevtushenko, who gave me this research opportunity and guided me throughout this project. I also thank Nick Schimpf for all his help and training, which were influential in shaping my experimental methods. My gratitude extends to Dr. Maria Munawar and Atta Ur Rahman for being the best lab mates I could ever ask for. I would also like to thank Drs. Igor Kovalchuk and Jenny McCune for acting as my supervisory committee members and for all your suggestions to improve this work. I would like to give additional thanks to Dr. Igor Kovalchuk for the use of his CL2 laboratory and equipment and to Yasamin Rostamian for training me in human cell culture techniques. Dr. Jie Feng is thanked for providing bacterial cultures. Lastly, I would like to thank the NSERC Discovery Grants Program, which provided funding for the majority of this research.

On a personal level, I would like to thank my husband, Rene, and my children for their encouragement, patience and support all through my studies: you gifted me with the will to see it through. Finally, my parents are also thanked for their help and support throughout this process.

Table of Contents

List of Tables

List of Figures

List of Abbreviations

Ala – Alanine
Arg- Arginine
Asn – Asparagine
CaMV – cauliflower mosaic virus
cfu – colony forming unit
CsMV – cassava mosaic virus
DMSO – Dimethyl sulfoxide
ER – endoplasmic reticulum
FBS – fetal bovine serum
gfp – green fluorescent protein
Gln - Glutamine
Gly – Glycine
GUS – β-glucuronidase
HDP – host defense peptide
His – Histidine
LB – Luria Burtani
LTP – lipid transfer protein
MES – (N-morpholino) ethanesulfonic acid
MET – Methionine
MIC – minimum inhibitory concentration
MS – Murashige and Skoog
PDA – potato dextrose agar
PDB – potato dextrose broth
PCR – polymerase chain reaction
RE – restriction enzyme
ROS – reactive oxygen species
Ser - Serine
Tyr – Tyrosine
Val - Valine

1. Introduction

1.1. Thesis Arrangement

This thesis is arranged into four chapters. Chapter 1 provides a literature review of the current knowledge regarding the topic and the objectives of the project that will aim to fill specific gaps in our knowledge. Chapter 2 briefly describes the experimental approach followed by the specific methods used during the experimental work. Chapter 3 provides the results of the experiments and analysis through text, figures, and tables. Chapter 4 encompasses an interpretation of the results and recommendations for further studies on this topic. Chapter 5 provides the conclusion, whereas Appendix A provides the composition of SW medium preparation.

1.2. Literature Review

1.2.1. Demand for Increased Crop Productivity

During the next few decades, we need to find ways to maximise crop yields on existing farmlands to maintain food security because global crop demand is increasing along with the environmental impacts of agricultural activities. This is due to the predicted 2.3 billion people increase to our populations by 2050, as well as the continually rising per capita income across the globe (Tilman et al., 2011). It is estimated that crop production will have to increase between 70% (FAO, 2009) and 110% (Tilman et al., 2011) by 2050 to meet this demand.

Land clearing and intensification of the use of existing croplands are both ways to increase food production to meet future food demand, but the environmental impacts would be severe (Tilman et al., 2011). The agricultural industry already causes extensive environmental impacts; for example, it accounts for approximately one quarter of global greenhouse gas emissions (Tilman et al., 2011), it is responsible for extensive land clearing and the ensuing loss

of biodiversity, and increased fertilizer and pesticide use pollutes bodies of water. However, taking advantage of, and furthering the development of technologies, as well as ensuring equal access to those technologies would allow us to meet the projected 2050 crop demand (FAO, 2009; Tilman et al., 2011) with far lower environmental impacts than relying on more conventional agricultural technologies and practices (Tilman et al., 2011).

An important crop which can help meet the nutritional needs of a growing population is the potato. In fact, it is one of the world's principal crops for ensuring food security (Bakhsh, 2020; Dolničar, 2021; Ortiz & Mares, 2017). Potato has become the choice crop in developing countries where there is limited purchasing power and land available for cultivation and which have an increasing demand for food (Bakhsh, 2020; Dolničar, 2021). For example, 40% of the world's potato crop area is in China and India, the world's two most populated countries (Dolničar, 2021). More evidence that the potato is a crop often chosen for its ability to provide food stability is the fact that North Korea turned to the potato as a main crop to solve the food shortages which led to severe famine in the late 1990s. Potatoes are grown as a major crop in 130 countries and are the world's fourth most important crop for many reasons (Dolničar, 2021). Potatoes are highly nutritious, containing more vitamins and nutrients than any other staple crop (Oritz & Mares, 2017). They provide large amounts of carbohydrates, are a good source of Vitamin C, iron, dietary fibre, potassium, and Vitamin B6 and B complex vitamins, such as thiamin, folate, riboflavin, and niacin. They are also a source of protein and minerals such as magnesium, phosphorus, and zinc. (Dolničar, 2021; Ortiz & Mares, 2017; Sood et al., 2017). Potatoes produce more dry matter and protein per hectare than any of the major cereal crops and can be cultivated in a very wide range of agro-ecosystems with different day lengths, temperatures, rainfall, soil types, and biotic stressors. They also need approximately 45% less

water than is needed for rice or wheat (Ortiz & Mares, 2017). All of these benefits make the potato an important candidate for further research aimed at increasing crop yields to their full potential. One of the ways we can achieve that goal is to reduce crop losses using technology to engineer plants with innate broad spectrum and durable disease resistance while also reducing agriculture's environmental impact by reducing the need for fungicidal and bactericidal crop applications. In order to effectively develop these crops, we need to fully understand the plant immune system components and how they function. Plant host defense peptides (HDPs) are one of the components which look most promising for the development of sustainable, disease resistant crops (Campos et al., 2018; Iqbal et al., 2019; Sathoff & Samac, 2019).

1.2.2. Host Defence Peptides (HDPs)

HDPs are found in most, if not all, life forms and in most tissues (Haney et al., 2017; Li et al., 2021; Yevtushenko & Misra, 2012). In plants, they are part of the innate immune system and act as the first line of defense against phytopathogens and although they are best known for their antimicrobial properties, it is increasingly clear that they perform other biological functions, such as immunomodulatory, anti cancer, antiviral and antibiofilm activities (Haney et al., 2017). HDPs are polypeptide sequences, which are usually synthesized as an inactive pro-peptide that must be cleaved and undergo further post-translational modifications to become the active peptide (Haney et al., 2017; Li et al., 2021) which often possesses a broad spectrum of activity with multiple antimicrobial targets (Li et al., 2021). Some HDPs are also synthesized by non-ribosomal synthases (Li et al., 2021), although this mode of synthesis mainly occurs in bacteria (Iqbal et al., 2019). They are generally small (consisting of less than 100 amino acids), cationic peptides that contain even numbers of cysteines, and they form disulfide bonds which make these peptides extremely stable (Iqbal et al., 2019). They form secondary structures such as alpha

helices and anti-parallel beta sheets and they are usually amphipathic (Nawrot et al., 2014). They comprise a large and diverse family of proteins which are broken up into classes based on amino acid sequence, structure, and the number of disulfide bonds (Goyal & Mattoo, 2016; Iqbal et al., 2019; Li et al., 2021; Nawrot et al., 2014).

Plant-derived HDPs are very promising candidates for ectopic expression in crop plants because they have the potential to provide crops with durable, broad-spectrum resistance to phytopathogens. Some HDPs from plants have proven to be capable of killing fungi, bacteria, and viruses within minutes of contact (Büyükkiraz & Kesmen, 2022). There is also a relatively low chance of pathogens developing resistance to these peptides because many HDPs target fundamental differences in the microbial cell membrane structure, which distinguishes them from plant and animal cell membranes. Because HDPs target these basic differences in the cell membranes, as opposed to specific receptors, the microorganisms would need to significantly redesign the structure of the cell membrane to develop resistance (Büyükkiraz & Kesmen, 2022; Yevtushenko & Misra, 2007). However, that is not to say that it is impossible for microorganisms to develop resistance to HDPs. There is the possibility of bacteria reducing the negative charge of their membrane, thus avoiding the initial electrostatic interaction of most HDPs. One example of this has been observed with gram-positive *Listeria monocytogenes*: it can neutralize its anionic charge by modifying teichoic acid with the addition of positively charged D-alanine residues (Nunes et al., 2021). However, the evolution of such resistance has not been the case so far: there has been no real evidence that the presence of HDPs can increase the mutation rate of bacteria. Microbial resistance to HDPs generally seems to evolve at a much lower rate than has been observed with conventional antibiotics (Nunes et al., 2021). Another advantage of HDPs is that some may act synergistically, allowing higher levels of inhibition with

the use of gene pyramiding or via synergism with the host's defense peptides. For example, Magainin 2 and PGLa from frog skin display synergistic levels of activity against bacteria by forming stable transmembrane pores (Büyükkiraz & Kesmen, 2022). Another example is that of abaecin, from bumble bee, combined with cecropin A, which showed synergistic activity levels against *E. coli* in the study of Rahnamaeian et al. (2016). Each peptide individually showed no effect on bacterial growth, but when combined they completely inhibited bacterial cell growth at those same concentrations. A further point in favour of plant derived HDPs is that plants, being stationary organisms, cannot escape threats, yet after millions of years they are still thriving. This indicates that the plant immune system, including the multifunctional HDPs, must be extremely robust despite lacking the adaptive immune system of higher organisms (Iqbal et al., 2019; Lacerda et al., 2014; Li et al., 2021; Park et al., 2000) . Some of these defence measures are physical such as possessing a waxy cuticle, but many are chemical, such as cell recognition systems, transcriptional pathways (Li et al., 2021), and production of defence factors, such as hydrogen peroxide, phenolics, alkaloids, pathogenesis-related defence proteins, and plant defence molecules such as HDPs (Lacerda et al., 2014). HDPs can often target multiple sites on the cellular membrane, while some are known to have intracellular targets, they usually display low levels of toxicity towards mammalian cells, they kill quickly at low concentrations, and are expressed in multiple organs (Li et al., 2021). Plant HDPs are also advantageous for crop development because they are often perceived as more natural than HDPs from other organisms, which generally makes them more acceptable to the public.

1.2.2.1 Classes of Plant HDPs. There are eight main classes of plant HDPs. One class represents thionins, which consist of 45 to 48 amino acids, and six or eight cysteines that form a ring structure (Li et al., 2021). They inhibit fungi, bacteria, and insects, and are known to bind

membrane phospholipids causing ion leakage which leads to cell death. An example of a thionin is Thi2 from *Arabidopsis thaliana* which strongly inhibits *Staphylococcus aureus* (Iqbal et al., 2019). Another class of HDPs are called plant defensins: they are 45-54 amino acids long and form a large superclass of plant HDPs. They possess a conserved structure consisting of three anti-parallel β sheets and an α helix parallel to the β sheets which are stabilized by 4 disulfide bonds (Lacerda et al., 2014; Li et al., 2021). Plant defensins have a number of functions such as, antimicrobial activity, and inhibition of α amylase and trypsin activity. They may also act as epigenetic factors, and mediate abiotic stress responses (Lacerda et al., 2014; Li et al., 2021). Plant defensins are also known to be involved in the growth and development of plants; for example, in the study of Stotz et al. (2009), the tomato defensin DEF2 was found to play a role in pollen and seed production, and organ growth while also inhibiting the growth of *Botrytis cinerea*.

Hevein-like peptides form a third class of HDPs. They are mainly known to inhibit fungal growth due to their chitin binding domains (Li et al., 2021) but they can also display antibacterial activity (Iqbal et al., 2019). An example of a hevein-like protein is GAFP, which was isolated from *Gingko biloba* and displayed antifungal activity towards *Pellicularia sasakii, Alternaria alternata, Fusarium graminearum,* and *F. moniliforme* (Huang et al., 2000). Their structure consists of an antiparallel β-sheet and a short α-helix with three to five disulfide bonds which stabilize the molecule (Li et al., 2021). The fourth class are knottin-type peptides which are approximately 30 amino acids long (Li et al., 2021) and possess a range of functions such as antimicrobial activity, enzyme inhibition, hormone-like functions, cytotoxic effects, anti-HIV, and insecticidal functions (Iqbal et al., 2019). They also participate in abiotic and biotic stress resistance, and they are known to stimulate root growth. Their structure contains multiple

disulfide bonds which result in the formation of a cysteine knot (Li et al., 2021). The fifth class of peptides is the α-hairpinin family, which are peptides rich in lysine and arginine and possess a helix-loop-helix motif, stabilized by two disulfide bonds. These HDPs display activity against a wide range of antimicrobial targets, they also possess ribosome-inactivating and trypsin-inactivating activities (Li et al., 2021).

The next, sixth class of HDPs are the lipid transfer proteins (LTPs). These are small and cationic, containing eight cysteine residues. They fold into a stable tertiary structure with four disulfide bonds and four flexible loop-linked helices with hydrophobic cavities which contain lipid binding sites (Li et al., 2021). LTPs are known to display activity toward phytopathogens, and they also play a role in abiotic stress resistance (Iqbal et al., 2019). The seventh class are the snakins; they possess six disulfide bonds and are approximately 63 amino acids in length. Snakins play a role in biotic and abiotic stress response, and plant hormone functions (Oliveira-Lima et al., 2017). The last class is the cyclotide family. These HDPs are 28 to 37 amino acids long and are long chain cyclic peptides stabilized by three disulfide bonds which are arranged and cross linked into a knotted pattern. Most of the anionic plant HDPs belong to this family. These are extremely stable peptides which resist denaturation and degradation by proteases (Li et al., 2021). Their biological activities include hemolytic and cytotoxic effects, anti-HIV effects, and insecticidal, antimicrobial, and anti helminthic activities (Iqbal et al., 2019).

1.2.2.2 Mechanisms of Action of Plant HDPs. The mechanisms of action of plant HDPs are not yet completely understood but currently there are two main categories: membranolytic and non-membranolytic. In general, membranolytic HDPs are cationic peptides which interact with bacterial membranes which are rich in anionic lipids such as phosphatidylserine. These interactions result in changes to membrane permeability which leads to cell death due to altered

cell transmembrane potential, altered pH gradients, inhibited cell respiration, and the effect on osmotic regulation (Li et al., 2021).

Membranolytic interactions. There are currently four main models of HDP interaction with cell membranes.

Barrel-stave pore model. In the barrel-stave pore model the HDPs first congregate at the cell membrane and align themselves horizontally on the plasma membrane. Then, as the hydrophobic region of the peptides align with the hydrophobic core of the lipid bilayer, the HDPs insert into the bilayer vertically, aligning themselves with the membrane lipids; the peptides bind together and form a stable transmembrane pore. There is evidence that some HDPs may then enter the cell through these pores and interact with intracellular targets, further disrupting cellular processes (Li et al., 2021; Nawrot et al., 2014).

Carpet mechanism model. In the carpet mechanism model the HDPs form a carpet-like layer by aligning themselves horizontally on the cell membrane and adsorbing to it. When a threshold concentration is reached then the membrane lipids lose directionality and break up into micelles, lined by HDPs on the outside, in a detergent like manner (Li et al., 2021; Nawrot et al., 2014).

Toroidal pore model. The toroidal pore model is in between the barrel-stave and carpet models. Once the HDPs form a carpet and adsorb to the cell membrane surface it causes the membrane to curve which allows the peptide to pass through the lipid bilayer and form a pore. The peptides line the pores, staying in contact with the lipid heads on one side and the cytosol on the other (Li et al., 2021; Nawrot et al., 2014).

Disordered toroidal pore model. The disordered toroidal pore model begins like the toroidal pore model but then the HDPs turn inwards, and the phospholipid head groups turn to

face the pore lining. The embedded peptides and the peptides at the pore openings help to stabilize and maintain the pore (Li et al., 2021).

While HDPs tend to be cationic, there are anionic HDPs which are known to interact with the negatively charged cell membrane. One example of this is the peptide AP2 which is anionic but contains some cationic amino acid residues which allows interaction with the plasma membrane (Li et al., 2021).

Non-membranolytic interactions. Some HDPs are also known to target other processes which lead to cell death without interacting with the cell membrane, sometimes by means of cell penetration through the utilization of some form of transmembrane transport, such as protein mediated transmembrane transport. Some of the processes which are often hindered are protein synthesis, nucleic acid function or synthesis, cell wall synthesis, such as with fungal cells by HDPs containing chitin binding domains, and by interfering with protein folding (Li et al., 2021; Nicolas, 2009). They may also stimulate reactive oxygen species (ROS) production; for example, *RsAFP2* stimulates ROS in *Candida albicans* which affects fungal growth as well as cell permeability, and some HDPs, such as MsDef1, block calcium cell signalling in fungi which inhibits tip growth in the hyphae (Iqbal et al.,2019; Nicolas, 2009).

1.2.2.3 Applications in Crop Development. There are several advantages to utilizing plant HDPs to engineer disease resistance in crops. Most plant HDPs are constitutively expressed in various organs at a low base level and increase their levels in response to pathogen invasion (Lacerdo et al., 2014; Li et al., 2021). Most HDPs also target pathogens in a non-specific way, which makes it more difficult for the pathogens to develop resistance against them; this makes them ideal for the development of crops which possess enduring resistance to phytopathogens. HDPs may also be modified to increase activity by applying the principles of peptide modelling

(Yevtushenko & Misra, 2012). One successful example of a crop transformed with an HDP is the heterologous expression of Mj-AMP1, a defensin from *Mirabilis jalapa,* in tomato which increased resistance to *Alternaria solani* (Li et al., 2021). HDPs also, when combined with an appropriate promoter, can be expressed in specific organs, such as potato tubers. When the benefits of such a stable, low energy method of pathogen defence is considered, along with the recent findings that many HDPs fulfill other roles, such as functions mediating growth and development, it is not surprising that yields may increase. In fact, transformed *Arabidopsis thaliana* expressing defensin Cn-AFP from chickpea displayed higher germination rates, root length, and biomass in a study by Kumar et al. (2019), and it was discovered that transformed potato plants expressing AMPs MsrA1, MsrA2, and MsrA3 experienced a 15-25% increase in tuber yield (Yevtushenko & Misra, 2012). Given all these benefits, and the fact that HDPs also display very low levels of toxicity towards mammalian cells (Li et al., 2021), utilizing HDPs in crop defence has become a promising area of research.

1.2.2.4 HDPs chosen for this experiment. Four HDPs were chosen for this experiment to be tested *in vitro* for activity against several potato pathogens. These peptides are: Skh-AMP1 from *Satureja khuzistanica*, Cr-ACP1 from *Cycas revoluta*, Cn-AMP1 from the green coconut water of *Cocos nucifera*, and Shepherin 2 from *Capsella bursa-pastoris*. All these HDPs are somewhat unusual because, unlike most known HDPs, they contain no disulfide bonds (Park et al., 2000; Santana et al., 2015; Silva et al., 2012).

Shepherin 2. In a study by Park et al. (2000) Shepherin 2 was isolated along with Shepherin 1 from the roots of *Capsella bursa-pastoris* (shepherd's purse) which has been traditionally used in North America and Korea for the healing of wounds and treatment of diarrhea (Park et al., 2000; Romero, 1954). This peptide is 38 amino acids in length and has a

molecular mass of 3260.6 Da, as determined by matrix assisted laser desorption/ionization (MALDI) mass spectroscopy (Park et al., 2000). The amino acid sequence of the active peptide is: Gly-Tyr-His-Gly-Gly-His-Gly-Gly-His-Gly-Gly-Gly-Tyr-Asn-Gly-Gly-Gly-Gly-His-Gly-Gly-His-Gly-Gly-Gly-Tyr-Asn-Gly-Gly-Gly-His-His-Gly-Gly-Gly-Gly-His-Gly. As can be seen by the sequence, Shepherin 2 is a very glycine (65.8% mol/mol glycine) and histidine (21.1% mol/mol histidine) rich polypeptide with its repeating Gly-Gly-His motif. The numerous histidine residues make Shepherin 2 highly cationic with a net charge of +8 and the circular dichroism (CD) spectra indicated that the secondary structure consists entirely of random coil in 50 mM sodium phosphate buffer but that in 50% trifluoroethanol the secondary structure consisted of 25% β sheets and 75% random coil, with no α helices detected (Park et al., 2000). The two Shepherin peptides are novel peptides because, while they share some characteristics of other HDPs, such as length and positive charge, they lack the characteristic even number of cysteine residues and resulting disulphide bridges. Both Shepherin 1 and 2 are produced from a single 120 amino acid polypeptide. This pro-peptide is thought to be localized in the vacuole where it is cleaved into the two separate HDPs (Park et al., 2000). When this pro-peptide was isolated, it was not found in the leaves and stems, only the roots contained the peptide. The yield was 7 micrograms of Shepherin 2 per gram of roots and it was found to be active against the gram-negative bacteria and most of the fungi it was tested against, although it displayed no activity against gram positive bacteria; even at a concentration of 100 μg/ml (Park et al., 2000). Most of the pathogens Shepherin 2 was tested against by Park et al. (2000) were human pathogens; however, a couple fungal phytopathogens were also assayed: *Alternaria alternata* was tested and found to be resistant up to 100 μg/ml and *Fusarium culmorum* was found to reach 50% inhibition at 68 μg/ml.

Skh-AMP1. Skh-AMP1 was isolated from the leaves of *Satureja khuzistanica* (jamzad) (Khani et al., 2019). Jamzad is a plant native to Iran and has been used in traditional medicine for wound healing, toothache, and stomach and intestinal issues. The essential oils from jamzad have also been noted to have antiviral, anti inflammatory, antimicrobial, and antioxidant activities which have been confirmed in several studies (Khani et al., 2019). This HDP is 25 amino acids in length, has a net charge of +2, a pI of 9.3, and a molecular mass of 2778.10 Da. It is a hydrophilic peptide with only 28% of the residues being hydrophobic and was stable at 30° C to 40° C but lost stability when tested at 80°C. The peptide also lost stability in acidic conditions (pH 2-4) but was very stable at pH 7-8. The sequence was determined to be: Gly-Arg-Thr-Ser-Lys-Gln-Glu-Leu-Cys-Thr-Trp-Glu-Arg-Gly-Ser-Val-Arg-Gln-Ala-Asp-Lys-Thr-Ile-Ala-Gly by high resolution mass spectrometry followed by Edman sequencing (Khani et al., 2019). Molecular modelling analysis determined that Skh-AMP1 would adopt an α-helix conformation. Khani et al. (2019) reported that the yield was 3.75 μg per gram of leaf tissue and that there was a negligible amount of hemolytic activity observed during assays as well as very low levels of cytotoxicity against HEK293 cells. The Khani et al. (2019) experiment conducted antifungal assays against species of *Aspergillus* and *Candida* which found that Skh-AMP1 completely inhibited fungal growth for these species at concentrations between 19.8 μM and 23.4 μM. Skh-AMP1 was found to interact with the fungal cell membrane which affected cell permeability and osmotic pressure which was confirmed by an increase in potassium ion leakage as well as propidium iodide uptake. This then leads to increased ROS production followed by apoptosis (Khani et al., 2020).

Cn-AMP1. Cn-AMP1 was isolated from *Cocos nucifera* L. (green coconut) water. Green coconut water contains sugars, vitamins, proteins, and minerals which has caused its popularity

as a health beverage. It is also used to this day in poor regions for the treatment of diarrhea and in traditional medicine to treat gastroenteritis, urinary stone dissolution, and coronary heart disease (Mandal et al., 2009). This HDP is only nine amino acids in length, has a net charge of +1, and a molecular mass of 858 Da. The amino acid sequence is: Ser-Val-Ala-Gly-Arg-Ala-Gln-Gly-Met which gives it a hydrophobic ratio of 44%. Cn-AMP forms an amphipathic α-helix in the presence of cell membranes (Mandal et al., 2009) and changes conformation to a loose coil conformation as the microenvironment changes to an aqueous environment (Mandal et al., 2009; Santana et al., 2015). In the Silva et al. (2012) study Cn-AMP1 was tested against a variety of human pathogens and displayed activity against all of them. The pathogens tested included gram-positive bacteria: *Bacillus subtilis, Enterococcus faecalis, Staphylococcus aureus,* and *Streptococcus pyogenes*: the minimum inhibitory concentration (MIC) was between 18 and 36 μM. The gram-negative pathogens tested were: *Escherichia coli, Klebsiella pneumoniae, Proteus mirabilis, Pseudomonas aeruginosa,* and *Salmonella typhimurium*; the MIC was found to be between 9 to 18 μM for this group. Several fungi were also tested; they included: *Candida albicans, Candida parapsilosis, Cryptococcus neoformans, Trichophyton mentagrophytes,* and *Trichophyton rubrum*; the MIC for fungi was between 18 and 144 μM (Silva et al., 2012). These findings indicate that Cn-AMP1 is most active against gram-negative bacteria, followed by gram-positive bacteria and fungi. Cn-AMP1 in the study of Silva et al. (2012) also displayed anti-cancerous and immunostimulatory activity.

Cr-ACP1. Cr-ACP1 was isolated from the seeds of *Cycas revoluta* (sago palm) whose trunks are the source of sago, a food starch. It has a molecular mass of 1050 Da and is only nine amino acids long. Its amino acid sequence is: Ala-Trp-Lys-Leu-Phe-Asp-Asp-Gly-Val, giving it a net charge of -1 (Mandal et al., 2012); it was the only negatively charged peptide tested during

this experiment. Three-dimensional modelling indicates that the secondary structure consists of an amphipathic α-helix, and it appears to target DNA leading to apoptosis (Mandala et al., 2012). The Mandala et al. (2012) study tested Cr-ACP1 against both gram-positive and gram-negative bacteria which are pathogenic to humans; the results gave an MIC between 30 and 60 μM for all tested species. The bacteria tested were *Staphylococcus epidermis, Bacillus subtilis, Pseudomonas aeruginosa,* and *E. coli*. Cr-ACP1 was also found to possess anti-cancerous properties and to cause no negative effects to red blood cells (Mandala et al., 2012).

1.2.3. Phytopathogens

More than forty pathogens are known to target potatoes causing significant damage to the plant foliage as well as the tubers, both pre- and postharvest. These pathogens, which consist of bacteria, fungi, viruses, insects, and nematodes, often cause significant losses to both yield and tuber quality (Tiwwari et al., 2020). Four major potato pathogenic species were assayed for susceptibility to the four HDPs used in this experiment: two bacterial species and two fungal species. The bacteria were both of the same genus: *Pectobacterium carotovorum* subsp. *carotovorum* and *P. carotovorum* subsp. *atrosepticum.* The two fungal species were from different genera: *Alternaria alternata* and *Fusarium culmorum*. The species of pathogen were chosen because they are important potato pathogens and because, in the case of the fungal species, it is relatively simple to induce sporulation and obtain an adequate number of spores from their cultures grown *in vitro*.

1.2.3.1 *Pectobacterium carotovorum* subsp. *carotovorum* and *P. carotovorum* subsp. *atrosepticum.* These are two subspecies of *P. carotovorum* but throughout this thesis I will refer to them as simply *P. atrosepticum* and *P. carotovorum*. *P. atrosepticum* is a gram-negative rod-shaped bacterium that is 0.5 to 0.8 μm by 1 to 2.5 μm. The bacterial cells possess flagella which

allow for motility; they are also facultative anaerobes. *P. carotovorum* are also a rod shaped, gram-negative, facultative anaerobic bacteria; they measure 0.5 to 0.8 μm by 1.0 to 3.0 μm and possess peritrichous flagella which allow them mobility. These bacteria cause blackleg and bacterial soft rot in potatoes (Howard et al., 1994). In regard to blackleg, the disease may be present in or on seed tubers, the roots of various crops and weeds, and in irrigation water. Although the bacteria are not thought to last more than a year without a host, it can spread quickly and easily from flies that land in cull piles or during activities such as seed cutting or tuber harvest and storage. If the disease overwinters in the seed tubers that are planted the following spring, then the disease cycle repeats. At that point the bacteria may also travel through soil water (up to 60 cm) and infect neighbouring seed tubers as well (Howard et al., 1994). Blackleg favours wet soil and temperatures below 18° C and plants in low lying areas. The first symptoms of blackleg usually appear during flowering; at which point one or more plant stems will suddenly wilt and sometimes leaf yellowing between the veins and leaf cupping will occur. Lower stems will usually blacken or darken, and the bottom 15 cm of the stem may turn absolutely black. The bacteria from infected tubers may move up the emerging stems and stunt the growth of young plants, the tubers may rot in the soil, and planting of infected tubers can cause reduced germination due to seed rotting, and reduced plant stands. Most common potato cultivars are susceptible to blackleg with only Russet Burbank possessing some resistance (Howard et al., 1994). The methods of disease transmission are the same for bacterial soft rot, but the symptoms are different. Soft rot often occurs alongside other infections and usually only affects the tubers. It causes brown, sunken lesions of up to one centimetre to form on the surface. A clear line separates the uninfected from the infected tuber tissues which appear creamy white in the beginning. The infected regions will then darken to a brown colour and become slimy with

a rotten odour. In wet conditions the tubers will rot while still in the soil; the disease prefers high temperatures to cool ones (Howard et al., 1994).

1.2.3.2 ***Alternaria solani.*** The conidia of *A. solani* are brown and are 150 to 300 µm by 15 to 19 µm which grow brown to black mycelium (Howard et al., 1994) (Fig. 1). *A. solani* causes early blight of potato. The first symptoms usually show themselves at the time of flowering and usually take the form of small brown dots on the older leaves, which become lesions surrounded by dead tissue, in a bullseye-like manner, and with margins on the leaf often becoming yellow (Bauske et al., 2018; Howard et al., 1994). This eventually spreads to the upper leaves and if it spreads enough, it will reduce tuber yields. The disease can also occur in stored tubers; the symptoms appear as dark and sunken circular lesions (Bauske et al., 2018; Howard et al., 1994). Early blight may persist and spread from infected tubers, soil, crop residues, and other infected plants, and the spores may be carried in wind and water to penetrate the leaves. Nitrogen deficiency can greatly increase susceptibility to early blight as well as the severity of the disease symptoms. The spores germinate in water and so favour cooler, under 15° C, dewy nights, and days that are around 20° C (Howard et al., 1994).

Figure 1 Light microscopy picture of an *Alternaria solani* spore (Paul Bachi, University of Kentucky Research and Education Center, Bugwood.org).

1.2.3.3 *Fusarium culmorum.* The macroconidia of *F. culmorum* have a slight crescent shape, are thick walled, usually have between 3 and 5 septae, are 30 to 50 µm by 5.0 to 7.5 µm (Fig. 2) and target a wide range of host species (Scherm et al., 2013). The *Fusarium* genus of fungi, including *F. culmorum*, cause potato dry rot (Tiwari et al., 2020) and seed-piece decay (Howard et al., 1994) in potato crops. *F. culmorum* also causes significant damage to wheat by being the causal agent of foot and root rot as well as *Fusarium* head blight (Scherm et al., 2013). Regarding seed-piece decay, the earliest symptoms of disease are missing hills and gaps in the plant cover, or delays in plant emergence due to the seed tuber having decayed in the ground; this can cause significant reductions to yield potential (Howard et al., 1994). Potato dry rot usually only affects the roots and tubers. The tubers shrivel up and shrink and develop lesions on the surface of the tubers and the roots; meanwhile, black or brown rot occurs within the tissues (Tiwari et al., 2020). *Fusarium* spores can survive for years in soil and can inoculate the seed tubers when planted in the infected soil, but many of the infections are caused by seed tubers which are already infected. The seeds may rot in the soil and infect young plants, or infected soil may be dug up with the tubers, which may then infect wounded or immature tubers. The infected soil may also contaminate the harvesting equipment, which can allow the equipment to introduce the pathogen to uninfected fields to further spread the disease (Howard et al., 1994). Unfortunately, most common potato cultivars remain susceptible to *Fusarium* dry rot causing significant loss to potential yields (Tiwari et al., 2020).

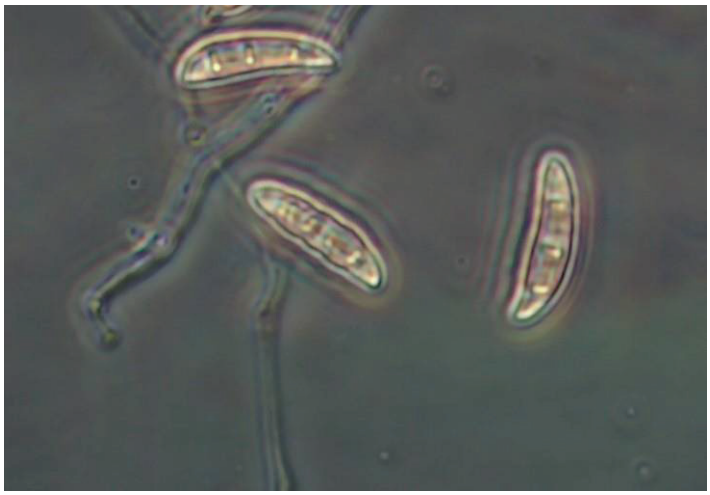

Figure 2 Light microscopy picture of *Fusarium culmorum* conidia in diluted potato dextrose broth.

1.2.4. Transgenic Crops

The genetic transformation of plants is defined as the transfer of DNA molecules from one organism to another, followed by the stable integration and expression of the introduced gene in the new host (Keshavareddy et al., 2018; Rivera et al., 2012). Genetic engineering is a powerful tool for crop breeders because it can reduce crop losses, which occur due to biotic and abiotic stresses, by allowing the introduction of agronomically useful components into complex pathways. Genetic engineering can also allow for the control of spatiotemporal expression of these transgenes (Keshavareddy et al., 2018; Rivera et al., 2012). Crop transformation has been used to genetically improve crops for qualities such as, improved yield, increased nutritional value, herbicide resistance, increased drought and salt tolerance, improved resistance to insects and microbial pathogens, and increased resistance to temperature or climate changes. Once the plant cells are transformed, they are regenerated into whole plants via tissue culture techniques. The transgenes are then inherited by future generations (Keshavareddy et al., 2018; Rivera et al., 2012). One example of an extremely successful transgenic crop is that of Bt cotton in India, which expresses toxins from the bacterium *Bacillus thuringiensis* that are harmful to the larva of

some insects; the use of Bt plants have increased the productivity of India's large cotton industry by 50% while also decreasing insecticidal spray use by 50% (Keshavareddy et al., 2018). Currently in the USA more than 75% of all cotton, soybean, sugar beet, and corn are genetically altered for insect and herbicide resistance (Anjanappa & Gruissem, 2021). However, several criteria must be met to make the production of transgenic crops feasible for mass production. Appropriate target cells or tissues, which can accept the new gene(s) and subsequently regenerate, must be available (Anjanappa & Gruissem, 2021; Keshavareddy et al., 2018), along with facilities which possess adequate aseptic conditions necessary for large scale plant production (Anjanappa & Gruissem, 2021; Rivera et al., 2012). A method for the introduction of the DNA into the cells or tissues is required along with a protocol for regenerating the transgenic tissues into full grown plants (Anjanappa & Gruissem, 2021; Keshavareddy et al., 2018). Any protocol to be used must be straight forward and efficient, economical, reproducible, and be able to produce a large number of transgenic plants (Keshavareddy et al., 2018; Rivera et al., 2012). The protocols must also be safe; hazardous components or procedures should be avoided (Keshavareddy et al., 2018; Rivera et al., 2012). The protocol applied should also result in a small copy number of genes introduced into each cell (Rivera et al., 2012) to minimize occurrences of gene disruption at insertion sites (Keshavareddy et al., 2018; Rivera et al., 2012). The procedures should strive for minimal time in tissue culture in order to lower costs and to avoid the introduction of somaclonal variation (genetic variation which may occur in tissue cultured plants) (Keshavareddy et al., 2018); and lastly, the protocol must yield stable, fertile transgenic lines which display expression of the transgenes in the desired manner for future propagation, preferably without the inclusion of unnecessary vector sequences in the genome (Keshavareddy et al., 2018; Rivera et al., 2012). There are two main types of plant

transformation: the first are called direct or non biological systems, and the second are called indirect or biological systems of transformation.

1.2.4.1 Transformation systems. While there have been a number of techniques for genetic transformation among these two types, when the above criteria for successful large scale transgenic production is taken into account, most of these techniques are usually judged to be impractical for the large-scale production of transgenic crops. Generally, two techniques end up being used, one is *Agrobacterium*-mediated transformation (a biological system) and the other is particle bombardment, also known as biolistics (a non-biological system) (Anjanappa & Gruissem, 2021; Keshavareddy et al., 2018; Rivera et al., 2012). There are pros and cons to both methods.

Agrobacterium-mediated transformation. During *Agrobacterium*-mediated transformation, the gene is introduced to the target cells via *Agrobacterium* cells, which contain a plasmid, which has been designed to express the gene of interest. This technique works because *Agrobacterium* has a natural ability to infect plants by transferring DNA which is located on a plasmid that produces plant tumors. The plasmid is introduced into the plant cell and is subsequently taken up by the genome, resulting in stable transgene expression (Keshavareddy et al., 2018). Some advantages to *Agrobacterium*-mediated transformation are that it works with a wide range of species, it is efficient and reproducible, the DNA can be introduced to various types of cells (Rivera et al., 2012), genes are introduced into the cell in low copy numbers and the insertions are more likely to be intact and have defined ends, and transgene integration is generally stable and inheritable, displaying consistent gene expression over subsequent generations (Anjanappa & Gruissem, 2021; Rivera et al., 2012). Some disadvantages of using *Agrobacterium* are that the levels of transformation efficiency and plant regeneration can be

highly variable, depending on the host plant species. This method is also time consuming and requires the use of aseptic protocols and facilities (Rivera et al., 2012). Issues may also occur with monocotyledonous species, such as cereal crops, because they are not naturally susceptible to *Agrobacterium* infection. However, new methods have been discovered to overcome this barrier in many species including rice, banana, wheat, sugar cane, and several species of commercially important trees (Keshavareddy et al., 2018). This is the most common form of crop transformation, with over 195 *Agrobacterium* transformed crops approved for production in species of alfalfa, canola, maize, potato, apple, cotton, tomato, and others (Anjanappa & Gruissem, 2021).

Particle bombardment. Particle bombardment, also known as biolistics, is another method used for the purpose of plant transformation. During this procedure a biolistics gun is used to shoot gene covered particles into the cell, through the cell wall. Some advantages of biolistics are that it is simple, with no need to remove the cell wall, as is necessary with some non biological methods, and more than a single gene may be included in the transformation (Rivera et al., 2012). Particle bombardment is also good for the transformation of cereals and other monocots which are more difficult to transform using *Agrobacterium*. This method also has a high rate of transformation efficiency, and the constructs can be linear cassettes, or circular or linear plasmids (Keshavareddy et al., 2018). Some disadvantages of biolistics are that the transformation efficiency tends to be lower than *Agrobacterium* mediated transformation as well as being more expensive. The targets are also random, the DNA is often damaged and multiple copy insertions often occur which can cause undesirable gene expression patterns or gene silencing in the host plant (Keshavareddy et al., 2018; Rivera et al., 2012). Despite these

disadvantages there are 45 biolistic crops approved for production including canola, maize, cotton, and soybean (Anjanappa & Gruissem, 2021).

1.2.4.2 Choice of promoter. The regulation of a gene may occur at various levels, but it is crucial at the stage of transcriptional initiation, which relies on the interaction between promoters, RNA polymerase II, and transcription factors (Kluge et al., 2018; Potenza et al., 2004). For this reason, promoter choice for the development of transgenics is very important. A promoter is a section of DNA located upstream of the gene's coding region: it contains the sequences recognized by proteins such as, RNA polymerase II and various transcription factors that are involved in transcription initiation (Kluge et al., 2018; Potenza et al., 2004). Plant promoters are usually composed of two regions; the first is a core region which contains a TATA box which specifies to other molecules where transcription begins. This core region is usually quite short (50-100 bp) and is adjacent to the transcription start site. The second region is an upstream flanking region, usually one to two kb long, which contain *cis*-regulatory elements that serve as binding sites for transcription factors (Potenza et al., 2004; Yevtushenko & Misra, 2018). The gene's pattern of expression, including when, where, and how much protein is produced, is driven by the interaction between the *cis*-acting elements and the transcription factors (Potenza et al., 2004; Yevtushenko & Misra, 2018). Many different promoters have been discovered which produce different patterns and levels of gene expression. The main difference is whether a promoter is constitutive or inducible; they may also promote gene expression during different developmental stages and in different parts of the organism (Potenza et al., 2004; Yoshida & Shinmyo, 2000).

Transgenic plants are developed to serve different purposes, such as disease control or drought tolerance, others are created to constitutively over-express a gene of interest. When

trying to achieve the latter goal, the most common type of promoters originate from plant virus sources, such as the *CaMV* (cauliflower mosaic virus) *35S* promoter or the *CsMV* (cassava mosaic virus) promoter. These types of promoters are isolated from double stranded DNA viral genomes, which use their target species' RNA polymerase for transcription (Potenza et al., 2004). There are also constitutive promoters of plant origin, such as the *ACT 2* promoter from the actin gene family of *Arabidopsis*, although these are less commonly used. These constitutive promoters are unregulated promoters that allow continuous expression of a gene. They are advantageous because they display high levels of transcription in both monocots and dicots (Potenza et al., 2004; Yoshida & Shinmyo, 2000), are easily obtained for research, and are already available in pre-constructed vectors (Potenza et al., 2004).

However, there are also disadvantages to the use of constitutive promoters for transformation. These disadvantages include possible detrimental effects on plant growth and development which may result from high levels of expression of foreign genes during a sensitive developmental phase (Potenza et al., 2004). Plant health can also be damaged by the high accumulation of the proteins being produced via transgene expression, which at some point may cross a threshold concentration and become toxic to the host plant (Yoshida & Shinmyo, 2000), and for many applications there is simply no benefit from constitutive expression of a gene (Yevtushenko & Misra, 2018). The viral promoters have additional disadvantages because sometimes the host cells may recognize and inactivate the viral genes via transcriptional gene silencing. Public perception is also an obstacle with the use of viral elements in crops because they are seen as a possible risk to human health (Potenza et al., 2004). In this regard, plant-derived promoters, which can be inducible in a predictable spatiotemporal manner, may be seen

as more natural and less intrusive to the plants and are thus perceived to be more acceptable by the public.

Inducible promoters induce or repress gene expression in response to stimuli such as, wounding, abiotic stress, and pathogen attack (Potenza et al., 2004). An ideal inducible promoter to produce transgenic crops will display resource efficient induction so that plant growth is not impacted by a loss of energy and resources due to the plant's stress response. It will reliably induce expression of the target gene and will tightly control regulation of the gene (Kluge et al., 2018). Inducible promoters are advantageous because gene expression can be targeted to the area of attack or infection, and gene expression is generally kept at a low or nonexistent basal level which is only increased when the organism responds to a stressor. This prevents a build up of proteins which may have detrimental effects on plant growth, health, and development (Potenza et al., 2004). An example of a promoter that increases its activity in response to stimuli is the *PmBiP Pro1* promoter of the luminal binding protein (*BiP*) from Douglas-fir. The *PmBiP Pro1* promoter regulates the expression of the endoplasmic reticulum (ER) molecular chaperone of the HSP70 stress-related protein family (Yevtushenko & Misra, 2018). In the Yevtushenko & Misra (2018) study, potato plants were transformed with the *BiP* promoter which regulated the expression of the *β-glucuronidase (GUS)* reporter gene. The study found that the promoter was fully functional in the potato host and was compatible with the potato transcription factors. Expression of GUS also increased beyond the basal expression level in response to wounding and pathogen invasion by approximately two-fold. High levels of GUS were detected in young tissues as well as other tissues that are associated with high rates of cell division and unusually high levels of GUS were also detected in tubers, suggesting some organ-specific activity as well (Yevtushenko & Misra, 2018). A truncated version of the *BiP* promoter, called *PmBiP Pro1-3*, is

one of the promoters that was used for transformation in this study because it was found to be fully functional in potato plants (Yevtushenko & Misra, 2018); the commonly used constitutive *CaMV35S* promoter from Cauliflower mosaic virus was the other promoter used in this study for comparisons between the two types of promoters.

1.3 Objectives

This research project had four objectives:

1. Evaluate antimicrobial activities of four selected plant HDPs against major potato pathogens *in vitro*.
2. Evaluate the cytotoxicity of these HDPs toward plant and mammalian cells *in vitro*.
3. Confirm the activity of the truncated Douglas-fir *PmBiP Pro1-3* promoter in plant tissues and organs using green fluorescent protein (gfp).
4. Construct plant transformation vector(s) with the gene encoding the most efficient HDP found in this study, under the control of one of the following promoters—the truncated Douglas-for *PmBiP Pro1-3* promoter and the constitutive *CaMV 35S* promoter, and introduce them into *Solanum tuberosum* L. cv. Desiree potato plants via *Agrobacterium*-mediated transformation.

The first two objectives focus on the identification of a promising HDP that has potent antimicrobial activity towards potato pathogens and is not harmful to plants or mammals. The third objective was chosen to verify that the *PmBiP Pro1-3* promoter would be suitable to drive the expression of the most promising HDP, and the last objective was to apply the results from the first three objectives and to create transgenic potato plants to be used for the next step of the research. Future research will include the evaluation of expression and antimicrobial activity of

the chosen HDP *in planta* against a range of potato pathogens under the control of two different types of promoters so that comparisons for growth, yield, plant health, and pathogen resistance may be made between the two.

The selection of the HDPs in this study had to meet three criteria: 1) the peptides must be of plant origin, to address the current trend in transgenic research to minimize the presence of non-plant DNA in transgenic crops; 2) the peptides must not have been expressed in non-host plants; and 3) the peptides must be linear, lacking disulfide bonds. The latter would keep the cost of peptide synthesis affordable.

These objectives resulted in the identification of an HDP, of plant origin, which displayed strong antimicrobial activity toward potato pathogens while demonstrating low levels of toxicity towards plant and mammalian cells. The study also utilized a plant promoter to induce expression of the HDP in transgenic potato in response to pathogen invasion and compare its efficacy with that of a constitutive promoter. The use of a green fluorescent protein (gfp) reporter gene, fused to the *PmBiPPro1-3* promoter, was intended to provide information about how the Douglas-fir promoter regulates gene expression throughout the potato plant life cycle.

The transgenic potato plants developed during this project may be used for future experiments, such as the development of a transgenic potato cultivar with potent and responsive antimicrobial defence.

2. Materials and Methods

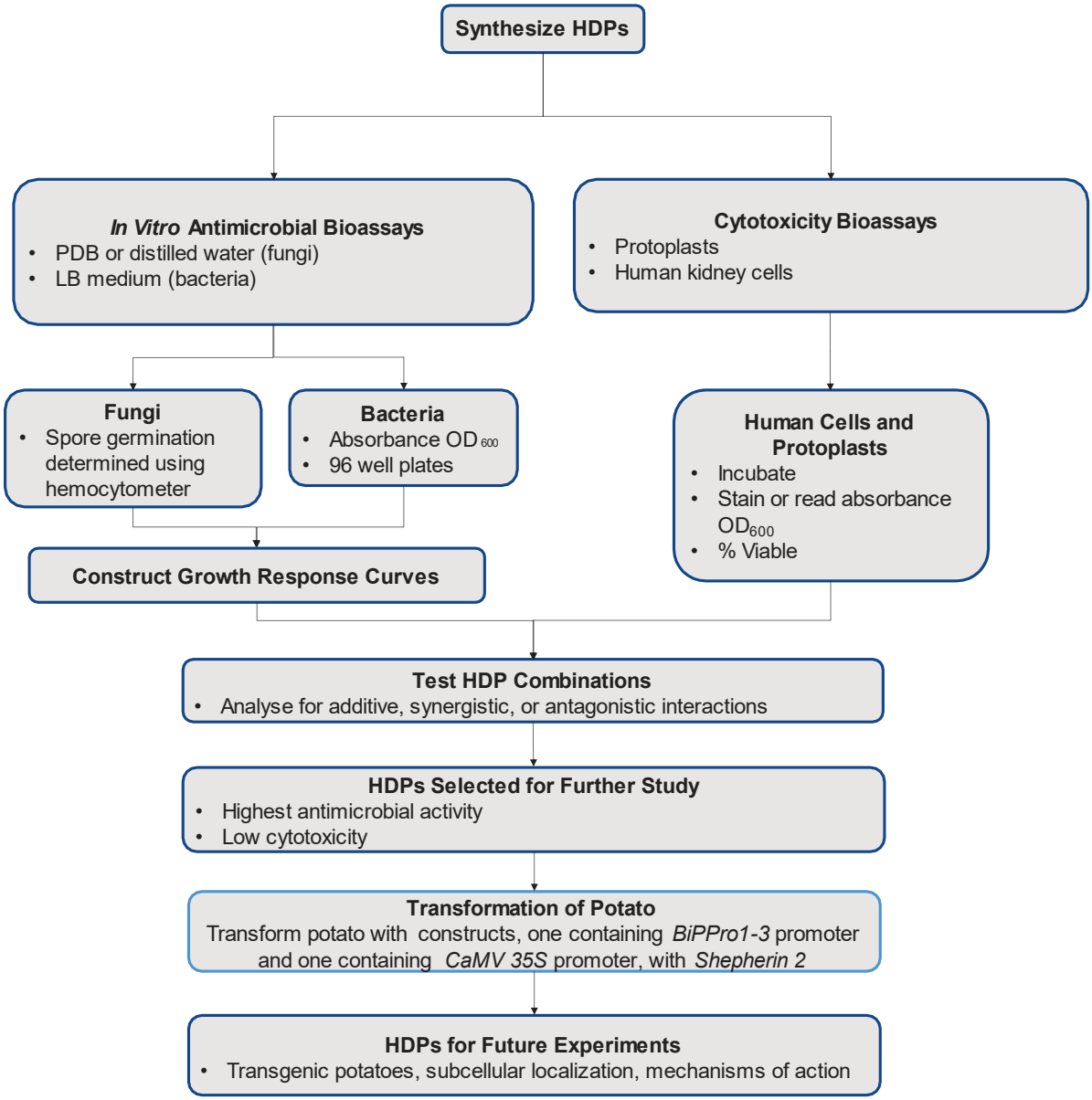

Figure 3. Summary of experimental approach.

2.1 Plant material and growth conditions. Potato plants (*Solanum tuberosum* L. cultivar Desiree) were grown aseptically in 15-cm culture tubes in Murashige and Skoog medium containing 3% sucrose and 0.5% agar at a pH of 5.85. The plant cultures were kept at 24 °C in a 16-hour photoperiod at a 200 μmol/m^2/s light intensity (Yevtushenko et al., 2004; Yevtushenko & Misra, 2007).

2.2 Pathogens. Two fungal species and two bacterial species, all pathogenic to potato, were used in this study. The fungi *Fusarium culmorum*, *Alternaria solani* and the bacterium *P. carotovorum* subsp. *carotovorum* were derived from the Phytopathogen Collection in the Potato Research Laboratory at the University of Lethbridge, whereas *P. carotovorum* subsp. *atrosepticum* was kindly provided by Dr. Jie Feng (The Alberta Plant Health Laboratory, Crop Diversification Centre North, Alberta Agriculture and Forestry, Canada). The *F. culmorum* culture was grown on either oatmeal agar (BD Difco™, Franklin Lakes, NJ, USA) or potato dextrose agar (PDA; BD Difco™) and maintained at room temperature in low light (Yevtushenko & Misra, 2007). The protocol to induce sporulation in the *A. solani* culture, so that the spores could be collected for use in the antimicrobial bioassays, was adapted from Rodrigues et al. (2010) as follows: fungal spores were incubated in liquid V8 medium [18% (v/v) V8® juice and 2 g/L $CaCO_3$] at 28 °C for seven days with gentle shaking and then blended in a sterile blender for 60 seconds at low speed, followed by plating on PDA medium in Petri dishes. The plates, without lids, were placed in a dark chamber under UV light set up for 12-hour UV photoperiods. After the agar and fungal mycelia were fully desiccated (approximately after one week), the plates were covered with lids, sealed and stored at room temperature in low light for 2 months. *F culmorum* culture was transferred to fresh oatmeal agar or potato dextrose agar plates and incubated in low light at room temperature for eleven to fourteen days before the conidia

were collected for use in the antifungal assays. The bacterium *P. atrosepticum* was grown in LB medium for 24 hours at 26 °C on a shaker to mid-logarithmic phase. For long-term storage, the bacterial culture was mixed with an equal volume of 50% sterile glycerol and stored in 100 µL aliquots at -80 °C. The concentration in colony forming units (cfu) was determined by plating serial dilutions of bacterial glycerol stock on LB agar from a one of the stock tubes (Yevtushenko & Misra, 2007).

2.3 Peptides. All peptides were ordered from and synthesized at AnaSpec, Inc. (Fremont, CA, USA) using fmoc solid-phase peptide synthesis; the purity of over 95% for all peptides was confirmed by high performance liquid chromatography (HPLC). Lyophilized peptides were dissolved in sterile, deionized water to stock concentrations of 10 µM, 100 µM, and 1mM, then dispensed into 0.6 mL Eppendorf tubes in 40-µL, 30-µL, and 10-µL aliquots, respectively, and stored at -80 °C.

2.4 Antifungal activity of HDPs. The antifungal activity of the peptides *in vitro* was quantified by observing the number of conidia that were able to germinate in the presence of the peptides. Following a protocol modified from Yevtushenko et al. (2005), *A. solani* conidia were collected aseptically by flooding the desiccated culture plate with 6-9 mL of sterile, deionized water and gently scrubbing the culture with a glass spreader, followed by filtration through a sterile mesh. The conidia were stored at 4 °C for up to three days before being discarded. The conidial suspension was adjusted to 1.5 x 10^5 conidia/mL in sterile, deionized water and dispensed into 15-µL aliquots in glass vials with increasing concentrations of the peptides. The conidial samples were incubated with different peptide concentrations for 24 hours in darkness at room temperature. The protocol for *F. culmorum* was similar to that for *A. solani*, except that the conidia were isolated fresh each day before use and adjusted to a concentration of 2.5 x 10^5

conidia/mL in 50-fold diluted PDB. After the 24-hour incubation, germination of conidia was determined using a haemocytometer and a light microscope. Conidia were considered germinated only if the freshly grown hyphae had reached a length at least three times the length of the conidia because in many cases the conidia would exhibit a very small amount of hyphal germination before the growth ceased when they were incubated with the HDPs . A negative control containing no peptides was included for each experiment to establish conidial germination in the absence of the peptides and to act as a base used to determine the growth inhibition of the fungi (Jacobi et al., 2000). A positive control using sodium dichloroisocyanurate (a known antimicrobial agent) was also included for all peptides and combinations; the Na-dichloroisocyanurate was tested at increasing concentrations using the same protocols as the HDPs. Each experiment was replicated three or four times. Note that for all of the bioassays carried out with peptide combinations, both antimicrobial and cytotoxicity, the concentrations tested were the total of the peptides combined in equal parts. For example, the combinations of two peptides at the 2 μM concentration consisted of 1 μM of each peptide.

2.5 Antibacterial activity of HDPs. The *in vitro* antibacterial assays were based on methods which use absorbance (optical density) of bacterial cultures in microtiter plates as a function of growth, such as the methods employed by Ali & Reddy (2000) and Broekaert et al. (1992). All antibacterial assays were conducted in sterile, 96-well, flat bottom microplates. The bacterial concentration was adjusted to 5 x 10^7 cfu/mL in 75-fold liquid LB medium and dispensed in 100-μL aliquots in plate wells with increasing HDP concentrations. The plates were sealed and incubated in very low light for 24 hours at 25 °C with slow shaking which was increased to a higher speed for the last hour of incubation. The absorbance of the wells was measured at OD_{600} using a FLUOstar Omega microplate reader (BMG Labtech, Ortenberg,

Germany) at the beginning of the incubation and again after the incubation. The net bacterial growth was calculated using the difference between the two absorbance readings. A negative control containing no peptides was included for each experiment to establish bacterial growth in the absence of the peptides and to act as a base used to determine the growth inhibition of the bacteria. A positive control using Na-dichloroisocyanurate was also included for all peptides and combinations; the Na-dichloroisocyanurate was tested at increasing concentrations using the same protocols as the HDPs. Each experiment was replicated three times.

2.6 Phytotoxicity of HDPs. The phytotoxicity bioassays were conducted using freshly isolated potato mesophyll protoplasts. Because of the absence of a cell wall, protoplasts are extremely sensitive to any potential cytotoxicity from the membrane-active HDPs (Yevtushenko et al., 2005). The fully expanded leaves of 4–6-week-old culture grown plants of *Solanum tuberosum* L. cultivar Desiree were used for the isolation of the mesophyll protoplasts using a modified version of the protocol from Yevtushenko & Misra (2007). The leaves were cut crosswise into thin 1-mm strips and incubated on the surface of 6-mL maceration enzyme solution, in a 9-cm Petri dish, for 16–18 hours, at 26 ° C in low light. The maceration enzyme solution consisted of 0.2% (w/v) Onozuka RS (BioWorld, Dublin, OH, USA), 0.6% (w/v) Macerozyme R-10 (BioWorld), 0.2% (w/v) Cellulysin (MilliporeSigma, Burlington, MA, USA), 0.4 M sucrose, 0.1 M L-glycine, 10 mM $CaCl_2$, and 10 mM 2-(N-morpholino) ethanesulfonic acid (MES). Following incubation, 5 mL of 0.5 M sucrose/5 mM $CaCl_2$ solution was added to the leaf digest and the Petri dish was gently shaken for 3 to 4 minutes to release the protoplasts. The protoplast solution was filtered through a 100-µm nylon mesh and transferred into a 15-mL centrifuge tube; after that, 0.5 M sucrose/5 mM $CaCl_2$ solution was added to top up the

protoplast suspension to 12 mL, then 1.5 mL of W5 solution (Medgyesy et al., 1980) was gently layered on top of the suspension so that it formed a clear top layer.

The protoplasts were centrifuged for 10 minutes at 500× *g* with a 1-minute acceleration/deceleration using Eppendorf 5810R centrifuge (Eppendorf, Hamburg, Germany). The viable protoplasts, which formed dark-green band at the solution interphase, were transferred to a centrifuge tube containing 11 mL of W5 washing solution and centrifuged for 4 minutes at 400× *g* with a 1-minute acceleration/deceleration. The supernatant was discarded (Yevtushenko & Misra, 2007) and 11 mL of modified SW medium (Sidorov et al., 1987; Appendix A) was added to the protoplasts and allowed to sit for a 1-minute wash. When the purified protoplasts settled to the bottom of the tube, the SW supernatant was carefully removed and discarded. Four milliliters of fresh SW medium were added to the pellet and gently resuspended. The protoplast suspension was then dispensed in 25 µL drops onto petri plates with increasing concentrations of the HDPs. Then the plates were sealed and incubated for 24 hours in low light at 24 °C with a 16-hour photoperiod. After incubation, 0.5 µL of neutral red (0.1% in 0.7 M sorbitol) (stains the vacuoles of living cells) or 0.5 µL of Evan's blue (0.5% in 0.7 M sorbitol) (stains dead cells) was added to each droplet of protoplast suspension and allowed to sit for one hour to allow time for the stain to diffuse throughout the suspension. The suspensions were viewed under an inverted light microscope and the percentage of viable protoplasts was estimated (Yevtushenko & Misra, 2007) via visual inspection by viewing the entire sample (a 25 µL droplet) under the microscope, left to right, and moving down until the entire sample had been viewed. The staining provided the main indicator of living vs. dead protoplasts; however, other visual indicators such as roundness, bright green chloroplasts, or how many cellular debris were present in the sample were also taken into consideration when estimating viability.

2.7 Cytotoxicity of HDPs. For the human cell cytotoxicity assays, the HEK293 human cell line was utilized to test the cytotoxicity of the HDPs towards mammalian cells *in vitro* similarly to Broekaert et al. (1992) because they are simple to grow and maintain, and they are readily available. First, the cell culture was grown from frozen stock kindly provided by Dr. I. Kovalchuk (University of Lethbridge, AB, Canada). Cells were collected from storage medium by centrifugation, resuspended in plates in growth medium [Minimum essential medium Eagle (Sigma Life Science) supplemented with 10% fetal bovine serum (FBS) (Sigma Life Science) and 292 mg/L L-glutamine], then incubated for four days (until 95% confluency was reached) at 37 °C and 6% CO_2. The cells were then harvested by removing liquid medium and adding 2 mL Trypsin-EDTA to the culture plates and incubating for 3 to 4 min before adding the cell suspension to 6 mL of fresh growth medium. A cell counter (Luna-II™ Automated Cell Counter) was used to determine the cell concentration: the culture was adjusted to a concentration of 10^4 cells/mL, dispensed into 96-well plates in 100-µL aliquots, and placed back into the incubator. After one day, the medium was removed and the prepared medium-peptide solutions were added to the cells and incubated for 24 hrs after which the MTT (tetrazolium salt) assay (Ab211091-MTT Cell Proliferation kit, Abcam, Cambridge, UK) was applied. The absorbance of the wells was measured at OD_{600} using a FLUOstar Omega microplate reader (BMG Labtech) at the beginning and after the incubation. The net cell growth was calculated using the difference between the two absorbance readings. A negative control containing no peptides was included for each experiment to establish cell growth in the absence of the peptides and to act as a baseline to determine the growth inhibition of the HEK cells. A control which contained the medium without cells was included as well. Additional control contained the medium with cells

and 10 μL of sterile deionized water (which corresponded to the volume of the dissolved peptide used in the test samples). Each experiment was replicated three times.

2.8 Vector construction. Two plant transformation vectors designed to express transgenes under the control of of the *PmBiPPro1-3* promoter, which is the 1259 bp truncated version of the full-length *PmBiPPro1* promoter (Yevtushenko and Misra, 2018), were constructed: PmBiPPro1-3/m-GFP5-ER contained the gene encoding the green fluorescent protein m-GFP5-ER, whereas PmBiPPro1-3/Shepherin2 contained the gene encoding HDP Shepherin 2 because it was found to have the highest antimicrobial activity in this study.

To make PmBiPPro1-3/m-GFP5-ER, the *Hin*dIII/XbaI DNA fragment containing the *PmBiPPro1-3* promoter was ligated into the corresponding sites of the plasmid pBI121 (Jefferson et al., 1987) in place of the deleted 35S promoter. The intermediate *PmBiPPro1-3/GUS* plasmid was cloned and digested with *XbaI* and *Sac*I to release the *β-glucuronidase (GUS)* gene, and the *Xba*I/*Sac*I DNA fragment containing the *m-GFP5-ER* gene was ligated into the corresponding sites of the plasmid in place of the deleted *GUS* sequence. All ligations were performed using T4 DNA ligase, following the New England Biolabs protocol (New England Biolabs, Ipswich, MA, USA). The resulting PmBiPPro1-3/m-GFP5-ER vector was maintained in DH5α *E. coli* cells, and the correct promoter-transgene insertion and their DNA sequences were confirmed by the restriction analyses and DNA sequences (Genewiz, South Plainfield, NJ, USA). It should be noted that the *m-GFP5-ER* region also contains an N-terminal signal peptide sequence from *Arabidopsis thaliana* basic chitinase and a C-terminal HDEL sequence for the retention of GFP in the endoplasmic reticulum (ER), which allows for the safe accumulation of GFP at high levels.

To make PmBiPPro1-3/Shepherin2, the *Shepherin 2* coding sequence was synthesized by Azenta (South Plainfield, NJ, USA) within the pUC19 vector. The *Shepherin 2*-contaning vector was digested with *Xba*I and *Sac*I, and the HDP-coding region was ligated into the corresponding sites of the plasmid PmBiPPro1-3/m-GFP5-ER in place of the deleted *m-GFP5-ER* sequence. *E. coli* colonies containing the *PmBiPPro1-3/ Shepherin2* constructs were identified by conventional PCR, and the whole plasmid sequencing was performed by Plasmidsaurus (Eugene, OR, USA) to verify the correct ligation and nucleotide sequences of the promotor-transgene region.

2.9 Transformation, selection, and regeneration of plants. The plant transformation vectors were introduced into electrocompetent *A. tumefaciens* LBA4404 cells (Takara Inc., San Jose, CA, USA) according to a modified protocol from the cell manufacturer. Briefly, 1 ng of plasmid DNA was added to 20 µL of cold competent cells, gently mixed, added to a chilled electroporation cuvette, and subjected to 2.25 kV electric pulse in an Eppendorf Electroporator 2510 (Eppendorf). Immediately, 1 mL of SOC media (20 g/L tryptone, 5 g/L yeast extract, 0.5 g/L NaCl, 20 mL/L glucose (1 M stock solution), and 5 mL/L $MgCl_2$ (2 M stock solution) at pH 7) was added to the cells. The cells were transferred to tubes and incubated for 1 hour at 28 °C with shaking (100 rpm). The cells were then plated, in both 50 µL and 100 µL aliquots, on LB agar plates containing selective antibiotics—100 mg/L kanamycin, 100 mg/L streptomycin, and 100 mg/L rifampicin,—and incubated for 36 hours at 28 °C in low light. Several individual colonies were picked and incubated in liquid LB containing 100 mg/L of each kanamycin, streptomycin, and rifampicin in low light at 28 °C and 230 rpm to mid-log phase (OD_{600} = 1). Plasmid DNA was isolated from each of the selected cell clones (i.e., grown cell suspensions) using GeneJET Plasmid Miniprep (Thermo Scientific). Restriction analyses of plasmid DNA

were performed to verify the presence of the desired DNA constructs in the selected *Agrobacterium* clones. The *Agrobacterium* clones that revealed the brightest indicative DNA bands during agarose gel electrophoreses were used for plant transformation.

Plant transformation was performed according to the protocol described in Yevtushenko et al. (2005). The *Agrobacterium* cultures, harbouring one of the plant transformation vectors, were grown for 1–2 d at 26–28 °C on a rotary shaker at 225 rpm to mid-log phase (OD600=1) in 15 ml liquid LB medium supplemented with 100 mg/L kanamycin, 100 mg/L streptomycin, and 100 mg/L rifampicin. The bacterial cells were collected using centrifugation for 10 min at 2000 *g* and then resuspended in liquid PetM containing MS basal salt mixture M524 (Phytotech Labs), 1 mL/L Gamborg vitamin solution (1000x) (Phytotech Labs), 40 mg/L adenine SO_4, 20 g/L glucose, 20 g/L mannitol, 900 mg/L MES, 0.25 mg/L gibberellic acid (GA_3), 0.1 mg/L 1-naphthalenacetic acid (NAA), and 1 mg/L zeatin riboside (ZR), at pH 5.7. Then 4 mL of this bacterial suspension was added to each plate of explants. The explants were the internodal stems and petioles of 4- to 6-week-old potato plants grown *in vitro,* which had been precultured in liquid PetM for two days at 24 °C in low light. Following the addition of the *Agrobacteria*, the explants were incubated for one hour at 27 °C and 60 rpm in low light. The explants were then thoroughly blotted on sterile filter paper and placed onto plates containing solid PetM (0.38% (w/v) agarose) and incubated at 24 °C in low light for 5 days. The infected explants were then washed in 20 mL of liquid PetM containing 500 mg/L cefotaxime for one hour at room temperature at 60 rpm and then placed onto plates with selective PetM containing 50 mg/L kanamycin and 500 mg/L cefotaxime (500 mg/L carbenicillin was included for the PmBiPPro1-3/m-GFP5-ER plant transformations). The plates were placed in a growth chamber set at 24 °C with a 16-hour photoperiod (200 µmol/m^2/s); they were covered by a single layer of white paper

towel to reduce the light intensity. The explants were transferred to fresh PetM medium every three weeks. Once the calluses formed and grew shoots, the shoots were excised and rooted in hormone-free MS medium (see Plant material and growth conditions) supplemented with 20 mg/L kanamycin and 400 mg/L cefotaxime (500 mg/L carbenicillin was included for the PmBiPPro1-3/m-GFP55-ER plants). The plants were subcultured every 2 to 3 months; after the third time they were subcultured, the antibiotics were no longer added to the MS medium.

2.10 PCR analysis of transgenic plants. PCR analysis was used to confirm the successful integration of the *gfp* gene in the potato genome. Plant DNA was isolated from culture grown potato plant leaves using a DNeasy Plant Pro kit (Qiagen, USA). PCR was carried out in 25 µL reaction mixtures consisting of 140 ng plant DNA, 6.25 µL All Taq Mastermix (Qiagen, USA), and 0.25 µM gene-specific DNA primers. The PCR was run using the following parameters: 94 °C for 3 minutes; 35 cycles of 94 °C for 30 seconds, 57 °C for 30 seconds, and 72° for 1 minute; followed by 72 °C for 10 minutes. The DNA primers used to amplify the gfp gene (816 bp) were: 21 mer forward primer, 5'-ATG AAG ACT AAT CTT TTT CTC-3', and 21-mer reverse primer, 5'-TTA AAG CTC ATC ATG TTT GTA-3'.

2.11 Transient transformation of tobacco plants. To confirm the transcriptional activity of the *Douglas-fir* promoter, the *Agrobacterium* cells containing the PmBiPPro1-3/m-GFP5-ER gene construct were grown in liquid LB medium until an absorbance of 0.1 to 0.2 (OD_{600}) was reached. The bacterial cells were collected by centrifugation and resuspended in infiltration buffer containing 2 mM $Na_3(PO_4)$, 50 mM MES, 20 mM acetosyringone in Dimethyl sulfoxide (DMSO), and 50 g/L glucose. Using the buffer, the bacteria was diluted five-fold and was then adjusted to absorbance 0.05 (OD_{600}). Using a sterile syringe, the leaves of fully grown greenhouse *Nicotiana tabacum* (tobacco) plants were inoculated. For this procedure, a leaf was

wrapped around the index finger and the syringe was pressed gently but firmly against the abaxial surface of the leaf while the plunger was slowly depressed. Note that the bacterial suspension should be visible as it enters the extracellular space in the leaf (the leaf darkens). After 2 to 4 days, green fluorescence in inoculated leaves was observed under a fluorescence microscope.

2.12 Analysis of data. For all assays, percent inhibition or percent cytotoxicity was calculated using the following formula: [(untreated control-treated sample)/untreated control]x100 with the net fungal growth based on the percentage of germinated conidia, bacterial or human cell net growth based on OD_{600} readings, and protoplast viability percentage was based on observed estimations of living protoplasts stained with either Evan's blue or neutral red dye (Ali & Reddy, 2000; Rongai et al., 2015). For each of the peptides or peptide combinations, dose response curves were graphed in Excel, and for each combination an expected value for percent inhibition was calculated using the Abbott formula: Expected inhibition = $x+y-(xy/100)$ was used for peptide combinations of two and Expected inhibition = $x+y+z-[(xy+xz+yz)/100]+(xyz/10\ 000)$ was used for combinations of three peptides where x, y, and z are the observed percent inhibition values for each single peptide treatment for that pathogen. For example, the observed growth inhibition of *F. culmorum* at 4 µM for Shepherin 2 was 32% and for Skh-AMP1 was 3%, so the equation would be: expected inhibition = 32+3–(32 x 3/100) = 34. This would mean that the expected inhibition for Shepherin 2 combined with Skh-AMP1 at 4 µM [2 µM of each (2:2)] is 34% (Abbott, 1925; Ali & Reddy, 2000; Graser et al., 2017).

3. Results

3.1 Antimicrobial activity of the HDPs *in vitro*

The antimicrobial activity of Shepherin 2, Skh-AMP1, Cn-AMP1, and Cr-ACP1 was evaluated *in vitro* to provide initial information on the possible disease resistance that they may provide *in planta*. The peptides were tested against the phytopathogens *F. culmorum*, *A. solani*, *P. carotovorum*, and *P. atrosepticum,* using increasing peptide concentrations. The results obtained after a 24-hour incubation period were used to construct dose-response curves for each peptide-pathogen combination.

3.1.1 *Fusarium culmorum.* Shepherin 2 was the only effective single peptide against *Fusarium culmorum*. It exhibited 87% growth inhibition at 8 μM and 98% at 16 μM, inhibition remained over 95% for all remaining concentrations (Fig. 4 & Table 1). The curve derived IC50, the half maximal inhibitory concentration, was 5 μM, and the MIC, the minimum inhibitory concentration defined as growth inhibition of 95% or over, was 10 μM.

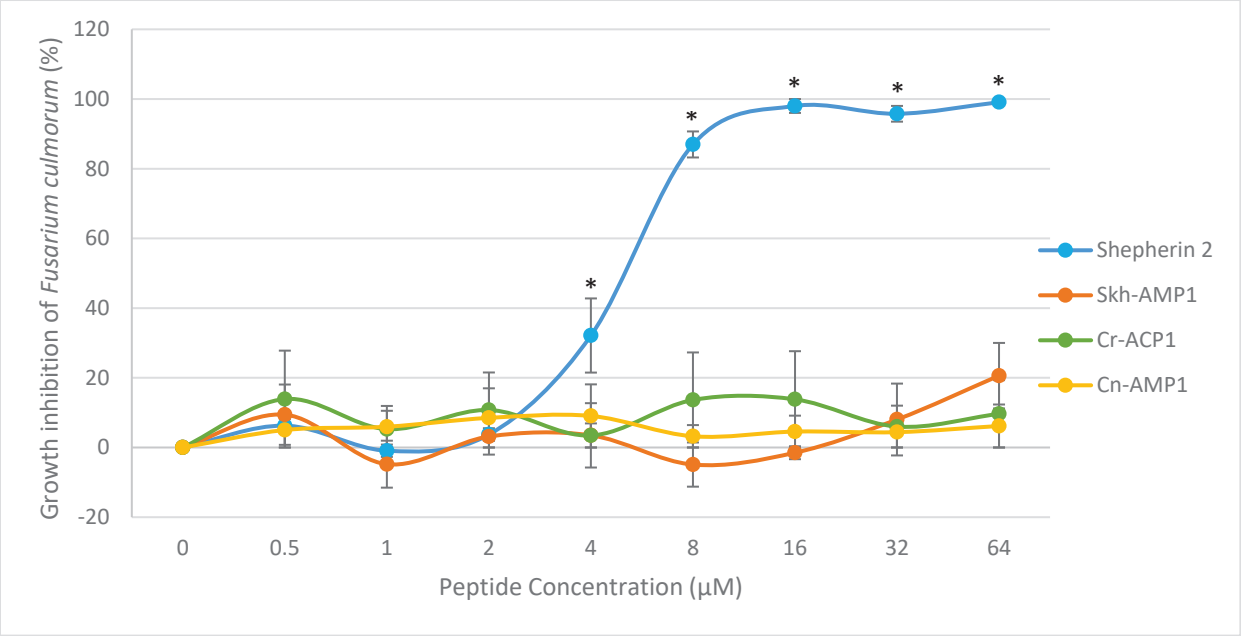

Figure 4 Effect of Shepherin 2, Skh-AMP1, Cr-ACP1, and Cn-AMP1 *in vitro* on the germination of *Fusarium culmorum* after 24 hr of incubation. Values are the means of three separate experiments; bars are the standard errors; asterisk (*) denotes a statistically significant difference compared to the no peptide control ($p \leq 0.05$) as determined by single factor ANOVA followed by Dunnett's test.

Table 1 Effect of Shepherin 2 on inhibiting the growth of *Fusarium culmorum in vitro*

Growth Inhibition of *Fusarium culmorum*	
Shepherin 2 Concentration (µM)	**Observed Inhibition (%)**
0.5	6 ± 1.90[b]
1	-1 ± 1.77
2	4 ± 1.82
4	32* ± 10.64[a]
8	87* ± 3.73
16	98* ± 1.99
32	96* ± 2.26
64	99* ± 0.58

[a] Means followed by an asterisk (*) are significantly different from the no peptide control at $P \leq 0.05$. [b] The values after ± are the standard errors of means.

The other three peptides achieved negligible levels of growth inhibition against *F. culmorum* (Fig. 4, Tables 2-4). The positive control, which tested the known antimicrobial agent Na-dichloroisocyanurate, displayed a dose response like that achieved with Shepherin 2 except at much higher concentrations, reaching 43% inhibition at 300 μM and 99% at 450 μM. The latter suggested that Shepherin 2 had significantly greater antimicrobial activity against *F. culmorum* than even positive control (Na-dichloroisocyanurate).

Table 2 Effect of Skh-AMP1 on inhibiting the growth of *Fusarium culmorum in vitro*

Growth Inhibition of *Fusarium culmorum*	
Skh-AMP1 Concentration (μM)	**Observed Inhibition (%)**
0.5	9 ± 8.66[a]
1	-5 ± 6.74
2	3 ± 5.19
4	3 ± 9.23
8	-5 ± 6.34
16	-1 ± 1.85
32	8 ± 10.31
64	21 ± 9.40

[a] The mean value ± standard error.

Table 3 Effect of Cn-AMP1 on inhibiting the growth of *Fusarium culmorum in vitro*

Growth Inhibition of *Fusarium culmorum*	
Cn-AMP1 Concentration (μM)	**Observed Inhibition (%)**
0.5	-9 ± 5.02[a]
1	5 ± 5.96
2	-15 ± 8.49
4	1 ± 9.06
8	-8 ± 3.22
16	-7 ± 4.57
32	-6 ± 4.40
64	-6 ± 6.17

[a] The mean value ± standard error.

Table 4 Effect of Cr-ACP1 on inhibiting the growth of *Fusarium culmorum in vitro*

Growth Inhibition of *Fusarium culmorum*	
Cr-ACP1 Concentration (μM)	**Observed Inhibition (%)**
0.5	19 ± 13.90[a]
1	7 ± 5.27
2	14 ± 10.76
4	4 ± 3.46
8	34 ± 13.64
16	16 ± 13.82
32	7 ± 6.00
64	12 ± 9.66

[a] The mean value ± standard error.

The peptides were combined in pairs to evaluate their interactions for possible synergistic, antagonistic, or additive effects on conidia germination. The highest growth inhibition was achieved with the combination of Shepherin 2 and Cn-AMP1 with an inhibition of 37% at 16 μM at which point inhibition went back down, indicating a narrow range of activity (Fig. 5) The expected inhibition for this peptide combination, as determined by Abbott's formula (Abbott, 1925), was 98% which indicated an antagonistic interaction occurred between these two peptides (Table 6). The other combination which displayed a significant level of inhibition was Shepherin 2 and Skh-AMP1, which achieved growth inhibition of 27% at 32 μM and rose to 32% at 64 μM (Table 5). Because the expected inhibition for these combinations was 96% and 99% respectively, the interaction that took place between these two peptides was defined as antagonistic. The other peptide combinations produced no significant inhibition of *F. culmorum.* (Tables 7–10).

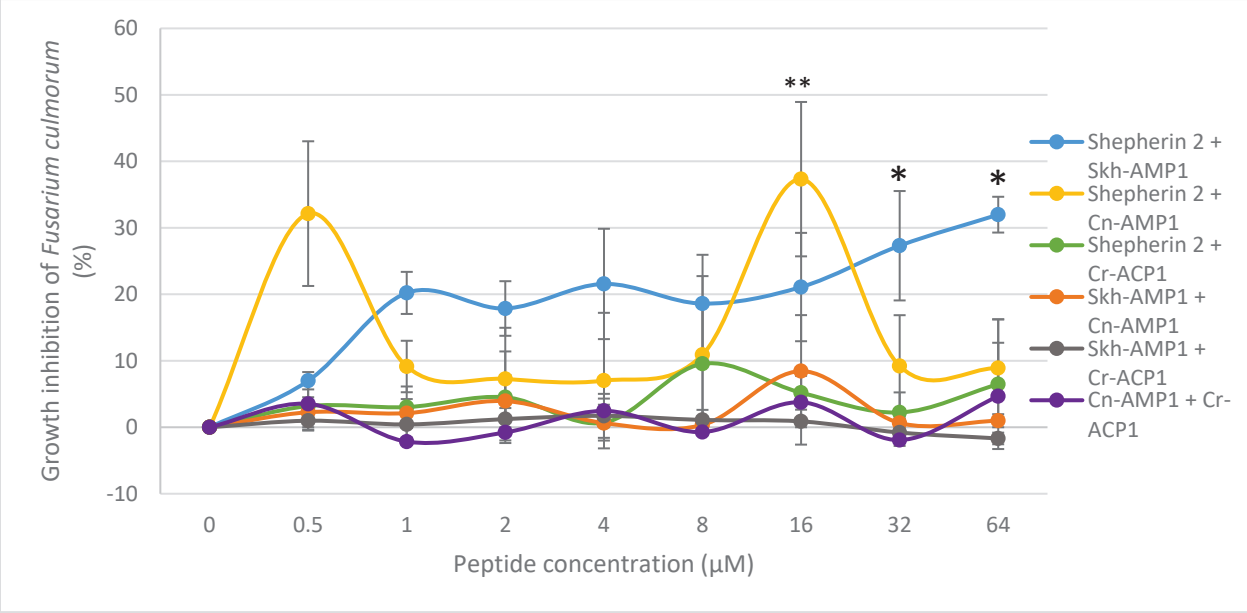

Figure 5 Effect of Shepherin 2, Skh-AMP1, Cr-ACP1, and Cn-AMP1 in combinations of two (1:1) *in vitro* on the germination of *Fusarium culmorum* after 24 hr of incubation. Values are the means of three separate experiments; bars are the standard errors; asterisk (*) denotes a statistically significant difference compared to the no peptide control ($p \leq 0.05$) as determined by single factor ANOVA followed by Dunnett's test. Double asterisk denotes statistical significance indicated by the Dunnett's test which was not indicated in the ANOVA results.

Table 5 Effect and interaction of Shepherin 2 combined with Skh-AMP1 on inhibiting germination of *Fusarium culmorum in vitro*

Growth inhibition *Fusarium culmorum*			
Peptide Concentrations (µM)	**Observed (%)**	**Expected (%)** [b]	**Interaction**[c]
Shepherin 2:Skh-AMP1 (0.25:0.25)	7 ± 1.31[d]	14	N/A
Shepherin 2:Skh-AMP1 (0.5:0.5)	20 ± 3.17	-6	N/A
Shepherin 2:Skh-AMP1 (1:1)	18 ± 4.11	7	N/A
Shepherin 2:Skh-AMP1 (2:2)	22 ± 8.30	34	N/A
Shepherin 2:Skh-AMP1 (4:4)	19 ± 7.34	86	N/A
Shepherin 2:Skh-AMP1 (8:8)	21 ± 8.15	98	N/A
Shepherin 2:Skh-AMP1 (16:16)	27* ± 8.23[a]	96	-
Shepherin 2:Skh-AMP1 (32:32)	32* ± 2.69	99	-

[a] Means followed by an asterisk (*) are significantly different from the no peptide control at $P \leq 0.05$. [b] Expected inhibition in growth was calculated using the Abbott formula: $I_{exp} = x + y - (xy/100)$ (Abbott, 1925), where x and y are the observed percent inhibition values for each corresponding single peptide treatment for *F. culmorum* (Table 1-2). [c] Interactions are considered synergistic (+) if the I_{exp} is lower than the I_{obs}, antagonistic (-) if I_{exp} is higher than I_{obs}, and additive (=) if they are equal (Kosman & Cohen, 1996). [d] The mean value ± standard error.

Table 6 Effect and interaction of Shepherin 2 combined with Cn-AMP1 on inhibiting germination of *Fusarium culmorum in vitro*

Growth inhibition *Fusarium culmorum*			
Peptide Concentrations (µM)	**Observed (%)**	**Expected (%)[b]**	**Interaction[c]**
Shepherin 2:Cn-AMP1 (0.25:0.25)	32 ± 10.88[d]	-2	N/A
Shepherin 2:Cn-AMP1 (0.5:0.5)	9 ± 3.87	4	N/A
Shepherin 2:Cn-AMP1 (1:1)	7 ± 7.69	-11	N/A
Shepherin 2:Cn-AMP1 (2:2)	7 ± 10.20	33	N/A
Shepherin 2:Cn-AMP1 (4:4)	11 ± 11.82	86	N/A
Shepherin 2:Cn-AMP1 (8:8)	37* ± 11.61[a]	98	-
Shepherin 2:Cn-AMP1 (16:16)	9 ± 7.64	96	N/A
Shepherin 2:Cn-AMP1 (32:32)	9 ± 7.32	99	N/A

[a] Means followed by an asterisk (*) are significantly different from the no peptide control at P≤0.05. [b] Expected inhibition in growth was calculated using the Abbott formula*:* $I_{exp} = x + y - (xy/100)$ (Abbott, 1925), where *x* and *y* are the observed percent inhibition values for each corresponding single peptide treatment for *F. culmorum* (Table 1 and 3). [c] Interactions are considered synergistic (+) if the I_{exp} is lower than the I_{obs}, antagonistic (-) if I_{exp} is higher than I_{obs}, and additive (=) if they are equal (Kosman & Cohen, 1996). [d] The mean value ± standard error.

Table 7 Effect and interaction of Shepherin 2 combined with Cr-ACP1 on inhibiting germination of *Fusarium culmorum in vitro*

Growth inhibition *Fusarium culmorum*			
Peptide Concentrations (µM)	**Observed (%)**	**Expected (%)[a]**	**Interaction[b]**
Shepherin 2:Cr-ACP1 (0.25:0.25)	3 ± 3.68[c]	24	N/A
Shepherin 2:Cr-ACP1 (0.5:0.5)	3 ± 3.10	6	N/A
Shepherin 2:Cr-ACP1 (1:1)	5 ± 6.89	17	N/A
Shepherin 2:Cr-ACP1 (2:2)	1 ± 2.7	35	N/A
Shepherin 2:Cr-ACP1 (4:4)	10 ± 8.83	91	N/A
Shepherin 2:Cr-ACP1 (8:8)	5 ± 2.55	98	N/A
Shepherin 2:Cr-ACP1 (16:16)	2 ± 3.02	96	N/A
Shepherin 2:Cr-ACP1 (32:32)	6 ± 9.76	99	N/A

[a] Expected inhibition in growth was calculated using the Abbott formula*:* $I_{exp} = x + y - (xy/100)$ (Abbott, 1925), where *x* and *y* are the observed percent inhibition values for each corresponding single peptide treatment for *F. culmorum* (Table 1 and 4). [b] Interactions are considered synergistic (+) if the I_{exp} is lower than the I_{obs} , antagonistic (-) if I_{exp} is higher than I_{obs}, and additive (=) if they are equal (Kosman & Cohen, 1996). [c] The mean value ± standard error.

Table 8 Effect and interaction of Skh-AMP1 combined with Cn-AMP1 on inhibiting germination of *Fusarium culmorum in vitro*

Growth inhibition *Fusarium culmorum*			
Peptide Concentrations (µM)	**Observed (%)**	**Expected (%)[a]**	**Interaction[b]**
Skh-AMP1:Cn-AMP1 (0.25:0.25)	-4 ± 2.26[c]	1	N/A
Skh-AMP1:Cn-AMP1 (0.5:0.5)	-7 ± 2.12	0	N/A
Skh-AMP1:Cn-AMP1 (1:1)	-6 ± 3.93	-12	N/A
Skh-AMP1:Cn-AMP1 (2:2)	-5 ± 0.63	4	N/A
Skh-AMP1:Cn-AMP1 (4:4)	-2 ± 0.35	-13	N/A
Skh-AMP1:Cn-AMP1 (8:8)	2 ± 8.43	-8	N/A
Skh-AMP1:Cn-AMP1 (16:16)	-5 ± 0.65	2	N/A
Skh-AMP1:Cn-AMP1 (32:32)	-9 ± 0.98	16	N/A

[a] Expected inhibition in growth was calculated using the Abbott formula*:* $I_{exp} = x + y - (xy/100)$ (Abbott, 1925), where *x* and *y* are the observed percent inhibition values for each corresponding single peptide treatment for *F. culmorum* (Table 2-3). [b] Interactions are considered synergistic (+) if the I_{exp} is lower than the I_{obs} , antagonistic (-) if I_{exp} is higher than I_{obs}, and additive (=) if they are equal (Kosman & Cohen, 1996). [c] The mean value ± standard error.

Table 9 Effect and interaction of Skh-AMP1 combined with Cr-ACP1 on inhibiting germination of *Fusarium culmorum in vitro*

Growth inhibition *Fusarium culmorum*			
Peptide Concentrations (µM)	**Observed (%)**	**Expected (%)[a]**	**Interaction[b]**
Skh-AMP1:Cr-ACP1 (0.25:0.25)	1 ± 1.34[c]	26	N/A
Skh-AMP1:Cr-ACP1 (0.5:0.5)	0 ± 1.96	2	N/A
Skh-AMP1:Cr-ACP1 (1:1)	1 ± 3.21	17	N/A
Skh-AMP1:Cr-ACP1 (2:2)	2 ± 3.31	7	N/A
Skh-AMP1:Cr-ACP1 (4:4)	1 ± 1.52	31	N/A
Skh-AMP1:Cr-ACP1 (8:8)	1 ± 3.49	15	N/A
Skh-AMP1:Cr-ACP1 (16:16)	-1 ± 2.02	14	N/A
Skh-AMP1:Cr-ACP1 (32:32)	-2 ± 0.88	30	N/A

[a] Expected inhibition in growth was calculated using the Abbott formula*:* $I_{exp} = x + y - (xy/100)$ (Abbott, 1925), where *x* and *y* are the observed percent inhibition values for each corresponding single peptide treatment for *F. culmorum* (Table 2 and 4). [b] Interactions are considered synergistic (+) if the I_{exp} is lower than the I_{obs} , antagonistic (-) if I_{exp} is higher than I_{obs}, and additive (=) if they are equal (Kosman & Cohen, 1996). [c] The mean value ± standard error.

Table 10 Effect and interaction of Cn-AMP1 combined with Cr-ACP1 on inhibiting germination of *Fusarium culmorum in vitro*

Growth inhibition *Fusarium culmorum*			
Peptide Concentrations (µM)	**Observed (%)**	**Expected (%)[a]**	**Interaction[b]**
Cn-AMP1:Cr-ACP1 (0.25:0.25)	4 ± 3.28[c]	12	N/A
Cn-AMP1:Cr-ACP1 (0.5:0.5)	-2 ± 3.10	12	N/A
Cn-AMP1:Cr-ACP1 (1:1)	-1 ± 3.67	1	N/A
Cn-AMP1:Cr-ACP1 (2:2)	2 ± 1.85	5	N/A
Cn-AMP1:Cr-ACP1 (4:4)	-1 ± 1.44	29	N/A
Cn-AMP1:Cr-ACP1 (8:8)	4 ± 4.04	10	N/A
Cn-AMP1:Cr-ACP1 (16:16)	-2 ± 2.48	2	N/A
Cn-AMP1:Cr-ACP1 (32:32)	5 ± 8.03	7	N/A

[a] Expected inhibition in growth was calculated using the Abbott formula*: $I_{exp} = x + y - (xy/100)$* (Abbott, 1925), where *x* and *y* are the observed percent inhibition values for each corresponding single peptide treatment for *F. culmorum* (Table 3-4). [b] Interactions are considered synergistic (+) if the I_{exp} is lower than the I_{obs} , antagonistic (-) if I_{exp} is higher than I_{obs}, and additive (=) if they are equal (Kosman & Cohen, 1996). [c] The mean value ± standard error.

There was no significant inhibition found with the triple peptide combinations (Fig. 6).

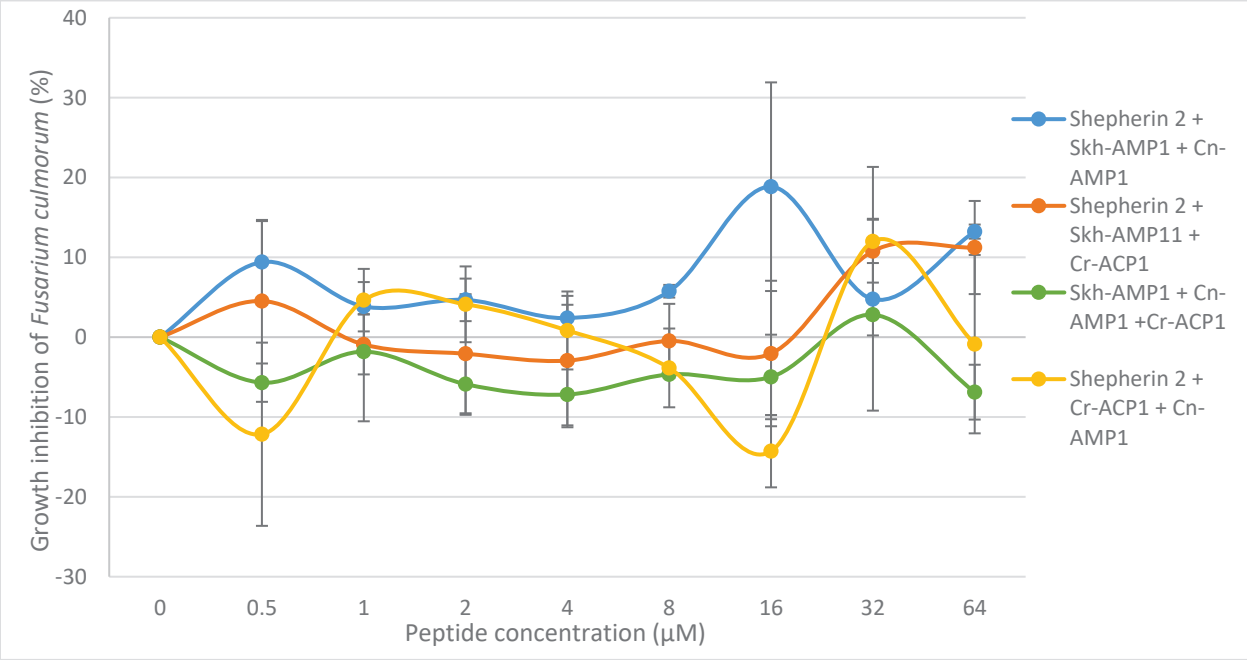

Figure 6 Effect of Shepherin 2, Skh-AMP1, Cr-ACP1, and Cn-AMP1 in combinations of three (1:1:1) *in vitro* on the germination of *Fusarium culmorum* after 24 hr of incubation. Values are the means of three separate experiments; bars are the standard errors. No statistical significance between the percent growth inhibition value and the no peptide control value ($p \leq 0.05$) as determined by single factor ANOVA followed by Dunnett's test.

Table 11 Effect and interaction of Shepherin 2 combined with Skh-AMP1 and Cn-AMP1 on inhibiting germination of *Fusarium culmorum in vitro*

Growth inhibition *Fusarium culmorum*			
Peptide Concentrations (µM)	**Observed (%)**	**Expected (%)[a]**	**Interaction[b]**
Shepherin 2:Skh-AMP1:Cn-AMP1 (0.17:0.17:0.17)	9 ± 5.28[c]	7	N/A
Shepherin 2:Skh-AMP1:Cn-AMP1 (033:0.33:0.33)	4 ± 0.95	-1	N/A
Shepherin 2:Skh-AMP1:Cn-AMP1 (0.67:0.67:0.67)	5 ± 2.66	-7	N/A
Shepherin 2:Skh-AMP1:Cn-AMP1 (1.33:1.33:1.33)	2 ± 1.66	35	N/A
Shepherin 2:Skh-AMP1:Cn-AMP1 (2.67:2.67:2.67)	6 ± 0.79	85	N/A
Shepherin 2:Skh-AMP1:Cn-AMP1 (5.33:5.33:5.33)	19 ± 13.06	98	N/A
Shepherin 2:Skh-AMP1:Cn-AMP1 (10.67:10.67:10.67)	5 ± 4.53	96	N/A
Shepherin 2:Skh-AMP1:Cn-AMP1 (21.33:21.33:21.33)	13 ± 0.88	99	N/A

[a] Expected inhibition in growth was calculated using the Abbott formula*: $I_{exp} = x + y + z - [(xy + xz + yz)/100] + (xyz/10\,000)$* (Abbott, 1925), where *x, y,* and *z* are the observed percent inhibition values for each corresponding single peptide treatment for *F. culmorum* (Table 1-3).[b] Interactions are considered synergistic (+) if the I_{exp} is lower than the I_{obs} , antagonistic (-) if I_{exp} is higher than I_{obs}, and additive (=) if they are equal (Kosman & Cohen, 1996). [c] The mean value ± standard error.

Table 12 Effect and interaction of Shepherin 2 combined with Skh-AMP1 and Cr-ACP1 on inhibiting germination of *Fusarium culmorum in vitro*

Growth inhibition *Fusarium culmorum*			
Peptide Concentrations (µM)	**Observed (%)**	**Expected (%)[a]**	**Interaction[b]**
Shepherin 2:Skh-AMP1:Cr-ACP1 (0.17:0.17:0.17)	5 ± 10.02[c]	32	N/A
Shepherin 2:Skh-AMP1:Cr-ACP1 (033:0.33:0.33)	-1 ± 3.75	1	N/A
Shepherin 2:Skh-AMP1:Cr-ACP1 (0.67:0.67:0.67)	-2 ± 7.46	20	N/A
Shepherin 2:Skh-AMP1:Cr-ACP1 (1.33:1.33:1.33)	-3 ± 8.11	37	N/A

Shepherin 2:Skh-AMP1:Cr-ACP1 (2.67:2.67:2.67)	0 ± 4.65	91	N/A
Shepherin 2:Skh-AMP1:Cr-ACP1 (5.33:5.33:5.33)	-2 ± 9.11	98	N/A
Shepherin 2:Skh-AMP1:Cr-ACP1 (10.67:10.67:10.67)	11 ± 3.94	97	N/A
Shepherin 2:Skh-AMP1:Cr-ACP1 (21.33:21.33:21.33)	11 ± 5.83	99	N/A

[a] Expected inhibition in growth was calculated using the Abbott formula*: $I_{exp} = x + y + z – [(xy + xz + yz)/100] + (xyz/10\ 000)$* (Abbott, 1925), where *x, y,* and *z* are the observed percent inhibition values for each corresponding single peptide treatment for *F. culmorum* (Table 1, 2 and 4).[b] Interactions are considered synergistic (+) if the I_{exp} is lower than the I_{obs} , antagonistic (-) if I_{exp} is higher than I_{obs}, and additive (=) if they are equal (Kosman & Cohen, 1996). [c] The mean value ± standard error.

Table 13 Effect and interaction of Skh-AMP1 combined with Cn-AMP1 and Cr-ACP1 on inhibiting germination of *Fusarium culmorum in vitro*

Growth inhibition *Fusarium culmorum*			
Peptide Concentrations (µM)	**Observed (%)**	**Expected (%)[a]**	**Interaction[b]**
Skh-AMP1:Cn-AMP1:Cr-ACP1 (0.17:0.17:0.17)	-6 ± 2.40[c]	20	N/A
Skh-AMP1:Cn-AMP1:Cr-ACP1 (0.33:0.33:0.33)	-2 ± 8.72	7	N/A
Skh-AMP1:Cn-AMP1:Cr-ACP1 (0.67:0.67:0.67)	-6 ± 3.84	4	N/A
Skh-AMP1:Cn-AMP1:Cr-ACP1 (1.33:1.33:1.33)	-7 ± 4.11	8	N/A
Skh-AMP1:Cn-AMP1:Cr-ACP1 (2.67:2.67:2.67)	-5 ± 0.15	25	N/A
Skh-AMP1:Cn-AMP1:Cr-ACP1 (5.33:5.33:5.33)	-5 ± 5.29	9	N/A
Skh-AMP1:Cn-AMP1:Cr-ACP1 (10.67:10.67:10.67)	3 ± 12.01	9	N/A
Skh-AMP1:Cn-AMP1:Cr-ACP1 (21.33:21.33:21.33)	-7 ± 3.43	26	N/A

[a] Expected inhibition in growth was calculated using the Abbott formula*: $I_{exp} = x + y + z – [(xy + xz + yz)/100] + (xyz/10\ 000)$* (Abbott, 1925), where *x, y,* and *z* are the observed percent inhibition values for each corresponding single peptide treatment for *F. culmorum* (Table 2-4).[b] Interactions are considered synergistic (+) if the I_{exp} is lower than the I_{obs} , antagonistic (-) if I_{exp} is higher than I_{obs}, and additive (=) if they are equal (Kosman & Cohen, 1996). [c] The mean value ± standard error.

Table 14 Effect and interaction of Shepherin 2 combined with Cn-AMP1 and Cr-ACP1 on inhibiting germination of *Fusarium culmorum in vitro*

Growth inhibition *Fusarium culmorum*			
Peptide Concentrations (µM)	**Observed (%)**	**Expected (%)[a]**	**Interaction[b]**
Shepherin 2:Cn-AMP1:Cr-ACP1 (0.17:0.17:0.17)	-12 ± 11.47	17	N/A
Shepherin 2:Cn-AMP1:Cr-ACP1 (0.33:0.33:0.33)	5 ± 3.91[c]	11	N/A
Shepherin 2:Cn-AMP1:Cr-ACP1 (0.67:0.67:0.67)	4 ± 4.75	5	N/A
Shepherin 2:Cn-AMP1:Cr-ACP1 (1.33:1.33:1.33)	1 ± 4.88	35	N/A
Shepherin 2:Cn-AMP1:Cr-ACP1 (2.67:2.67:2.67)	-4 ± 4.93	91	N/A
Shepherin 2:Cn-AMP1:Cr-ACP1 (5.33:5.33:5.33)	-14 ± 4.53	98	N/A
Shepherin 2:Cn-AMP1:Cr-ACP1 (10.67:10.67:10.67)	12 ± 9.33	96	N/A
Shepherin 2:Cn-AMP1:Cr-ACP1 (21.33:21.33:21.33)	-1 ± 11.17	99	N/A

[a] Expected inhibition in growth was calculated using the Abbott formula*: $I_{exp} = x + y + z – [(xy + xz + yz)/100] + (xyz/10\ 000)$* (Abbott, 1925), where *x, y,* and *z* are the observed percent inhibition values for each corresponding single peptide treatment for *F. culmorum* (Table 1, 3, and 4).[b] Interactions are considered synergistic (+) if the I_{exp} is lower than the I_{obs} , antagonistic (-) if I_{exp} is higher than I_{obs}, and additive (=) if they are equal (Kosman & Cohen, 1996). [c] The mean value ± standard error.

3.1.2 ***Alternaria solani*.** When these HDPs were incubated with spores of *A. solani,* none of the peptides had statistically significant levels of activity when applied alone, as a single peptide (Fig. 7, Table 15-18). The Na-dichloroisocyanurate control treatment reached 64% inhibition at 900 µM and 99% at 1200 µM, which were physiologically relatively high inhibitory concentrations.

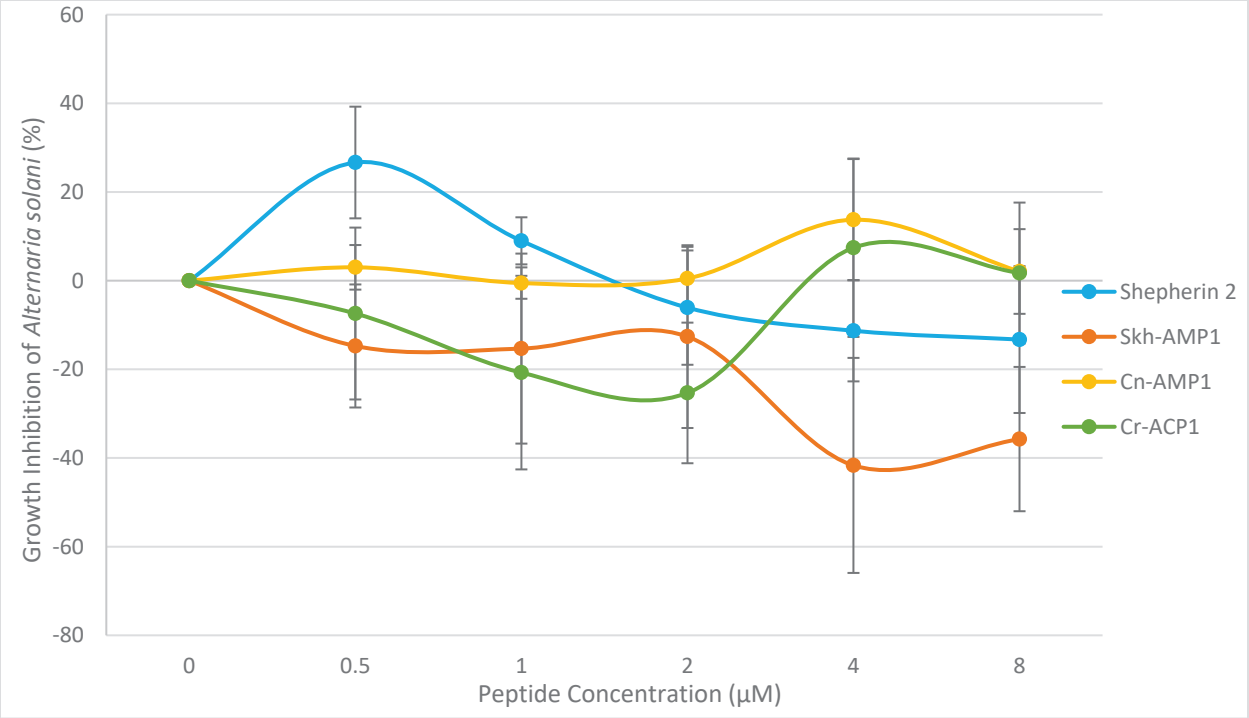

Figure 7 Effect of Shepherin 2, Skh-AMP1, Cr-ACP1, and Cn-AMP1 *in vitro* on the germination of *Alternaria solani* after 24 hr of incubation. Results for concentration 16 µM – 64 µM are not included in this figure to focus attention on the lower concentrations and because the results do not show any significance in that range. Values are the means of three or four separate experiments; bars are the standard errors. No statistical significance ($p \leq 0.05$) as determined by single factor ANOVA followed by Dunnett's test.

Table 15 Effect of Shepherin 2 on inhibiting the growth of *Alternaria solani in vitro*

Growth inhibition *Alternaria solani*	
Shepherin 2 Concentration (µM)	**Observed Inhibition %**
0.5	27 ± 12.6[a]
1	9 ± 5.31
2	-6 ± 12.89
4	-11 ± 11.43
8	-13 ± 16.56
16	-5 ± 6.46
32	-18 ± 17.66
64	-2 ± 19.84

[a] The mean value ± standard error.

Table 16 Effect of Skh-AMP1 on inhibiting the growth of *Alternaria solani in vitro*

Growth inhibition *Alternaria solani*	
Skh-AMP1 Concentration (µM)	**Observed Inhibition %**
0.5	-15 ± 13.88[a]
1	-15 ± 21.43
2	-13 ± 20.61
4	-42 ± 24.24
8	-36 ± 16.27
16	-62 ± 26.29
32	-71 ± 32.18
64	-74 ± 28.44

[a] The mean value ± standard error.

Table 17 Effect of Cn-AMP1 on inhibiting the growth of *Alternaria solani in vitro*

Growth inhibition *Alternaria solani*	
Cn-AMP1 Concentration (µM)	**Observed Inhibition %**
0.5	3 ± 5.03[a]
1	-1 ± 3.54
2	0 ± 7.13
4	14 ± 13.67
8	2 ± 9.55
16	-1 ± 7.02
32	1 ± 3.52
64	13 ± 5.77

[a] The mean value ± standard error.

Table 18 Effect of Cr-ACP1 on inhibiting the growth of *Alternaria solani in vitro*

Growth inhibition *Alternaria solani*	
Cr-ACP1 Concentration (µM)	**Observed Inhibition %**
0.5	-7 ± 19.38[a]
1	-21 ± 21.83
2	-25 ± 15.86
4	7 ± 20.12
8	2 ± 15.89
16	15 ± 22.28
32	-48 ± 21.58
64	-43 ± 22.35

[a] The mean value ± standard error.

Inhibition of *A. solani* was increased by combining the peptides. The greatest growth inhibition conferred by a double peptide combination resulted from Shepherin 2 and Cn-AMP1 at 0.5 µM, which inhibited germination of 53% spores (Fig. 8), the curve derived IC50 is also 0.5 µM. Because the expected growth inhibition for this combination is 29%, the observed results indicated a synergistic interaction occurred (Table 20).

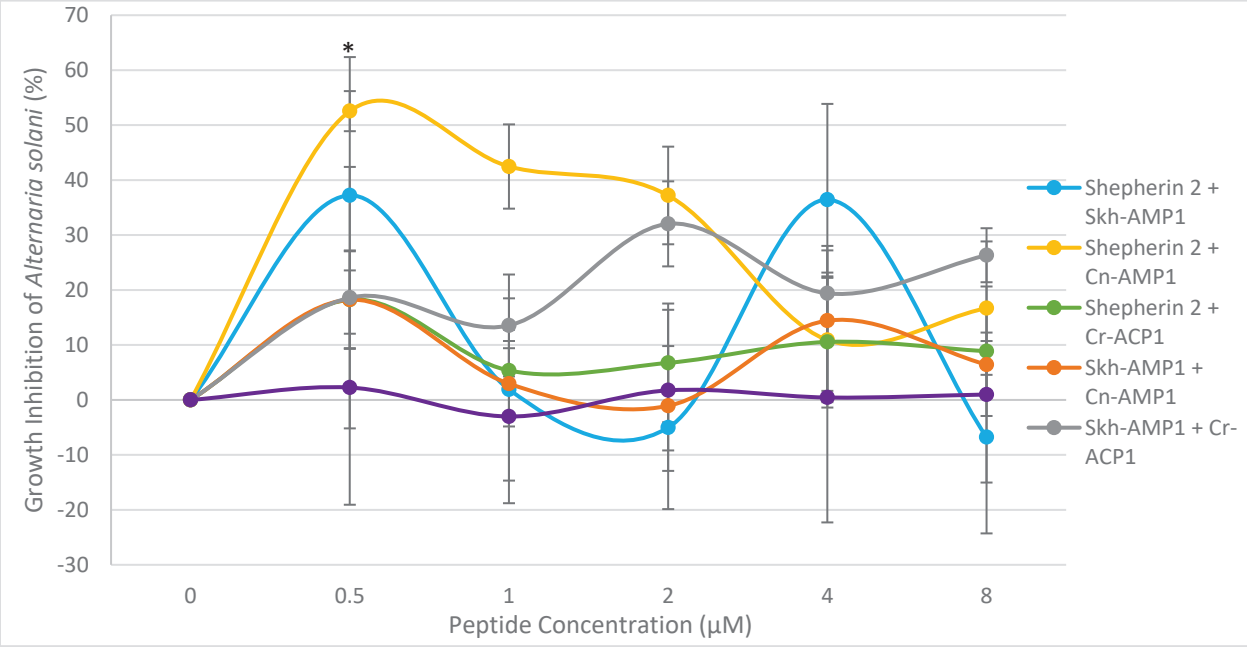

Figure 8 Effect of Shepherin 2, Skh-AMP1, Cr-ACP1, and Cn-AMP1 in combinations of two (1:1) *in vitro* on the germination of *Alternaria solani* after 24 hr of incubation. Results for concentration 16 µM – 64 µM are not included in this figure to focus attention on the lower concentrations and because the results do not show any significance in that range. Values are the means of three or four separate experiments; bars are the standard errors; asterisk (*) denotes a statistically significant difference compared to the no peptide control ($p \leq 0.05$) as determined by single factor ANOVA followed by Dunnett's test.

Table 19 Effect and interaction of Shepherin 2 combined with Skh-AMP1 on inhibiting germination *of Alternaria solani in vitro*

Growth inhibition *Alternaria solani*			
Peptide Concentrations (µM)	**Observed (%)**	**Expected (%)[a]**	**Interaction[b]**
Shepherin 2:Skh-AMP1 (0.25:0.25)	37 ± 25.17[c]	16	N/A
Shepherin 2:Skh-AMP1 (0.5:0.5)	2 ± 16.58	-5	N/A
Shepherin 2:Skh-AMP1 (1:1)	-5 ± 14.83	-20	N/A
Shepherin 2:Skh-AMP1 (2:2)	36 ± 17.42	-58	N/A
Shepherin 2:Skh-AMP1 (4:4)	-7 ± 17.50	-54	N/A
Shepherin 2:Skh-AMP1 (8:8)	-19 ± 21.08	-70	N/A
Shepherin 2:Skh-AMP1 (16:16)	-51 ± 27.01	-102	N/A
Shepherin 2:Skh-AMP1 (32:32)	-67 ± 16.20	-77	N/A

[a] Expected inhibition in growth was calculated using the Abbott formula*:* $I_{exp} = x + y - (xy/100)$ (Abbott, 1925), where *x* and *y* are the observed percent inhibition values for each corresponding single peptide treatment for *A. solani* (Table 15-16).[b] Interactions are considered synergistic (+) if the I_{exp} is lower than the I_{obs} , antagonistic (-) if I_{exp} is higher than I_{obs}, and additive (=) if they are equal (Kosman & Cohen, 1996). [c] The mean value ± standard error.

Table 20 Effect and interaction of Shepherin 2 combined with Cn-AMP1 on inhibiting germination of *Alternaria solani in vitro*

Growth inhibition *Alternaria solani*			
Peptide Concentrations (µM)	**Observed (%)**	**Expected (%)[b]**	**Interaction[c]**
Shepherin 2:Cn-AMP1 (0.25:0.25)	53* ± 3.65[a]	29	+
Shepherin 2:Cn-AMP1 (0.5:0.5)	42 ± 7.67[d]	8	N/A
Shepherin 2:Cn-AMP1 (1:1)	37 ± 8.88	-6	N/A
Shepherin 2:Cn-AMP1 (2:2)	11 ± 11.31	5	N/A
Shepherin 2:Cn-AMP1 (4:4)	17 ± 12.14	-11	N/A
Shepherin 2:Cn-AMP1 (8:8)	20 ± 3.51	-6	N/A
Shepherin 2:Cn-AMP1 (16:16)	4 ± 18.19	-17	N/A
Shepherin 2:Cn-AMP1 (32:32)	33 ± 19.95	11	N/A

[a] Means followed by an asterisk (*) are significantly different from the no peptide control at P≤0.05. [b] Expected inhibition in growth was calculated using the Abbott formula*:* $I_{exp} = x + y - (xy/100)$ (Abbott, 1925), where *x* and *y* are the observed percent inhibition values for each corresponding single peptide treatment for *A. solani* (Table 15 and 17). [c] Interactions are considered synergistic (+) if the I_{exp} is lower than the I_{obs} , antagonistic (-) if I_{exp} is higher than I_{obs}, and additive (=) if they are equal (Kosman & Cohen, 1996). [d] The mean value ± standard error.

Table 21 Effect and interaction of Shepherin 2 combined with Cr-ACP1 on inhibiting germination of *Alternaria solani in vitro*

Growth inhibition *Alternaria solani*			
Peptide Concentrations (µM)	**Observed (%)**	**Expected (%)[a]**	**Interaction[b]**
Shepherin 2:Cr-ACP1 (0.25:0.25)	18 ± 8.96[c]	22	N/A
Shepherin 2:Cr-ACP1 (0.5:0.5)	5 ± 4.07	-10	N/A
Shepherin 2:Cr-ACP1 (1:1)	7 ± 10.80	-33	N/A
Shepherin 2:Cr-ACP1 (2:2)	11 ± 11.94	-3	N/A
Shepherin 2:Cr-ACP1 (4:4)	9 ± 11.78	-11	N/A
Shepherin 2:Cr-ACP1 (8:8)	-7 ± 8.82	-21	N/A
Shepherin 2:Cr-ACP1 (16:16)	-25 ± 8.21	-75	N/A
Shepherin 2:Cr-ACP1 (32:32)	-11 ± 11.98	-46	N/A

[a] Expected inhibition in growth was calculated using the Abbott formula*: $I_{exp} = x + y - (xy/100)$* (Abbott, 1925), where *x* and *y* are the observed percent inhibition values for each corresponding single peptide treatment for *A. solani* (Table 15 and 18).[b] Interactions are considered synergistic (+) if the I_{exp} is lower than the I_{obs} , antagonistic (-) if I_{exp} is higher than I_{obs}, and additive (=) if they are equal (Kosman & Cohen, 1996). [c] The mean value ± standard error.

Table 22 Effect and interaction of Skh-AMP1 combined with Cn-AMP1 on inhibiting germination of *Alternaria solani in vitro*

Growth inhibition *Alternaria solani*			
Peptide Concentrations (µM)	**Observed (%)**	**Expected (%)[a]**	**Interaction[b]**
Skh-AMP1:Cn-AMP1 (0.25:0.25)	18 ± 8.81[c]	-12	N/A
Skh-AMP1:Cn-AMP1 (0.5:0.5)	3 ± 7.78	-16	N/A
Skh-AMP1:Cn-AMP1 (1:1)	-1 ± 8.11	-13	N/A
Skh-AMP1:Cn-AMP1 (2:2)	14 ± 12.78	-22	N/A
Skh-AMP1:Cn-AMP1 (4:4)	6 ± 5.84	-33	N/A
Skh-AMP1:Cn-AMP1 (8:8)	14 ± 13.07	-64	N/A
Skh-AMP1:Cn-AMP1 (16:16)	-15 ± 6.33	-69	N/A
Skh-AMP1:Cn-AMP1 (32:32)	-15 ± 16.39	-51	N/A

[a] Expected inhibition in growth was calculated using the Abbott formula*: $I_{exp} = x + y - (xy/100)$* (Abbott, 1925), where *x* and *y* are the observed percent inhibition values for each corresponding single peptide treatment for *A. solani* (Table 16 -17).[b] Interactions are considered synergistic (+) if the I_{exp} is lower than the I_{obs} , antagonistic (-) if I_{exp} is higher than I_{obs}, and additive (=) if they are equal (Kosman & Cohen, 1996). [c] The mean value ± standard error.

Table 23 Effect and interaction of Skh-AMP1 combined with Cr-ACP1 on inhibiting germination of *Alternaria solani in vitro*

Growth inhibition *Alternaria solani*			
Peptide Concentrations (µM)	**Observed (%)**	**Expected (%)[a]**	**Interaction[b]**
Skh-AMP1:Cr-ACP1 (0.25:0.25)	19 ± 23.79[c]	-23	N/A
Skh-AMP1:Cr-ACP1 (0.5:0.5)	14 ± 9.27	-39	N/A
Skh-AMP1:Cr-ACP1 (1:1)	32 ± 7.74	-41	N/A
Skh-AMP1:Cr-ACP1 (2:2)	19 ± 8.64	-32	N/A
Skh-AMP1:Cr-ACP1 (4:4)	26 ± 4.91	-33	N/A
Skh-AMP1:Cr-ACP1 (8:8)	6 ± 8.68	-86	N/A
Skh-AMP1:Cr-ACP1 (16:16)	23 ± 11.28	-153	N/A
Skh-AMP1:Cr-ACP1 (32:32)	30 ± 9.52	-149	N/A

[a] Expected inhibition in growth was calculated using the Abbott formula*: $I_{exp} = x + y - (xy/100)$* (Abbott, 1925), where *x* and *y* are the observed percent inhibition values for each corresponding single peptide treatment for *A. solani* (Table 15 and 18).[b] Interactions are considered synergistic (+) if the I_{exp} is lower than the I_{obs} , antagonistic (-) if I_{exp} is higher than I_{obs}, and additive (=) if they are equal (Kosman & Cohen, 1996). [c] The mean value ± standard error.

Table 24 Effect and interaction of Cn-AMP1 combined with Cr-ACP1 on inhibiting germination of *Alternaria solani in vitro*

Growth inhibition *Alternaria solani*			
Peptide Concentrations (µM)	**Observed (%)**	**Expected (%)[a]**	**Interaction[b]**
Cn-AMP1:Cr-ACP1 (0.25:0.25)	2 ± 31.32[c]	-4	N/A
Cn-AMP1:Cr-ACP1 (0.5:0.5)	-3 ± 15.78	-22	N/A
Cn-AMP1:Cr-ACP1 (1:1)	2 ± 14.66	-25	N/A
Cn-AMP1:Cr-ACP1 (2:2)	0 ± 22.73	20	N/A
Cn-AMP1:Cr-ACP1 (4:4)	1 ± 16.01	4	N/A
Cn-AMP1:Cr-ACP1 (8:8)	6 ± 19.09	-16	N/A
Cn-AMP1:Cr-ACP1 (16:16)	8 ± 21.77	-47	N/A
Cn-AMP1:Cr-ACP1 (32:32)	-22 ± 13.59	-24	N/A

[a] Expected inhibition in growth was calculated using the Abbott formula*: $I_{exp} = x + y - (xy/100)$* (Abbott, 1925), where *x* and *y* are the observed percent inhibition values for each corresponding single peptide treatment for *A. solani* (Table 17 - 18).[b] Interactions are considered synergistic (+) if the I_{exp} is lower than the I_{obs} , antagonistic (-) if I_{exp} is higher than I_{obs}, and additive (=) if they are equal (Kosman & Cohen, 1996). [c] The mean value ± standard error.

The triple peptide combinations demonstrated significantly greater growth inhibition than the single peptides and most of the double peptide combinations. Shepherin 2 combined with Skh-AMP1 and Cn-AMP1had a curve-derived IC50 of 1 μM showing 43% inhibition at 0.5 μM, which rose further to 57% at 4 μM, after which the level of growth inhibition was reduced, indicating a relatively narrow range of peak activity (Fig. 9). The expected inhibition of 19% and -36% at those two concentrations respectively indicate a strong synergistic reaction occurred between these three peptides (Table 25). In fact, all the interactions for the triple peptide combinations which produced significant levels of growth inhibition, when tested against *A. solani*, were strongly synergistic (Tables 25–28). Skh-AMP1, combined with Cn-AMP1 and Cr-ACP1, also significantly inhibited germination of *A. solani* spores, although to a lesser extent than the other combinations. Inhibition for this combination reached 40% at both 0.5 μM and 4 μM before dropping off: the curve-derived IC50 was 1 μM. The interactions between these peptides were also synergistic with an expected inhibition of -19% and -14%, respectively. The combination of Shepherin 2 with Cn-AMP1 and Cr-ACP1 had the widest range of concentrations displaying significant levels of inhibition against *A. solani*. Inhibition began at 48% at 0.5 μM and peaked at 54% at 2 μM, remained over 30% at 4, 16, and 32 μM before dropping to 13% at 64 μM, the curve derived IC50 was 1 μM. All these interactions were synergistic (Table 28). However, the highest level of growth inhibition was achieved by the combination of Shepherin 2 with Skh-AMP1 and Cr-ACP1, which showed inhibition of 58% at 1 μM and remained at nearly that level until a concentration of 4 μM, which achieved 54% inhibition before dropping off with the remaining tested concentrations. Once again, all these interactions are considered strongly synergistic with an expected inhibition of -27% at 1 μM and -47% at 4 μM (Table 26).

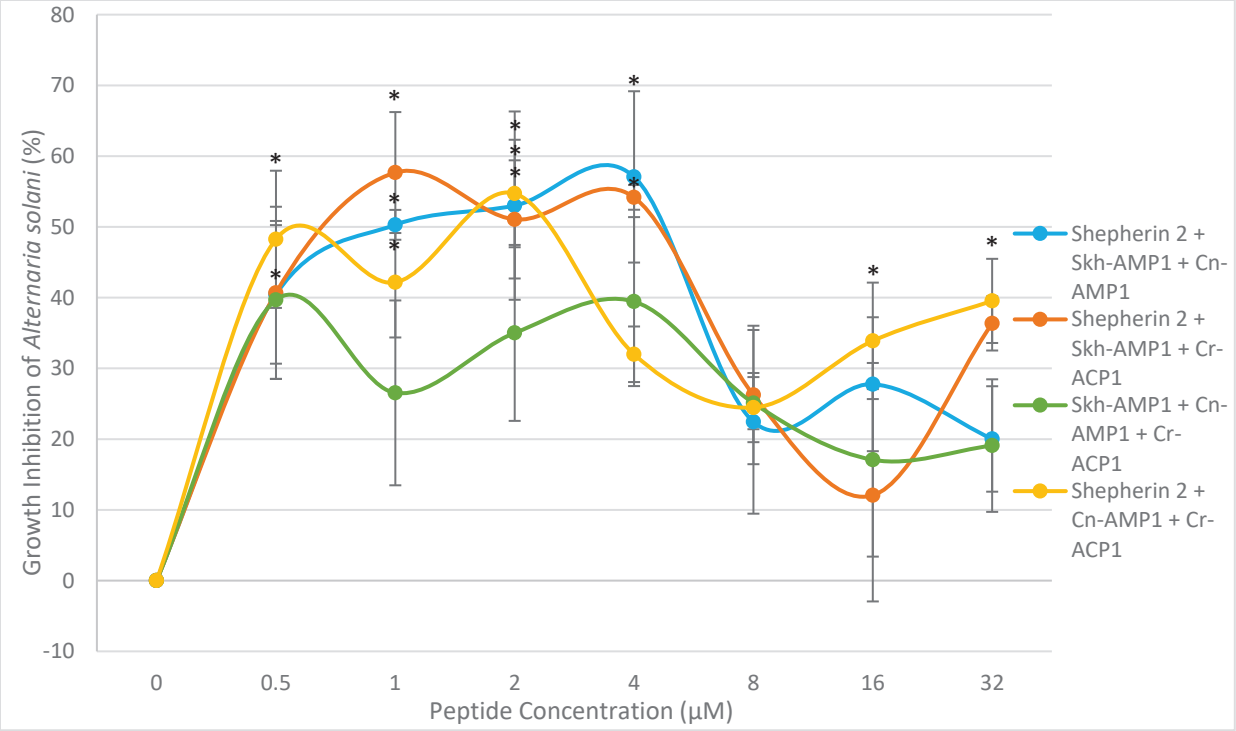

Figure 9 Effect of Shepherin 2, Skh-AMP1, Cr-ACP1, and Cn-AMP1 in combinations of three (1:1:1) *in vitro* on the germination of *Alternaria solani* after 24 hr of incubation. Results for 64 µM are not included in this figure to focus attention on the lower concentrations and because the results do not show any significance. Values are the means of three separate experiments; bars are the standard errors; asterisk (*) denotes a statistically significant difference compared to the no peptide control ($p \leq 0.05$) as determined by single factor ANOVA followed by Dunnett's test.

Table 25 Effect and interaction of Shepherin 2 combined with Skh-AMP1 and Cn-AMP1 on inhibiting germination of *Alternaria solani in vitro*

	Growth inhibition *Alternaria solani*		
Peptide Concentrations (µM)	**Observed (%)**	**Expected[b] (%)**	**Interaction[c]**
Shepherin 2:Skh-AMP1:Cn-AMP1 (0.17:0.17:0.17)	40* ± 9.79[a]	19	+
Shepherin 2:Skh-AMP1:Cn-AMP1 (033:0.33:0.33)	50* ± 2.11[d]	-6	+
Shepherin 2:Skh-AMP1:Cn-AMP1 (0.67:0.67:0.67)	53* ± 13.31	-20	+

Shepherin 2:Skh-AMP1:Cn-AMP1 (1.33:1.33:1.33)	57* ± 12.11	-36	+
Shepherin 2:Skh-AMP1:Cn-AMP1 (2.67:2.67:2.67)	22 ± 12.98	-51	N/A
Shepherin 2:Skh-AMP1:Cn-AMP1 (5.33:5.33:5.33)	28 ± 9.46	-72	N/A
Shepherin 2:Skh-AMP1:Cn-AMP1 (10.67:10.67:10.67)	20 ± 7.45	-100	N/A
Shepherin 2:Skh-AMP1:Cn-AMP1 (21.33:21.33:21.33)	33 ± 8.70	-54	N/A

[a] Means followed by an asterisk (*) are significantly different from the no peptide control at P≤0.05. [b] Expected inhibition in growth was calculated using the Abbott formula: $I_{exp} = x + y + z - [(xy + xz + yz)/100] + (xyz/10\ 000)$ (Abbott, 1925), where *x, y,* and *z* are the observed percent inhibition values for each corresponding single peptide treatment for *A. solani* (Table 15-17). [c] Interactions are considered synergistic (+) if the I_{exp} is lower than the I_{obs} , antagonistic (-) if I_{exp} is higher than I_{obs}, and additive (=) if they are equal (Kosman & Cohen, 1996). [d] The mean value ± standard error.

Table 26 Effect and interaction of Shepherin 2 combined with Skh-AMP1 and Cr-ACP1 on inhibiting germination of *Alternaria solani in vitro*

Growth inhibition *Alternaria solani*			
Peptide Concentrations (µM)	**Observed (%)**	**Expected (%)[b]**	**Interaction [c]**
Shepherin 2:Skh-AMP1:Cr-ACP1 (0.17:0.17:0.17)	41 ± 12.17[d]	10	N/A
Shepherin 2:Skh-AMP1:Cr-ACP1 (033:0.33:0.33)	58* ± 8.55[a]	-27	+
Shepherin 2:Skh-AMP1:Cr-ACP1 (0.67:0.67:0.67)	51* ± 8.35	-50	+
Shepherin 2:Skh-AMP1:Cr-ACP1 (1.33:1.33:1.33)	54* ± 1.75	-47	+
Shepherin 2:Skh-AMP1:Cr-ACP1 (2.67:2.67:2.67)	26 ± 9.79	-51	N/A
Shepherin 2:Skh-AMP1:Cr-ACP1 (5.33:5.33:5.33)	12 ± 15.01	-96	N/A
Shepherin 2:Skh-AMP1:Cr-ACP1 (10.67:10.67:10.67)	36 ± 3.83	-199	N/A
Shepherin 2:Skh-AMP1:Cr-ACP1 (21.33:21.33:21.33)	-22 ± 16.55	-154	N/A

[a] Means followed by an asterisk (*) are significantly different from the no peptide control at P≤0.05. [b] Expected inhibition in growth was calculated using the Abbott formula*: $I_{exp} = x + y + z - [(xy + xz + yz)/100] + (xyz/10\ 000)$* (Abbott, 1925), where *x, y,* and *z* are the observed percent inhibition values for each corresponding single peptide treatment for *A. solani* (Table 15, 16 and 18). [c] Interactions are considered synergistic (+) if the I_{exp} is lower than the I_{obs} , antagonistic (-) if I_{exp} is higher than I_{obs}, and additive (=) if they are equal (Kosman & Cohen, 1996). [d] The mean value ± standard error.

Table 27 Effect and interaction of Skh-AMP1 combined with Cn-AMP1 and Cr-ACP1 on inhibiting germination of *Alternaria solani in vitro*

Growth inhibition *Alternaria solani*			
Peptide Concentrations (µM)	**Observed (%)**	**Expected (%)[a]**	**Interaction[b]**
Skh-AMP1:Cn-AMP1:Cr-ACP1 (0.17:0.17:0.17)	40 ± 11.16[c]	-19	N/A
Skh-AMP1:Cn-AMP1:Cr-ACP1 (0.33:0.33:0.33)	27 ± 13.06	-41	N/A
Skh-AMP1:Cn-AMP1:Cr-ACP1 (0.67:0.67:0.67)	35 ± 12.43	-41	N/A
Skh-AMP1:Cn-AMP1:Cr-ACP1 (1.33:1.33:1.33)	39 ± 11.94	-14	N/A
Skh-AMP1:Cn-AMP1:Cr-ACP1 (2.67:2.67:2.67)	25 ± 3.68	-31	N/A
Skh-AMP1:Cn-AMP1:Cr-ACP1 (5.33:5.33:5.33)	17 ± 13.69	-88	N/A
Skh-AMP1:Cn-AMP1:Cr-ACP1 (10.67:10.67:10.67)	19 ± 9.37	-151	N/A
Skh-AMP1:Cn-AMP1:Cr-ACP1 (21.33:21.33:21.33)	-22 ± 4.65	-116	N/A

[a] Expected inhibition in growth was calculated using the Abbott formula*: $I_{exp} = x + y + z - [(xy + xz + yz)/100] + (xyz/10\ 000)$* (Abbott, 1925), where *x, y,* and *z* are the observed percent inhibition values for each corresponding single peptide treatment for *A. solani* (Table 16-18). [b] Interactions are considered synergistic (+) if the I_{exp} is lower than the I_{obs} , antagonistic (-) if I_{exp} is higher than I_{obs}, and additive (=) if they are equal (Kosman & Cohen, 1996). [c] The mean value ± standard error.

Table 28 Effect and interaction of Shepherin 2 combined with Cn-AMP1 and Cr-ACP1 on inhibiting germination of *Alternaria solani in vitro*

Growth inhibition *Alternaria solani*			
Peptide Concentrations (µM)	**Observed (%)**	**Expected (%)[b]**	**Interaction[c]**
Shepherin 2:Cn-AMP1:Cr-ACP1 (0.17:0.17:0.17)	48* ± 9.70[a]	24	+
Shepherin 2:Cn-AMP1:Cr-ACP1 (0.33:0.33:0.33)	42* ± 7.79[d]	-11	+
Shepherin 2:Cn-AMP1:Cr-ACP1 (0.67:0.67:0.67)	55* ± 7.60	-30	+
Shepherin 2:Cn-AMP1:Cr-ACP1 (1.33:1.33:1.33)	32* ± 3.93	11	+
Shepherin 2:Cn-AMP1:Cr-ACP1 (2.67:2.67:2.67)	24 ± 4.89	-9	N/A
Shepherin 2:Cn-AMP1:Cr-ACP1 (5.33:5.33:5.33)	34* ± 8.23	-22	+
Shepherin 2:Cn-AMP1:Cr-ACP1 (10.67:10.67:10.67)	40* ± 5.95	-73	+
Shepherin 2:Cn-AMP1:Cr-ACP1 (21.33:21.33:21.33)	14 ± 9.76	-27	N/A

[a] Means followed by an asterisk (*) are significantly different from the no peptide control at P≤0.05. [b] Expected inhibition in growth was calculated using the Abbott formula*: $I_{exp} = x + y + z - [(xy + xz + yz)/100] + (xyz/10\ 000)$* (Abbott, 1925), where *x, y,* and *z* are the observed percent inhibition values for each corresponding single peptide treatment for *A. solani* (Table 15, 17 and 18). [c] Interactions are considered synergistic (+) if the I_{exp} is lower than the I_{obs} , antagonistic (-) if I_{exp} is higher than I_{obs}, and additive (=) if they are equal (Kosman & Cohen, 1996). [d] The mean value ± standard error.

3.1.3 *Pectobacterium carotovorum* subsp. *carotovorum*. When *P. carotovorum* was treated with single peptides, Shepherin 2 showed the highest level of growth inhibition among all peptides tested. The curve derived IC50 was 7 µM and at 8 µM, 56% inhibition was observed, this increased to 69% at 16 µM and continued increasing to 84% at 64 µM. Cn-AMP1 also demonstrated statistically significant, although much lower, growth inhibition with 37% at 32 µM; Skh-AMP1 did as well, reaching 22% inhibition at 4 µM and 25% at 32 µM (Fig. 10, Table 29-31). The Na-dichloroisocyanurate control reached 29% inhibition at 150 µM and reached a

peak of 90% inhibition at 600 µM, complete inhibition was not achieved at any tested concentration up to the 900 µM.

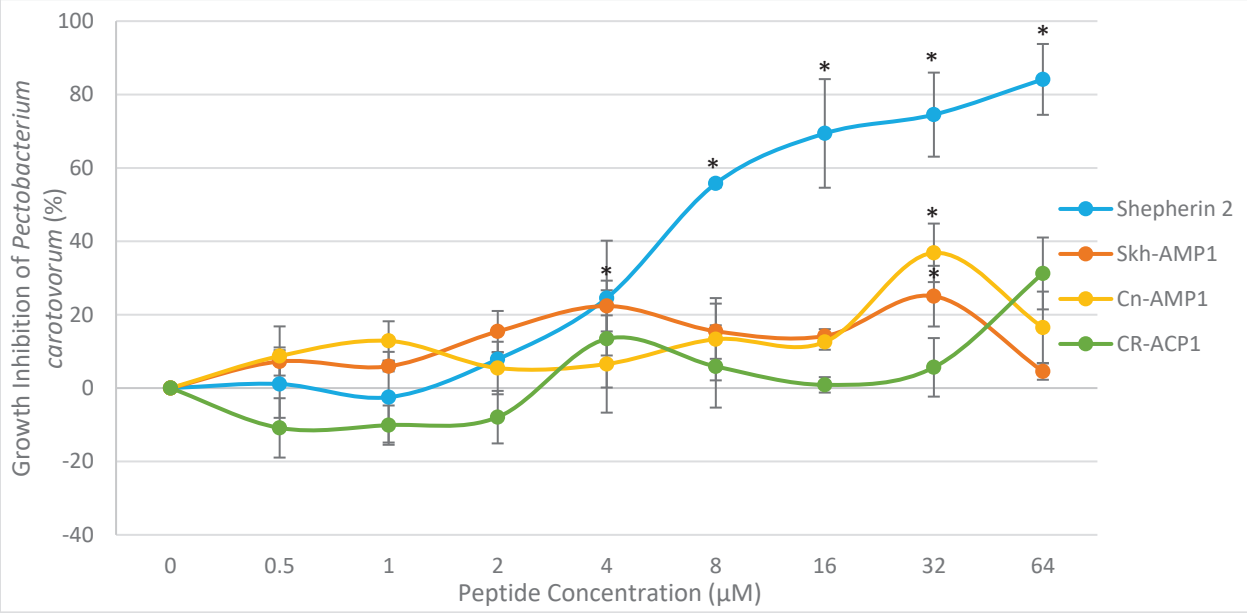

Figure 10 Effect of Shepherin 2, Skh-AMP1, Cr-ACP1, and Cn-AMP1 *in vitro* on the growth of *P. carotovorum*, determined by absorbance at OD_{600} after 24 h of incubation with the bacterium. Values are the means of three separate experiments; bars are the standard errors; asterisk (*) denotes a statistically significant difference compared to the no peptide control ($p \leq 0.05$) as determined by single factor ANOVA followed by Dunnett's test.

Table 29 Effect of Shepherin 2 on inhibiting the growth of *Pectobacterium carotovorum in vitro*

Growth inhibition *Pectobacterium carotovorum*	
Shepherin 2 Concentration (µM)	**Observed Inhibition (%)**
0.5	1 ± 9.21[b]
1	-2 ± 12.36
2	0 ± 1.83
4	25 ± 15.65
8	56* ± 1.05[a]
16	69* ± 14.80
32	75* ± 11.46
64	84* ± 9.66

[a] Means followed by an asterisk (*) are significantly different from the no peptide control at $P \leq 0.05$. [b] The mean value ± standard error.

Table 30 Effect of Skh-AMP1 on inhibiting the growth of *Pectobacterium carotovorum in vitro*

Growth inhibition *Pectobacterium carotovorum*	
Skh-AMP1 Concentration (µM)	**Observed Inhibition (%)**
0.5	7 ± 3.83[b]
1	6 ± 1.39
2	15 ± 5.60
4	22* ± 6.92
8	15 ± 7.52
16	14 ± 1.88
32	25* ± 8.27[a]
64	5 ± 2.28

[a] Means followed by an asterisk (*) are significantly different from the no peptide control at P≤0.05. [b] The mean value ± standard error.

Table 31 Effect of Cn-AMP1 on inhibiting the growth of *Pectobacterium carotovorum in vitro*

Growth inhibition *Pectobacterium carotovorum*	
Cn-AMP1 Concentration (µM)	**Observed Inhibition (%)**
0.5	9 ± 5.86[b]
1	13 ± 9.44
2	7 ± 5.79
4	7 ± 9.00
8	13 ± 12.53
16	13 ± 7.63
32	37* ± 11.49[a]
64	17 ± 3.42

[a] Means followed by an asterisk (*) are significantly different from the no peptide control at P≤0.05. [b] The mean value ± standard error.

Table 32 Effect of Cr- ACP1 on inhibiting the growth of *Pectobacterium carotovorum in vitro*

Growth inhibition *Pectobacterium carotovorum*	
Cr-ACP1 Concentration (µM)	**Observed Inhibition (%)**
0.5	-11 ± 8.09[a]
1	-10 ± 5.35
2	-11 ± 7.16
4	13 ± 13.25
8	6 ± 11.21
16	1 ± 2.11
32	6 ± 7.98
64	31 ± 9.79

[a] The values after the ± are the standard errors of means.

The inhibitory activities of these HDPs increased when the peptides were combined into pairs, particularly the combinations including Shepherin 2. The combination which reached the highest level of growth inhibition for *P. carotovorum* was Shepherin 2 combined with Cr-ACP1, which had a curve derived IC50 of 11 μM and displayed 89% inhibition at 16 μM, which decreased to 50% at 64 μM (Fig. 11). The expected inhibition for this combination at 16 μM was 69%, indicating a synergistic interaction. However, at 32 μM the observed inhibition was 74% and the expected inhibition was 77% which indicated that the interaction had become slightly antagonistic at higher concentrations which became more antagonistic at 64 μM when the expected inhibition was 89% while the observed inhibition was only 50% (Table 35). Shepherin 2 combined with Cn-AMP1, and Shepherin 2 combined with Skh-AMP1 also demonstrated significant inhibition in a narrow range of concentrations. They both peaked at 16 μM with 73% and 62% inhibition, respectively. Shepherin 2 combined with Skh-AMP1 reached 67% inhibition at 64 μM with an IC50 of 13 μM. The IC50 for the combination of Shepherin 2 with Cn-AMP1 was 12 μM. The expected inhibition was 73%, making this interaction additive, while both Shepherin 2 with Skh-AMP1 interactions were mildly antagonistic (Tables 33-34). Cn-AMP1 combined with Cr-ACP1 showed statistically significant levels of growth inhibition, although it was far lower than other peptide combinations: 29% inhibition was reached at 4 μM and 25% at 64 μM. The expected inhibition at 4 μM was 19% which indicates a synergistic interaction, and at 64 μM the expected inhibition was 43% which is an antagonistic interaction (Table 38).

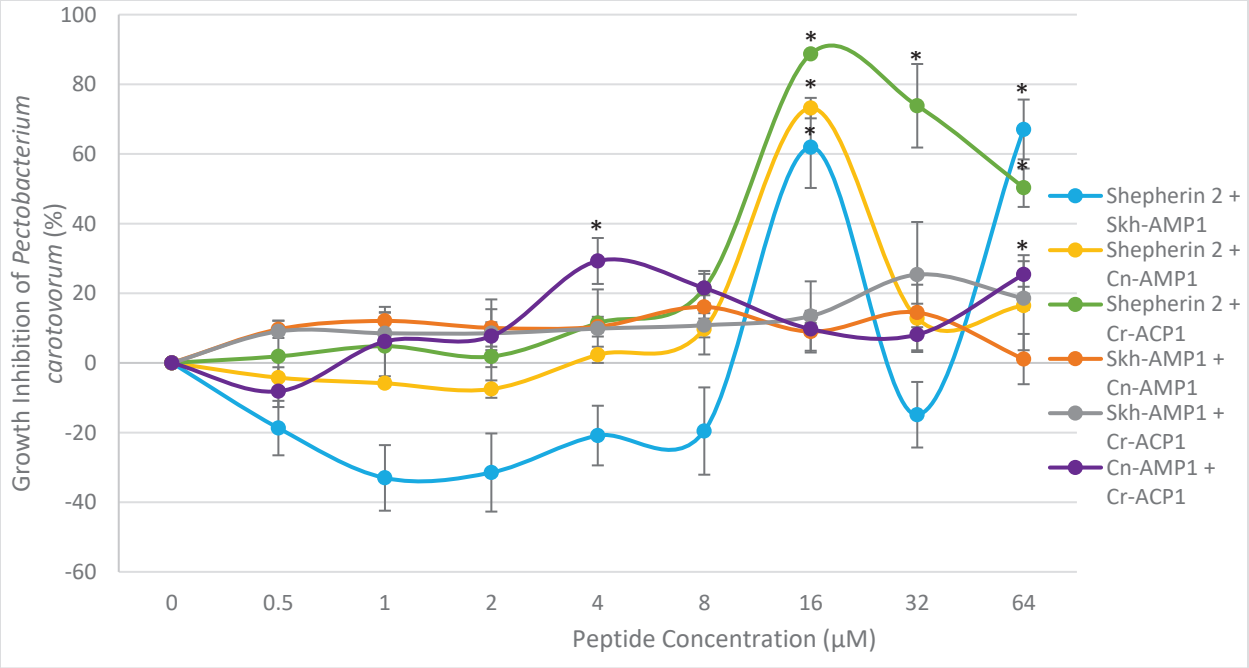

Figure 11 Effect of Shepherin 2, Skh-AMP1, Cr-ACP1, and Cn-AMP1 in combinations of 2 (1:1) *in vitro* on the growth of *P. carotovorum*, determined by absorbance at OD_{600} after 24 h of incubation with the bacterium. Values are the means of three separate experiments; bars are the standard errors; asterisk (*) denotes a statistically significant difference compared to the no peptide control ($p \leq 0.05$) as determined by single factor ANOVA followed by Dunnett's test.

Table 33 Effect and interaction of Shepherin 2 combined with Skh-AMP1 on inhibiting germination of *Pectobacterium carotovorum in vitro*

Growth inhibition *Pectobacterium carotovorum*			
Peptide Concentrations (µM)	**Observed (%)**	**Expected (%)[b]**	**Interaction [c]**
Shepherin 2:Skh-AMP1 (0.25:0.25)	-19 ± 7.82[d]	8	N/A
Shepherin 2:Skh-AMP1 (0.5:0.5)	-33 ± 9.42	4	N/A
Shepherin 2:Skh-AMP1 (1:1)	-35 ± 11.22	15	N/A
Shepherin 2:Skh-AMP1 (2:2)	-21 ± 8.56	42	N/A
Shepherin 2:Skh-AMP1 (4:4)	-20 ± 12.53	63	N/A
Shepherin 2:Skh-AMP1 (8:8)	62* ± 11.68[a]	73	-
Shepherin 2:Skh-AMP1 (16:16)	-15 ± 9.42	81	N/A
Shepherin 2:Skh-AMP1 (32:32)	67* ± 8.59	85	-

[a] Means followed by an asterisk (*) are significantly different from the no peptide control at $P \leq 0.05$. [b] Expected inhibition in growth was calculated using the Abbott formula: $I_{exp} = x + y - (xy/100)$ (Abbott, 1925), where x and y are the observed percent inhibition values for each corresponding single peptide treatment for *P. carotovorum* (Table 29-30). [c] Interactions are considered synergistic (+) if the I_{exp} is lower than the I_{obs} , antagonistic (-) if I_{exp} is higher than I_{obs}, and additive (=) if they are equal (Kosman & Cohen, 1996). [d] The mean value ± standard error.

Table 34 Effect and interaction of Shepherin 2 combined with Cn-AMP1 on inhibiting germination of *Pectobacterium carotovorum in vitro*

Growth inhibition *Pectobacterium carotovorum*			
Peptide Concentrations (µM)	**Observed (%)**	**Expected (%)[b]**	**Interaction[c]**
Shepherin 2:Cn-AMP1 (0.25:0.25)	-4 ± 2.99[d]	10	N/A
Shepherin 2:Cn-AMP1 (0.5:0.5)	-6 ± 0.85	11	N/A
Shepherin 2:Cn-AMP1 (1:1)	-6 ± 2.50	7	N/A
Shepherin 2:Cn-AMP1 (2:2)	2 ± 2.33	30	N/A
Shepherin 2:Cn-AMP1 (4:4)	10 ± 7.28	62	N/A
Shepherin 2:Cn-AMP1 (8:8)	73* ± 2.94[a]	73	=
Shepherin 2:Cn-AMP1 (16:16)	13 ± 9.66	83	N/A
Shepherin 2:Cn-AMP1 (32:32)	16 ± 12.78	87	N/A

[a] Means followed by an asterisk (*) are significantly different from the no peptide control at P≤0.05. [b] Expected inhibition in growth was calculated using the Abbott formula*: $I_{exp} = x + y - (xy/100)$* (Abbott, 1925), where *x* and *y* are the observed percent inhibition values for each corresponding single peptide treatment for *P. carotovorum* (Table 29 and 31). [c] Interactions are considered synergistic (+) if the I_{exp} is lower than the I_{obs} , antagonistic (-) if I_{exp} is higher than I_{obs}, and additive (=) if they are equal (Kosman & Cohen, 1996). [d] The mean value ± standard error.

Table 35 Effect and interaction of Shepherin 2 combined with Cr-ACP1 on inhibiting germination of *Pectobacterium carotovorum in vitro*

Growth inhibition *Pectobacterium carotovorum*			
Peptide Concentrations (µM)	**Observed (%)**	**Expected (%)[b]**	**Interaction[c]**
Shepherin 2:Cr-ACP1 (0.25:0.25)	2 ± 10.23[d]	-10	N/A
Shepherin 2:Cr-ACP1 (0.5:0.5)	5 ± 9.59	-12	N/A
Shepherin 2:Cr-ACP1 (1:1)	4 ± 8.85	-11	N/A
Shepherin 2:Cr-ACP1 (2:2)	11 ± 9.66	35	N/A
Shepherin 2:Cr-ACP1 (4:4)	21 ± 4.18	59	N/A
Shepherin 2:Cr-ACP1 (8:8)	89* ± 0.72[a]	69	+
Shepherin 2:Cr-ACP1 (16:16)	74* ± 11.99	77	-
Shepherin 2:Cr-ACP1 (32:32)	50* ± 5.51	89	-

[a] Means followed by an asterisk (*) are significantly different from the no peptide control at P≤0.05. [b] Expected inhibition in growth was calculated using the Abbott formula*: $I_{exp} = x + y - (xy/100)$* (Abbott, 1925), where *x* and *y* are the observed percent inhibition values for each corresponding single peptide treatment for *P. carotovorum* (Table 29 and 32). [c] Interactions are considered synergistic (+) if the I_{exp} is lower than the I_{obs} , antagonistic (-) if I_{exp} is higher than I_{obs}, and additive (=) if they are equal (Kosman & Cohen, 1996). [d] The mean value ± standard error.

Table 36 Effect and interaction of Skh-AMP1 combined with Cn-AMP1 on inhibiting germination of *Pectobacterium carotovorum in vitro*

Growth inhibition *Pectobacterium carotovorum*			
Peptide Concentrations (µM)	**Observed (%)**	**Expected (%)[a]**	**Interaction[b]**
Skh-AMP1:Cn-AMP1 (0.25:0.25)	10 ± 2.48[c]	15	N/A
Skh-AMP1:Cn-AMP1 (0.5:0.5)	12 ± 2.51	18	N/A
Skh-AMP1:Cn-AMP1 (1:1)	10 ± 5.37	21	N/A
Skh-AMP1:Cn-AMP1 (2:2)	10 ± 2.83	27	N/A
Skh-AMP1:Cn-AMP1 (4:4)	16 ± 3.34	26	N/A
Skh-AMP1:Cn-AMP1 (8:8)	9 ± 5.99	25	N/A
Skh-AMP1:Cn-AMP1 (16:16)	14 ± 2.54	53	N/A
Skh-AMP1:Cn-AMP1 (32:32)	1 ± 7.22	20	N/A

[a] Expected inhibition in growth was calculated using the Abbott formula*: $I_{exp} = x + y - (xy/100)$* (Abbott, 1925), where *x* and *y* are the observed percent inhibition values for each corresponding single peptide treatment for *P. carotovorum* (Table 30-31). [b] Interactions are considered synergistic (+) if the I_{exp} is lower than the I_{obs} , antagonistic (-) if I_{exp} is higher than I_{obs}, and additive (=) if they are equal (Kosman & Cohen, 1996). [c] The mean value ± standard error.

Table 37 Effect and interaction of Skh-AMP1 combined with Cr-ACP1 on inhibiting germination of *Pectobacterium carotovorum in vitro*

Growth inhibition *Pectobacterium carotovorum*			
Peptide Concentrations (µM)	**Observed (%)**	**Expected (%)[a]**	**Interaction[b]**
Skh-AMP1:Cr-ACP1 (0.25:0.25)	9 ± 0.37[c]	-3	N/A
Skh-AMP1:Cr-ACP1 (0.5:0.5)	9 ± 4.30	-3	N/A
Skh-AMP1:Cr-ACP1 (1:1)	3 ± 9.72	6	N/A
Skh-AMP1:Cr-ACP1 (2:2)	10 ± 1.07	32	N/A
Skh-AMP1:Cr-ACP1 (4:4)	11 ± 3.47	20	N/A
Skh-AMP1:Cr-ACP1 (8:8)	13 ± 9.96	15	N/A
Skh-AMP1:Cr-ACP1 (16:16)	25 ± 15.10	30	N/A
Skh-AMP1:Cr-ACP1 (32:32)	19 ± 3.32	34	N/A

[a] Expected inhibition in growth was calculated using the Abbott formula*: $I_{exp} = x + y - (xy/100)$* (Abbott, 1925), where *x* and *y* are the observed percent inhibition values for each corresponding single peptide treatment for *P. carotovorum* (Table 30 and 32). [b] Interactions are considered synergistic (+) if the I_{exp} is lower than the I_{obs} , antagonistic (-) if I_{exp} is higher than I_{obs}, and additive (=) if they are equal (Kosman & Cohen, 1996). [c] The mean value ± standard error.

Table 38 Effect and interaction of Cn-AMP1 combined with Cr-ACP1 on inhibiting germination of *Pectobacterium carotovorum in vitro*

Growth inhibition *Pectobacterium carotovorum*			
Peptide Concentrations (µM)	**Observed (%)**	**Expected (%)[b]**	**Interaction[c]**
Cn-AMP1:Cr-ACP1 (0.25:0.25)	-8 ± 4.52[d]	-1	N/A
Cn-AMP1:Cr-ACP1 (0.5:0.5)	6 ± 9.96	4	N/A
Cn-AMP1:Cr-ACP1 (1:1)	7 ± 4.00	-3	N/A
Cn-AMP1:Cr-ACP1 (2:2)	29* ± 6.60[a]	19	+
Cn-AMP1:Cr-ACP1 (4:4)	21 ± 4.92	18	N/A
Cn-AMP1:Cr-ACP1 (8:8)	10 ± 1.74	14	N/A
Cn-AMP1:Cr-ACP1 (16:16)	8 ± 4.50	41	N/A
Cn-AMP1:Cr-ACP1 (32:32)	25* ± 5.55	43	-

[a] Means followed by an asterisk (*) are significantly different from the no peptide control at P≤0.05. [b] Expected inhibition in growth was calculated using the Abbott formula*:* $I_{exp} = x + y - (xy/100)$ (Abbott, 1925), where *x* and *y* are the observed percent inhibition values for each corresponding single peptide treatment for *P. carotovorum* (Table 31-32). [c] Interactions are considered synergistic (+) if the I_{exp} is lower than the I_{obs} , antagonistic (-) if I_{exp} is higher than I_{obs}, and additive (=) if they are equal (Kosman & Cohen, 1996). [d] The mean value ± standard error.

3.1.4 *Pectobacterium carotovorum* subsp. *atrosepticum*. When the peptides were tested alone against *P. atrosepticum*, there was no statistically significant inhibition from any peptide or combination at the concentrations tested. The highest growth inhibition for a single peptide was observed with Skh-AMP1, which achieved 34% inhibition at 4 µM. Although at only 1 µM Cn-AMP1 achieved 33% inhibition (Fig. 12). The Na-dichloroisocyanurate control achieved 24% inhibition at 50 µM, which increased to 87% at 5000 µM, which was the highest concentration tested for this pathogen.

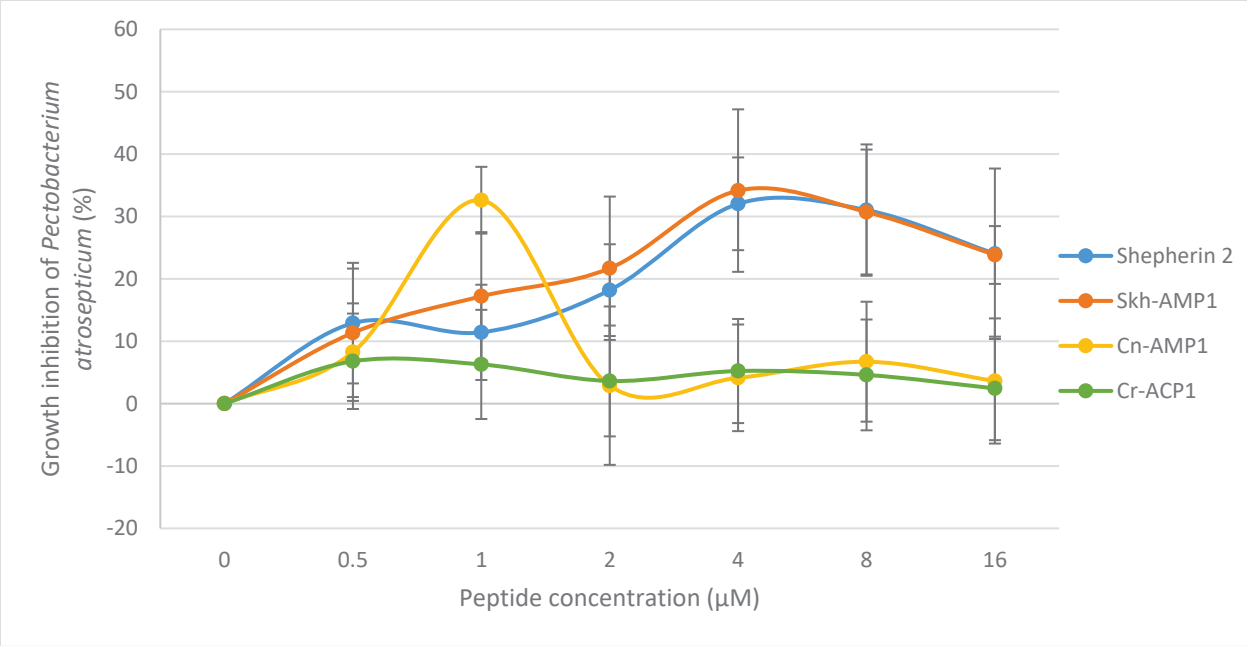

Figure 12 Effect of Shepherin 2, Skh-AMP1, Cr-ACP1, and Cn-AMP1 *in vitro* on the growth of *P. atrosepticum*, determined by absorbance at OD_{600} after 24 h of incubation with the bacterium. Results for concentration 32 µM – 64 µM are not included in this figure to focus attention on the lower concentrations and because the results do not show any significance in that range. Values are the means of three separate experiments; bars are the standard errors.

Table 39 Effect of Shepherin 2 on inhibiting the growth of *Pectobacterium atrosepticum in vitro*

Growth inhibition *Pectobacterium atrosepticum*	
Shepherin 2 Concentration (µM)	**Observed Inhibition (%)**
0.5	13 ± 9.66[a]
1	11 ± 7.63
2	18 ± 7.36
4	32 ± 7.43
8	31 ± 10.53
16	24 ± 13.66
32	6 ± 10.32
64	-28 ± 16.10

[a] The mean value ± standard error.

Table 40 Effect of Skh-AMP1 on inhibiting the growth of *Pectobacterium atrosepticum in vitro*

Growth inhibition *Pectobacterium atrosepticum*	
Skh-AMP1 Concentration (µM)	**Observed Inhibition (%)**
0.5	11 ± 10.30
1	17 ± 10.29
2	22 ± 11.49
4	34 ± 13.02
8	31 ± 10.01
16	24 ± 4.63
32	12 ± 9.02
64	6 ± 11.14

[a] The mean value ± standard error.

Table 41 Effect of Cn-AMP1 on inhibiting the growth of *Pectobacterium atrosepticum in vitro*

Growth inhibition *Pectobacterium atrosepticum*	
Cn-AMP1 Concentration (µM)	**Observed Inhibition (%)**
0.5	8 ± 7.82[a]
1	33 ± 5.35
2	3 ± 12.69
4	4 ± 8.55
8	7 ± 9.61
16	4 ± 10.03
32	6 ± 10.58
64	-3 ± 13.62

[a] The mean value ± standard error.

Table 42 Effect of Cr-ACP1 on inhibiting the growth of *Pectobacterium atrosepticum in vitro*

Growth inhibition *Pectobacterium atrosepticum*	
Cr-ACP1 Concentration (µM)	**Observed Inhibition (%)**
0.5	7 ± 7.65[a]
1	6 ± 8.75
2	4 ± 8.89
4	5 ± 8.35
8	5 ± 8.88
16	2 ± 8.30
32	-1 ± 10.07
64	-8 ± 13.13

[a] The mean value ± standard error.

The strongest inhibition for the double peptides was 36% at 16 µM by Skh-AMP1 and Cn-AMP1; however, this result was not statistically significant (Fig. 13, Tables 43-48).

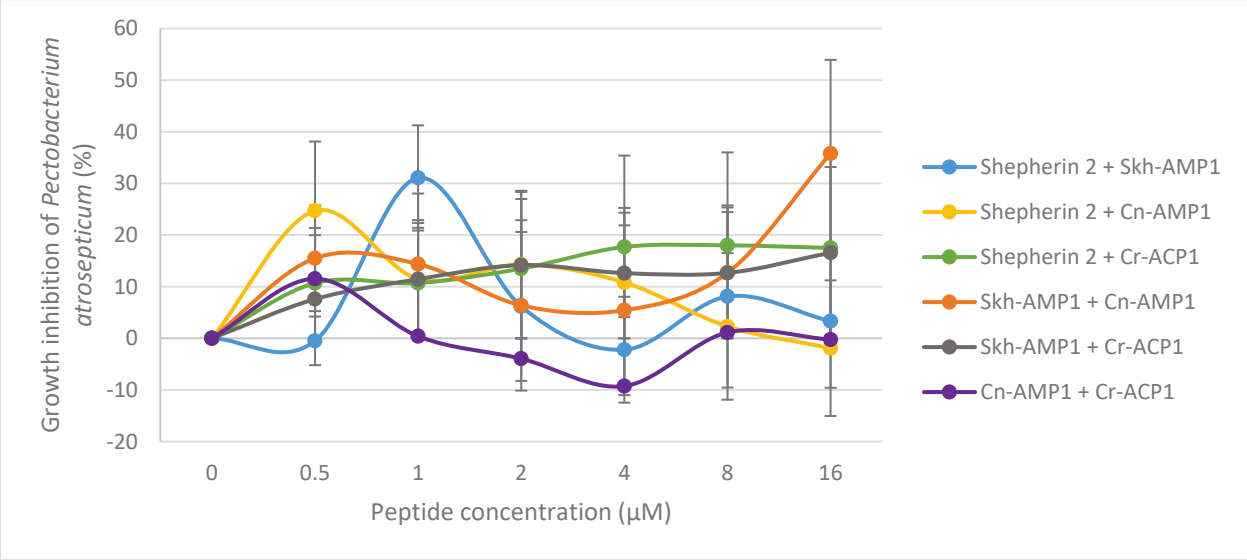

Figure 13 Effect of Shepherin 2, Skh-AMP1, Cr-ACP1, and Cn-AMP1 in combinations of 2 (1:1) *in vitro* on the growth of *P. atrosepticum*, determined by absorbance at OD_{600} after 24 h of incubation with the bacterium. Results for concentration 16 µM – 64 µM are not included in this figure to focus attention on the lower concentrations and because the results do not show any significance in that range. Values are the means of three separate experiments.No statistical significance ($p \leq 0.05$) as determined by single factor ANOVA followed by Dunnett's test.

Table 43 Effect and interaction of Shepherin 2 combined with Skh-AMP1 on inhibiting germination of *Pectobacterium atrosepticum in vitro*

Growth inhibition *Pectobacterium atrosepticum*			
Peptide Concentrations (µM)	**Observed (%)**	**Expected (%)[a]**	**Interaction[b]**
Shepherin 2:Skh-AMP1 (0.25:0.25)	0 ± 4.70[c]	23	N/A
Shepherin 2:Skh-AMP1 (0.5:0.5)	31 ± 10.19	26	N/A
Shepherin 2:Skh-AMP1 (1:1)	6 ± 14.42	36	N/A
Shepherin 2:Skh-AMP1 (2:2)	-2 ± 10.25	55	N/A
Shepherin 2:Skh-AMP1 (4:4)	8 ± 17.64	52	N/A
Shepherin 2:Skh-AMP1 (8:8)	3 ± 12.88	42	N/A
Shepherin 2:Skh-AMP1 (16:16)	-6 ± 16.94	17	N/A
Shepherin 2:Skh-AMP1 (32:32)	-14 ± 9.03	-20	N/A

[a] Expected inhibition in growth was calculated using the Abbott formula: $I_{exp} = x + y - (xy/100)$ (Abbott, 1925), where x and y are the observed percent inhibition values for each corresponding single peptide treatment for *P. atrosepticum* (Table 39-40).[b] Interactions are considered synergistic (+) if the I_{exp} is lower than the I_{obs} , antagonistic (-) if I_{exp} is higher than I_{obs}, and additive (=) if they are equal (Kosman & Cohen, 1096). [c] The mean value ± standard error.

Table 44 Effect and interaction of Shepherin combined with Cn-AMP1 on inhibiting germination of *Pectobacterium atrosepticum in vitro*

Growth inhibition *Pectobacterium atrosepticum*			
Peptide Concentrations (µM)	**Observed (%)**	**Expected (%)[a]**	**Interaction[b]**
Shepherin 2:Cn-AMP1 (0.25:0.25)	25 ± 13.43[c]	20	N/A
Shepherin 2:Cn-AMP1 (0.5:0.5)	11 ± 10.87	40	N/A
Shepherin 2:Cn-AMP1 (1:1)	14 ± 14.29	20	N/A
Shepherin 2:Cn-AMP1 (2:2)	11 ± 13.50	35	N/A
Shepherin 2:Cn-AMP1 (4:4)	2 ± 14.20	36	N/A
Shepherin 2:Cn-AMP1 (8:8)	-2 ± 13.14	27	N/A
Shepherin 2:Cn-AMP1 (16:16)	-2 ± 13.79	12	N/A
Shepherin 2:Cn-AMP1 (32:32)	-13 ± 11.69	-32	N/A

[a] Expected inhibition in growth was calculated using the Abbott formula*: $I_{exp} = x + y - (xy/100)$* (Abbott, 1925), where *x* and *y* are the observed percent inhibition values for each corresponding single peptide treatment for *P. atrosepticum* (Table 39 and 41).[b] Interactions are considered synergistic (+) if the I_{exp} is lower than the I_{obs} , antagonistic (-) if I_{exp} is higher than I_{obs}, and additive (=) if they are equal (Kosman & Cohen, 1096). [c] The mean value ± standard error.

Table 45 Effect and interaction of Shepherin combined with Cr-ACP1 on inhibiting germination of *Pectobacterium atrosepticum in vitro*

Growth inhibition *Pectobacterium atrosepticum*			
Peptide Concentrations (µM)	**Observed (%)**	**Expected (%)[a]**	**Interaction[b]**
Shepherin 2:Cr-ACP1 (0.25:0.25)	8 ± 10.69[c]	19	N/A
Shepherin 2:Cr-ACP1 (0.5:0.5)	4 ± 10.70	16	N/A
Shepherin 2:Cr-ACP1 (1:1)	1 ± 13.49	21	N/A
Shepherin 2:Cr-ACP1 (2:2)	3 ± 17.70	35	N/A
Shepherin 2:Cr-ACP1 (4:4)	-7 ± 18.00	34	N/A
Shepherin 2:Cr-ACP1 (8:8)	3 ± 17.50	26	N/A
Shepherin 2:Cr-ACP1 (16:16)	-4 ± 14.79	5	N/A
Shepherin 2:Cr-ACP1 (32:32)	-21 ± 8.92	-38	N/A

[a] Expected inhibition in growth was calculated using the Abbott formula*: $I_{exp} = x + y - (xy/100)$* (Abbott, 1925), where *x* and *y* are the observed percent inhibition values for each corresponding single peptide treatment for *P. atrosepticum* (Table 39 and 42).[b] Interactions are considered synergistic (+) if the I_{exp} is lower than the I_{obs} , antagonistic (-) if I_{exp} is higher than I_{obs}, and additive (=) if they are equal (Kosman & Cohen, 1096). [c] The mean value ± standard error.

Table 46 Effect and interaction of Skh-AMP1 combined with Cn-AMP1 on inhibiting germination of *Pectobacterium atrosepticum in vitro*

Growth inhibition *Pectobacterium atrosepticum*			
Peptide Concentrations (µM)	**Observed (%)**	**Expected (%)[a]**	**Interaction[b]**
Skh-AMP1:Cn-AMP1 (0.25:0.25)	16 ± 10.24[c]	18	N/A
Skh-AMP1:Cn-AMP1 (0.5:0.5)	14 ± 13.65	44	N/A
Skh-AMP1:Cn-AMP1 (1:1)	6 ± 16.50	24	N/A
Skh-AMP1:Cn-AMP1 (2:2)	5 ± 16.44	37	N/A
Skh-AMP1:Cn-AMP1 (4:4)	13 ± 11.76	36	N/A
Skh-AMP1:Cn-AMP1 (8:8)	36 ± 18.12	27	N/A
Skh-AMP1:Cn-AMP1 (16:16)	24 ± 15.83	17	N/A
Skh-AMP1:Cn-AMP1 (32:32)	16 ± 10.81	3	N/A

[a] Expected inhibition in growth was calculated using the Abbott formula*:* $I_{exp} = x + y - (xy/100)$ (Abbott, 1925), where *x* and *y* are the observed percent inhibition values for each corresponding single peptide treatment for *P. atrosepticum* (Table 40-41).[b] Interactions are considered synergistic (+) if the I_{exp} is lower than the I_{obs} , antagonistic (-) if I_{exp} is higher than I_{obs}, and additive (=) if they are equal (Kosman & Cohen, 1096). [c] The mean value ± standard error.

Table 47 Effect and interaction of Skh-AMP1 combined with Cr-ACP1 on inhibiting germination of *Pectobacterium atrosepticum in vitro*

Growth inhibition *Pectobacterium atrosepticum*			
Peptide Concentrations (µM)	**Observed (%)**	**Expected (%)[a]**	**Interaction[b]**
Skh-AMP1:Cr-ACP1 (0.25:0.25)	4 ± 7.59[c]	17	N/A
Skh-AMP1:Cr-ACP1 (0.5:0.5)	6 ± 11.45	22	N/A
Skh-AMP1:Cr-ACP1 (1:1)	14 ± 14.17	25	N/A
Skh-AMP1:Cr-ACP1 (2:2)	11 ± 12.63	37	N/A
Skh-AMP1:Cr-ACP1 (4:4)	13 ± 12.67	34	N/A
Skh-AMP1:Cr-ACP1 (8:8)	8 ± 16.58	26	N/A
Skh-AMP1:Cr-ACP1 (16:16)	10 ± 12.29	11	N/A
Skh-AMP1:Cr-ACP1 (32:32)	-3 ± 4.48	-2	N/A

[a] Expected inhibition in growth was calculated using the Abbott formula*:* $I_{exp} = x + y - (xy/100)$ (Abbott, 1925), where *x* and *y* are the observed percent inhibition values for each corresponding single peptide treatment for *P. atrosepticum* (Table 40 and 42).[b] Interactions are considered synergistic (+) if the I_{exp} is lower than the I_{obs} , antagonistic (-) if I_{exp} is higher than I_{obs}, and additive (=) if they are equal (Kosman & Cohen, 1096). [c] The mean value ± standard error.

Table 48 Effect and interaction of Cn-AMP1 combined with Cr-ACP1 on inhibiting germination of *Pectobacterium atrosepticum in vitro*

Growth inhibition *Pectobacterium atrosepticum*			
Peptide Concentrations (µM)	**Observed (%)**	**Expected (%)[a]**	**Interaction[b]**
Cn-AMP1:Cr-ACP1 (0.25:0.25)	12 ± 8.45[c]	14	N/A
Cn-AMP1:Cr-ACP1 (0.5:0.5)	0 ± 13.19	37	N/A
Cn-AMP1:Cr-ACP1 (1:1)	-4 ± 11.15	7	N/A
Cn-AMP1:Cr-ACP1 (2:2)	-9 ± 13.35	9	N/A
Cn-AMP1:Cr-ACP1 (4:4)	1 ± 1.59	12	N/A
Cn-AMP1:Cr-ACP1 (8:8)	0 ± 3.06	6	N/A
Cn-AMP1:Cr-ACP1 (16:16)	-1 ± 2.79	5	N/A
Cn-AMP1:Cr-ACP1 (32:32)	-8 ± 1.13	-11	N/A

[a] Expected inhibition in growth was calculated using the Abbott formula*: $I_{exp} = x + y – (xy/100)$* (Abbott, 1925), where *x* and *y* are the observed percent inhibition values for each corresponding single peptide treatment for *P. atrosepticum* (Table 41-42).[b] Interactions are considered synergistic (+) if the I_{exp} is lower than the I_{obs} , antagonistic (-) if I_{exp} is higher than I_{obs}, and additive (=) if they are equal (Kosman & Cohen, 1096). [c] The mean value ± standard error.

3.2 Cytotoxic effects of HDPs *in vitro*

The application of HDPs for the development of disease-resistant crops will only be useful if they are not harmful to their host plants and mammals. To address this issue, I have evaluated human kidney cells and potato mesophyll protoplasts for viability, by culturing them *in vitro* in the presence of the HDPs.

3.2.1 Cytotoxicity to human cells. These graphs (Fig. 14, 15, & 16) show the results of the human cell cytotoxicity assays. No statistically significant inhibitory effects were observed for any of the peptides, alone or in combinations, at any tested concentration ranging from 0 to 100 µM.

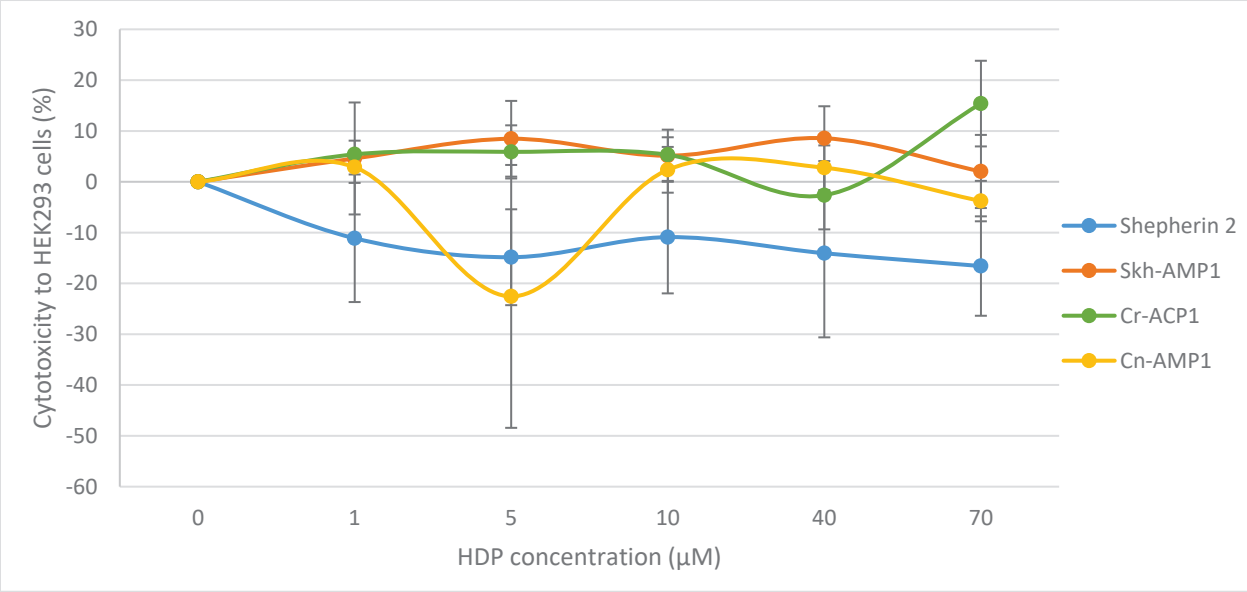

Figure 14 Percent cytotoxicity to HEK293 human embryonic kidney cells after 24-h incubation with peptides (Shepherin 2, Skh-AMP1, Cn-AMP1, and Cr-ACP1), as determined by absorbance at OD_{600}. Results for 100 µM are not included in this figure to focus attention on the concentrations relevant to the antimicrobial activity and because the results do not show any significance in that range. No statistical significance was found between the cytotoxicity value and no peptide control value ($p \leq 0.05$) as determined by single factor ANOVA followed by Dunnett's test. Values are the means of 3 technical repeats and bars are the standard error of the mean.

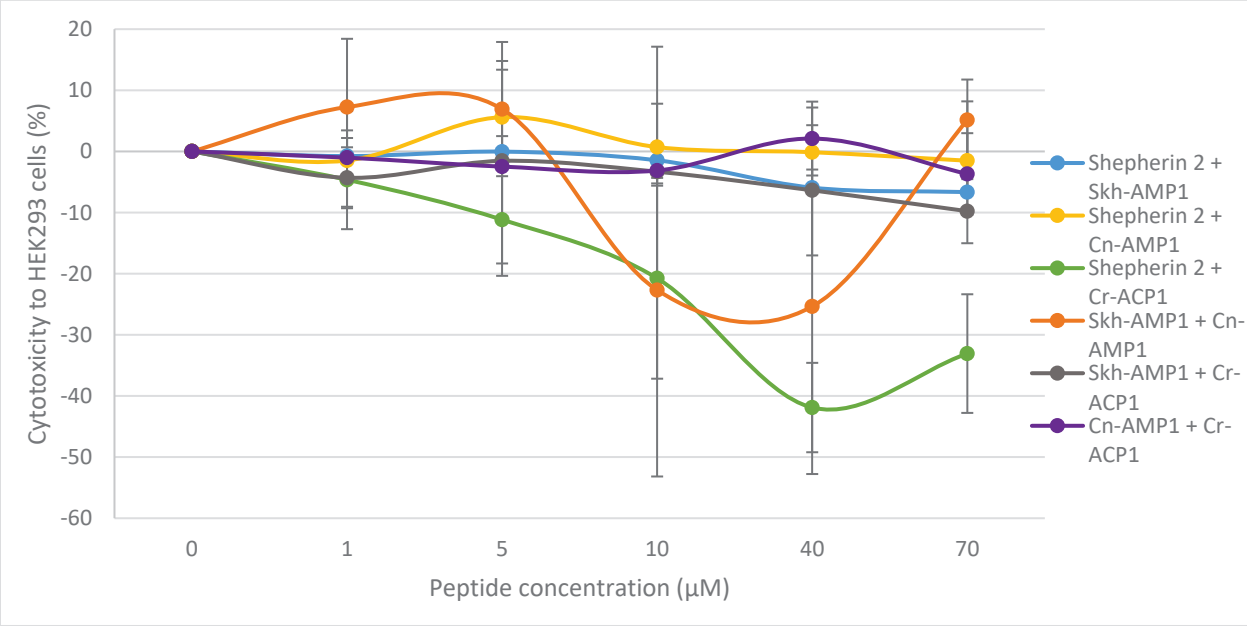

Figure 15 Percent cytotoxicity to HEK293 human embryonic kidney cells after 24-h incubation with combinations of two peptides (1:1 ratio) (Shepherin 2, Skh-AMP1, Cn-AMP1, and Cr-ACP1), as determined by absorbance at OD_{600}. Results for 100 µM are not included in this figure

to focus attention on the concentrations relevant to the antimicrobial activity and because the results do not show any significance in that range. No statistical significance was found between the cytotoxicity value and no peptide control value ($p \leq 0.05$) as determined by single factor ANOVA followed by Dunnett's test. Values are the means of 3 technical repeats and bars are the standard error of the mean.

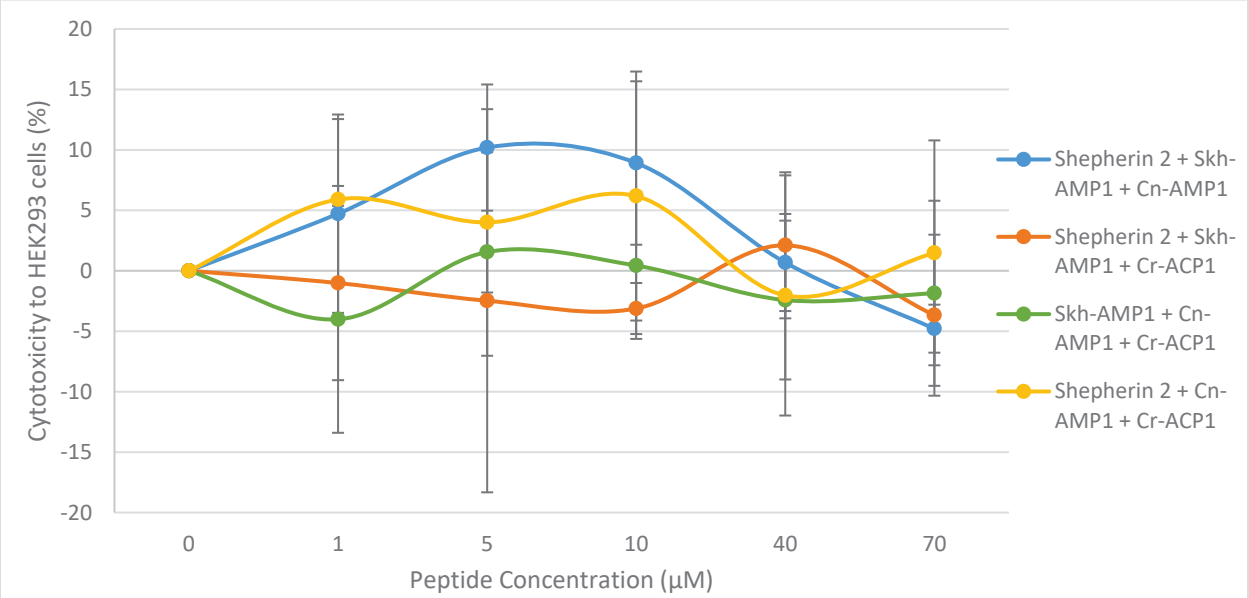

Figure 16 Percent cytotoxicity to HEK293 human embryonic kidney cells after 24-h incubation with combinations of three peptides (1:1:1 ratio) (Shepherin 2, Skh-AMP1, Cn-AMP1, and Cr-ACP1), as determined by absorbance at OD_{600}. Results for 100 µM are not included in this figure to focus attention on the concentrations relevant to the antimicrobial activity and because the results do not show any significance in that range. No statistical significance was found between the cytotoxicity value and no peptide control value ($p \leq 0.05$) as determined by single factor ANOVA followed by Dunnett's test. Values are the means of 3 technical repeats and bars are the standard error of the mean.

3.2.2 Phytotoxicity to potato mesophyll protoplasts. The protoplast phytotoxicity assays were based on staining the potato mesophyll protoplast cultures with Evan's blue and neutral red dyes (three repeats of each) following incubation in the presence of the HDPs. The two stains showed similar results, but the protoplasts stained with neutral red generally appeared to be healthier because the blue stain made the cellular debris in the sample more noticeable.

When the protoplasts were stained with Evan's blue, cell viability was impacted to a statistically significant degree with Shepherin 2, Skh-AMP1 and Cr-ACP1. Shepherin 2 caused

the greatest reduction in viability, reaching a maximum value of 35% toxicity at 100 µM and the loss of viability was statistically significant at all other concentrations tested as well. Skh-AMP1 and Cr-ACP1 only had a significant impact at 70 and 100 µM, which was a higher inhibitory concentration than that observed in the antimicrobial assays (Fig. 17).

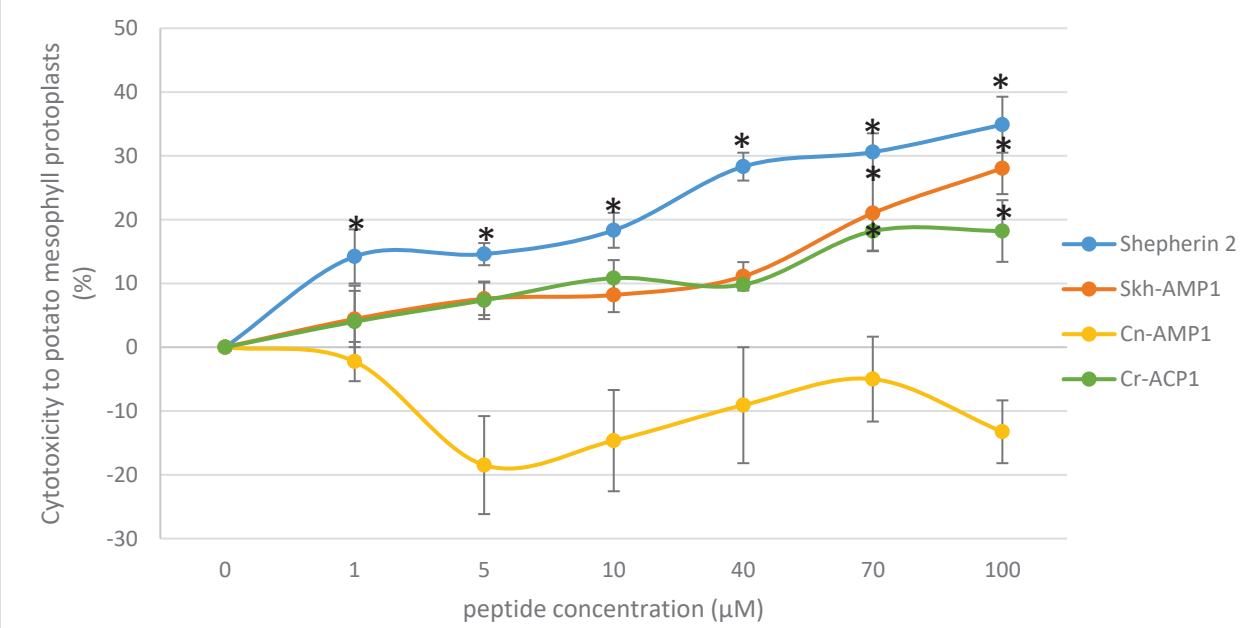

Figure 17 Percent phytotoxicity to potato mesophyll protoplasts after 24-h incubation with single peptides (Shepherin 2, Skh-AMP1, Cn-AMP1, and Cr-ACP1), as determined by visual inspection after staining with Evan's blue. Values are the means of three separate experiments; bars are the standard errors of the mean; asterisk (*) denotes a statistically significant difference compared to the no peptide control ($p \leq 0.05$) as determined by single factor ANOVA followed by Dunnett's test.

When the protoplasts were stained with neutral red, the trend was similar but a reduced impact to cell viability was observed. The only statistically significant phytotoxic effects were observed with Shepherin 2, Sk-AMP1, and Cr-ACP1 at 100 µM, with phytotoxicities of 36%, 24%, and 16%, respectively (Fig. 18).

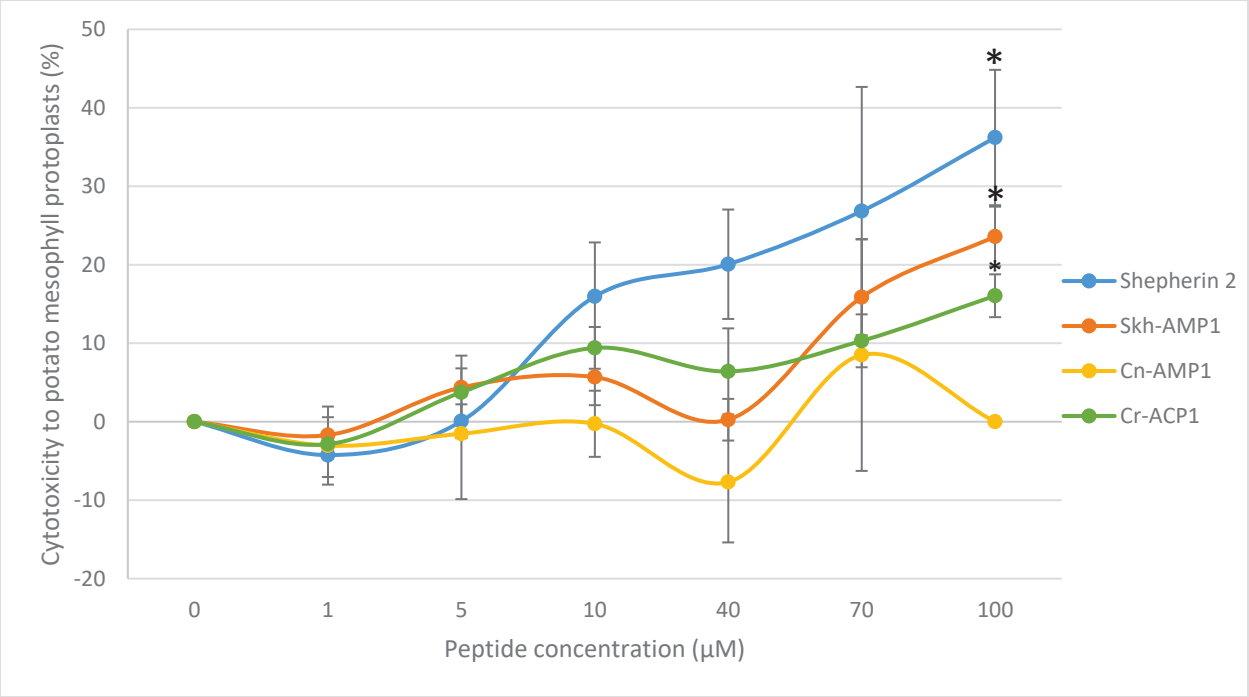

Figure 18 Percent phytotoxicity to potato mesophyll protoplasts after 24-h incubation with peptides (Shepherin 2, Skh-AMP1, Cn-AMP1, and Cr-ACP1), as determined by visual inspection after staining with neutral red. Values are the means of three separate experiments; bars are the standard errors of the mean; asterisk (*) denotes a statistically significant difference compared to the no peptide control ($p \leq 0.05$) as determined by single factor ANOVA followed by Dunnett's test.

Figure 19 shows the appearance of the protoplasts after incubation with Shepherin 2, the most toxic HDP to the protoplasts: the representative images include control protoplast culture and the culture treated with 100 µM Shepherin 2, the highest concentration tested in this study. The Evan's blue stained dead cells and the neutral red stained the vacuoles of viable cells.

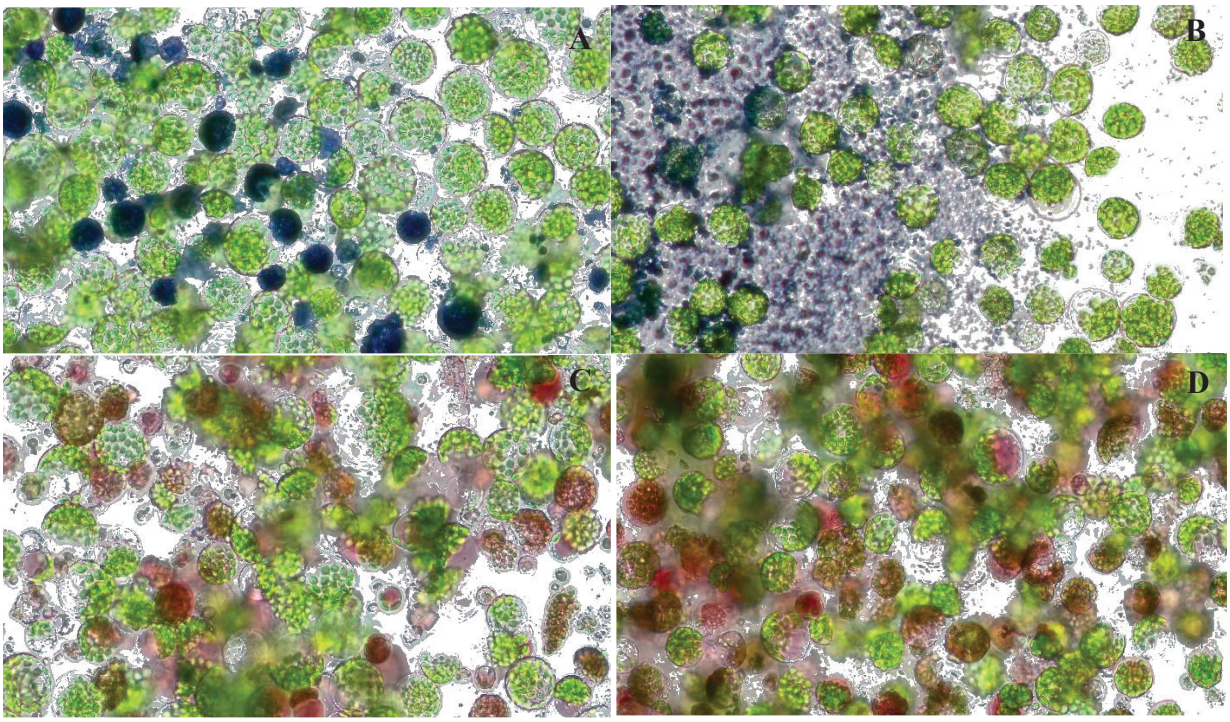

Figure 19 Potato mesophyll protoplasts stained with either Evan's blue or neutral red stain after 24-hours incubation with Shepherin 2. A. Evan's blue; no peptide control. B. Evan's blue; 100 µM Shepherin 2. C. Neutral red; no peptide control. D. Neutral red; 100 µM.

When the peptides were evaluated in combinations of two, the deleterious effects to the protoplasts increased dramatically for Shepherin 2 when combined with either Skh-AMP1 or Cn-AMP1. When Shepherin 2 was combined with Skh-AMP1 at 40 micromoles, percent phytotoxicity increased from only 16% to 62%, and then to 85% at 70 and 100 µM respectively. Shepherin 2 combined with Cn-AMP1 produced 43%, 48%, and 61% phytotoxicity at the same concentrations (Fig. 20).

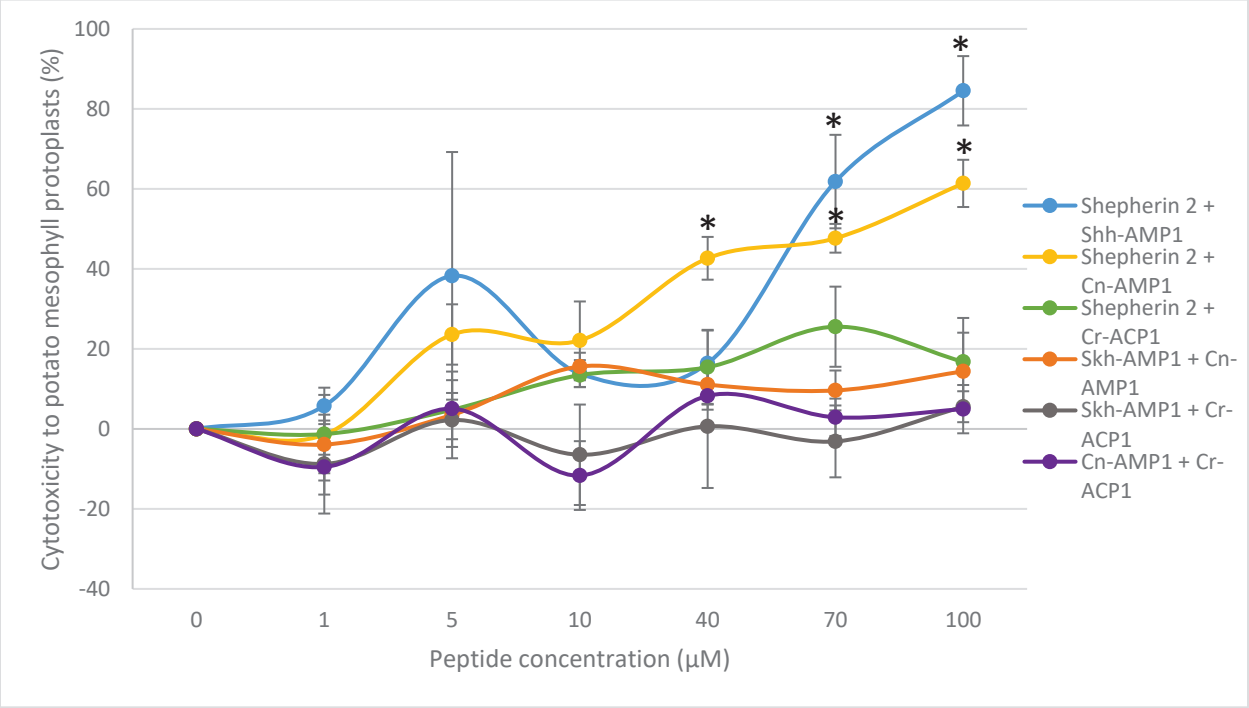

Figure 20 Percent phytotoxicity to potato mesophyll protoplasts after 24-hour incubation with peptides in combinations of two (1:1 ratio) (Shepherin 2, Skh-AMP1, Cn-AMP1, and Cr-ACP1), as determined by visual inspection after staining with Evan's blue. Values are the means of three experiments; bars are the standard errors of the mean; asterisk (*) denotes a statistically significant difference compared to the no peptide control ($p \leq 0.05$) as determined by single factor ANOVA followed by Dunnett's test.

This phytotoxicity trend was closely matched when the protoplasts were stained with neutral red. Shepherin 2 combined with Skh-AMP1 reduced protoplast viability by 35% at 40 µM, which increased to 77% at 100 µM. When Shepherin 2 was combined with Cn-AMP1, the protoplast viability was reduced by 37% at 10 µM and by 61% at 100 µM (Fig. 21).

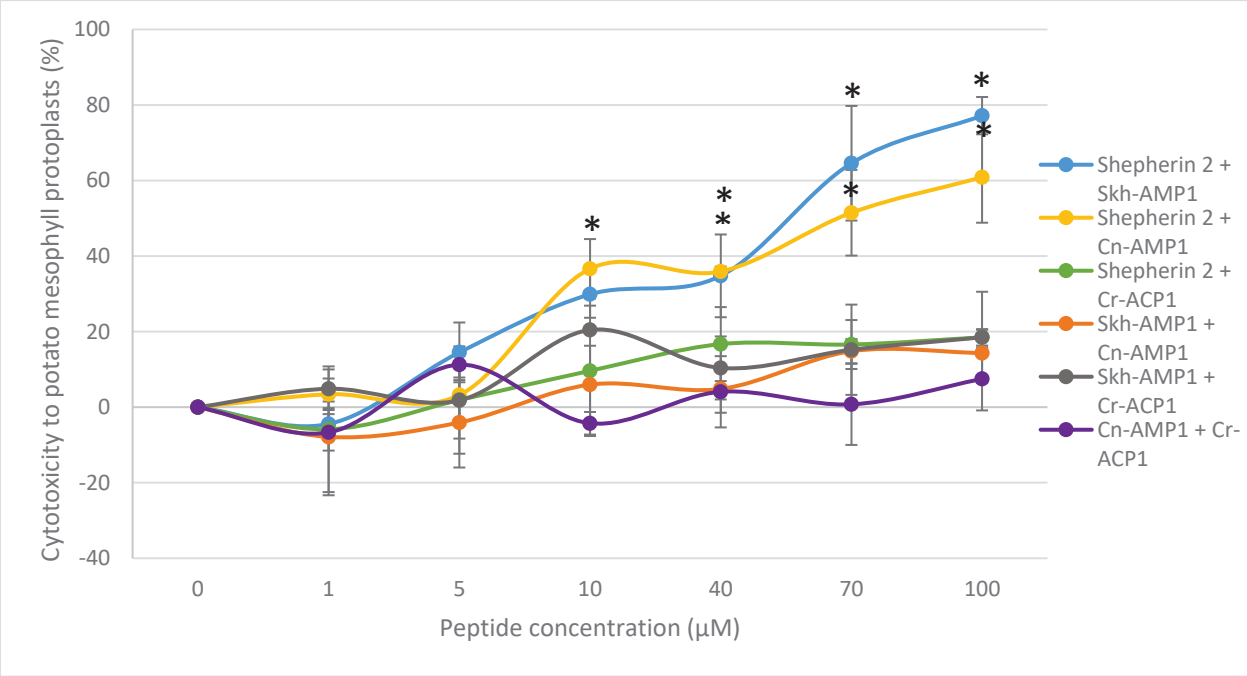

Figure 21 Percent phytotoxicity to potato mesophyll protoplasts after 24-h incubation with peptides in combinations of two (1:1 ratio) (Shepherin 2, Skh-AMP1, Cn-AMP1, and Cr-ACP1), as determined by visual inspection after staining with neutral red. Values are the means of three experiments; bars are the standard errors of the mean; asterisk (*) denotes a statistically significant difference compared to the no peptide control ($p \leq 0.05$) as determined by single factor ANOVA followed by Dunnett's test.

The triple peptide combinations proved to be far less toxic to the protoplasts. The experiments which utilized Evan's blue displayed no significant levels of toxicity to the protoplasts. The strongest phytotoxicity was produced by Shepherin 2 when combined with Skh-AMP1 and Cn-AMP1, with a mean of 28%±9.11 toxicity at 100 µM.

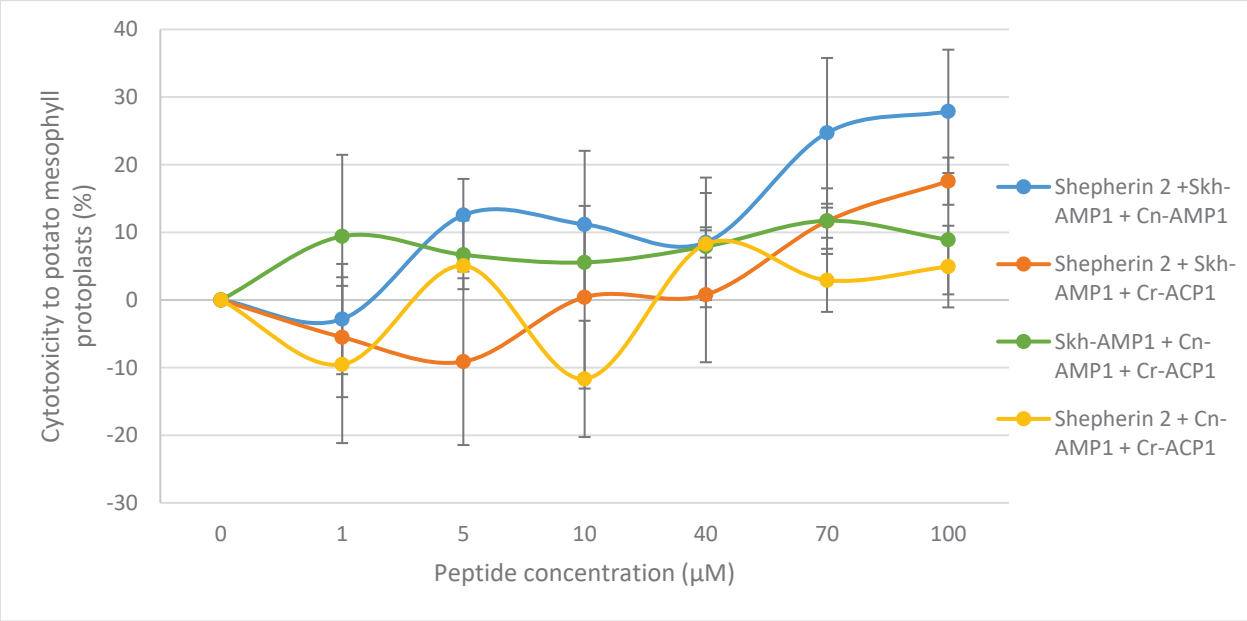

Figure 22 Percent phytotoxicity to potato mesophyll protoplasts after 24-h incubation with peptides in combinations of three (1:1:1 ratio) (Shepherin 2, Skh-AMP1, Cn-AMP1, and Cr-ACP1), as determined by visual inspection after staining with Evans blue. Values are the means of three experiments; bars are the standard errors of the mean. No statistical significance between cytotoxicity values and the no peptide control value ($p \leq 0.05$) as determined by single factor ANOVA followed by Dunnett's test.

When stained with the neutral red dye, Shepherin 2 combined with Skh-AMP1 and Cn-AMP1 displayed significant phytotoxicity at 70 and 100 µM, which caused 22% and 31% cell death, respectively.

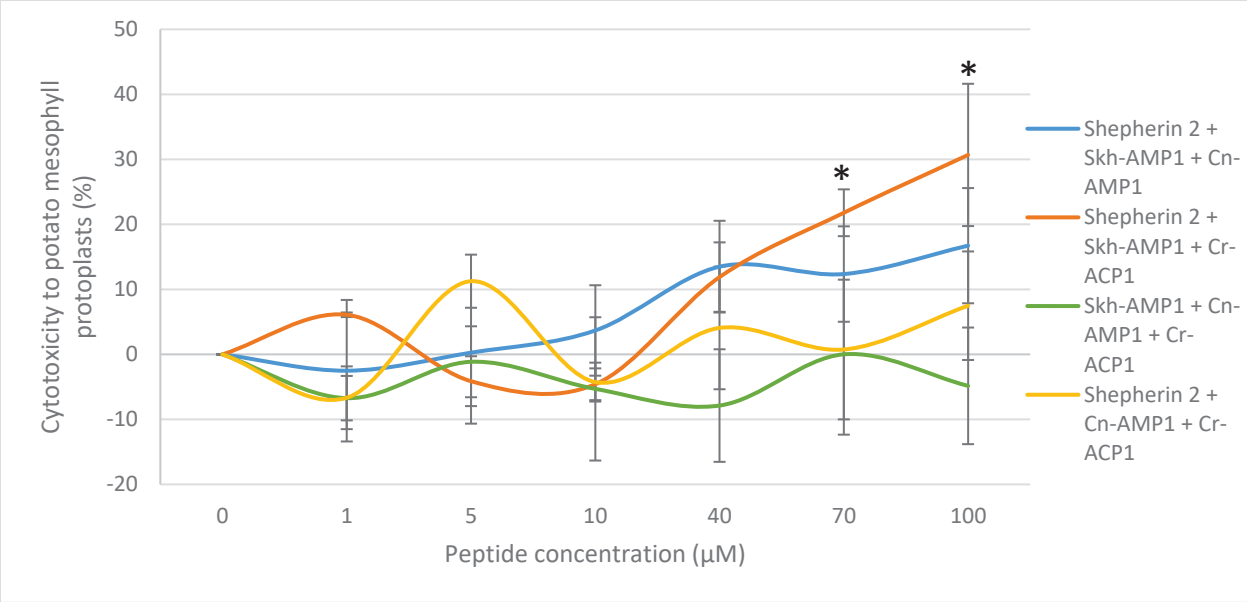

Figure 23 Percent phytotoxicity to potato mesophyll protoplasts after 24-h incubation with peptides in combinations of three (1:1:1 ratio) (Shepherin 2, Skh-AMP1, Cn-AMP1, and Cr-ACP1), as determined by visual inspection after staining with neutral red. Values are the means of three experiments; bars are the standard errors of the mean; asterisk (*) denotes a statistically significant difference compared to the no peptide control ($p \leq 0.05$) as determined by single factor ANOVA followed by Dunnett's test.

3.3 Production of transgenic potato

3.3.1 Transformation of potato with the PmBiPPro1-3/m-GFP5-ER

construct. The green fluorescent protein (gfp) gene was inserted into a plant expression vector under the control of the truncated 1259 bp wound-inducible *PmBiPPro1-3* promoter from Douglas-fir and introduced into potato plants (*Solanum tuberosum* L. cv. Desiree) using *Agrobacterium*-mediated transformation. From 143 explants cultured on kanamycin-containing selection culture medium, five explants produced green calli (Fig. 24A) and regenerated into plantlets. Putative transgenic lines 2 and 3 were the only morphologically normal lines (Fig. 24B); all other lines displayed abnormalities, such as stunted growth, shortened internodes, and small, dark, waxy leaves. Polymerase chain reaction (PCR) analyses using primers designed to amplify the gfp transgene region confirmed the presence of the transgenes in regenerated plant lines 2B, 3, and 4 (Fig 25).

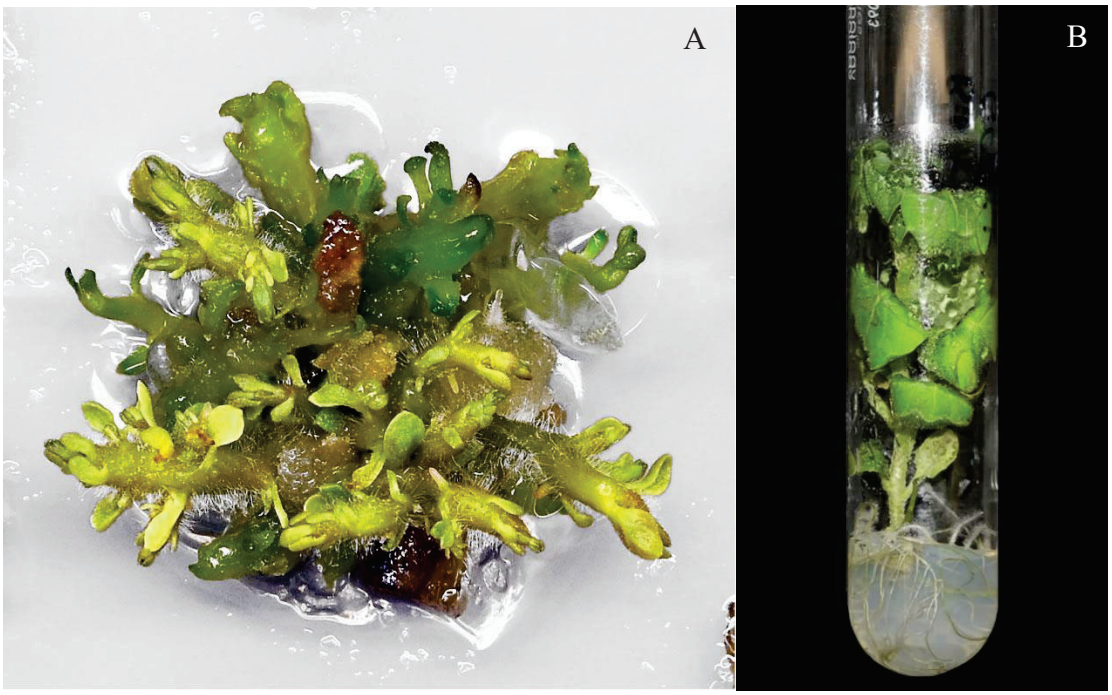

Figure 24 A. *Solanum tuberosum* L. cultivar Desiree callus regenerated from stem explant transformed with PmBiPPro1-3/m-GFP55-ER construct, (line 3). B. *Solanum tuberosum* L. cultivar Desiree PmBiPPro1-3/m-gfp5-ER 4-week-old plantlet (line 3).

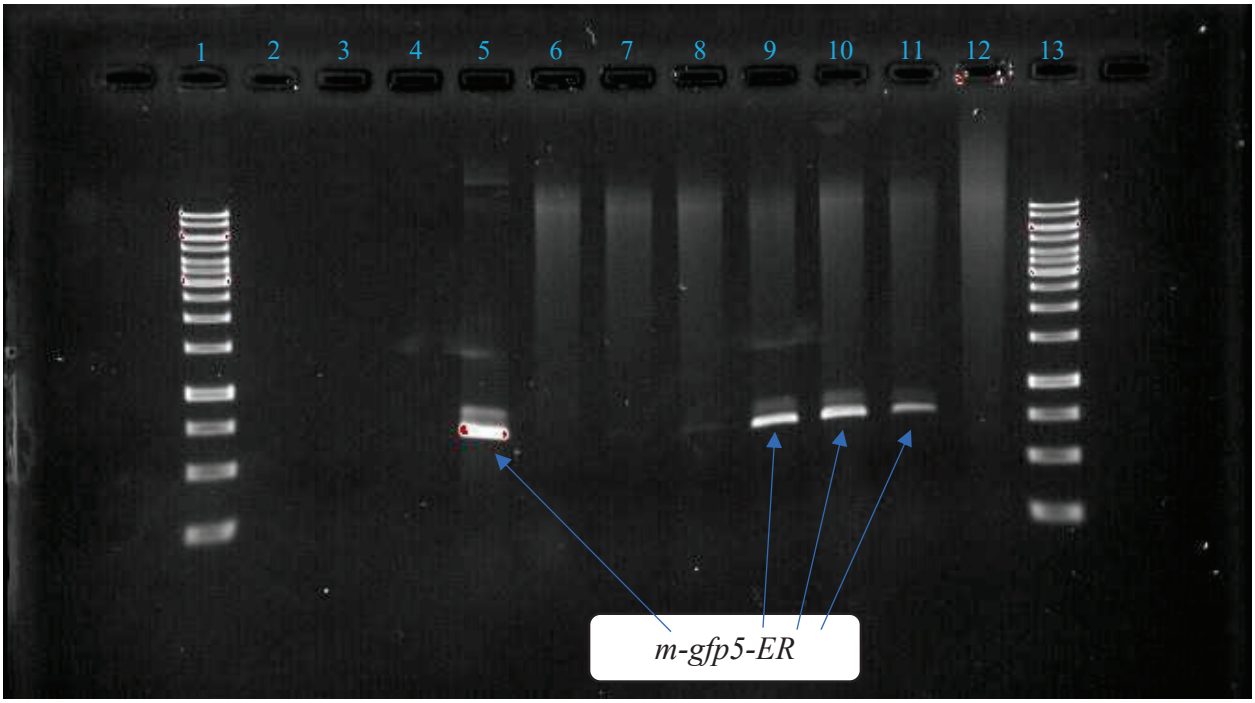

Figure 25 Agarose gel electrophoresis (1%) of the PCR product of the m-GFP5-ER gene from DNA extracted from PmBiPPro1-3/m-GFP5-ER transgenic potato lines: Lanes 1 and 13 - GeneRuler 1 kb DNA ladder; 2 - no template control; 3 - positive control; 4 - left primer control;

5 - right primer control; 6 - Desiree control; 7 - line 1; 8 - line 2; 9 - line 2B; 10 - line 3; 11 – line 4; 12 – line 5.

3.3.2 Transient transformation of tobacco with the PmBiPPro1-3/m-GFP5-ER construct. To confirm the transcriptional activity of the *PmBiPPro1-3* promoter, the leaves of fully grown greenhouse tobacco plants (*Nicotiana tabacum* L.), were inoculated with the suspension of *Agrobacterium* cells containing the PmBiPPro1-3/m-GFP5-ER vector. Green fluorescence was observed under a fluorescence microscope four days after inoculation.

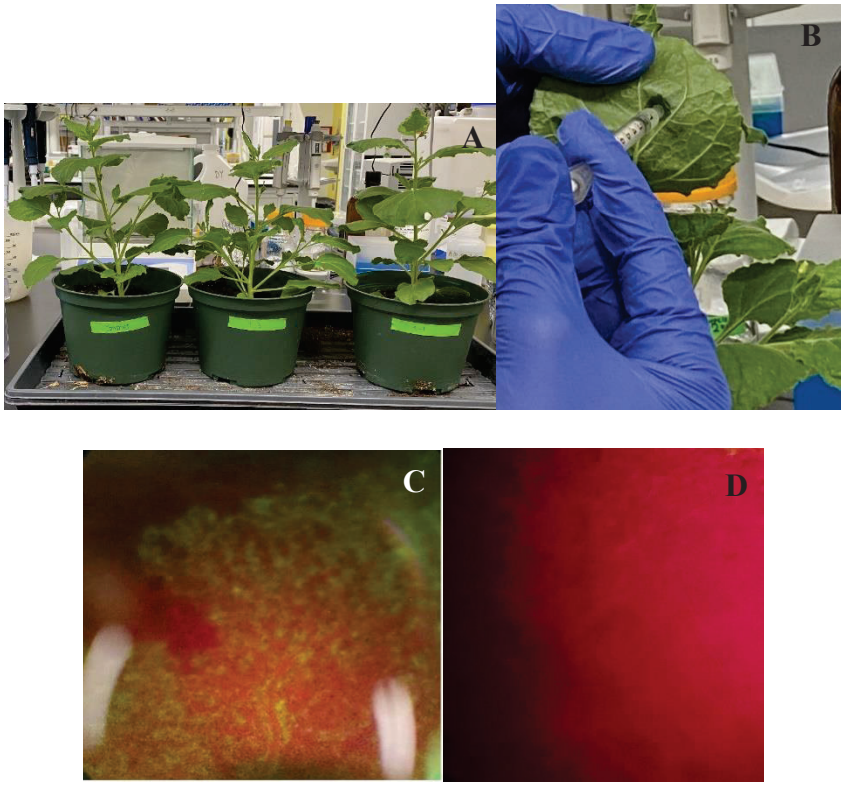

Figure 26 Transient transformation of tobacco with PmBiPPro1-3/m-GFP5-ER vector. A. Greenhouse grown tobacco plants used for transient transformation. B. Inoculation of tobacco leaf with infiltration buffer containing *A. tumefaciens* transformed with PmBipPro1-3/m-GFP5-ER. C. Transient expression of gfp fluorescence in tobacco leaf; the green sections show gfp fluorescence and the red portions show non-transformed sections of the leaf; viewed under fluorescence microscope using gfp filters. D. Buffer only control in tobacco leaf showing non-transformed tissue: viewed under fluorescence microscope using gfp filters.

3.3.3 Transformation of potato with the PmBiPPro1-3/Shepherin2 and CaMV35S/Shepherin2 constructs. Because Shepherin 2 was found to be the most promising

HDP for expression in plants among all peptides tested, the nucleotide sequence encoding for the *Shepherin 2* gene was inserted into plant transformation vectors under the control of one of the following two promoters: the *PmBiPPro1-3* promoter and the constitutive *CaMV 35S* (cauliflower mosaic virus) promoter. These expression constructs were introduced into *S. tuberosum* L. cv. Desiree potato plants via *Agrobacterium* mediated transformation. To date, of 114 *Agrobacterium*-treated explants, two *PmBiPPro1-3/Shepherin2* and three *CaMV35S/Shepherin2* putative transgenic green calli were formed after two months of culture on kanamycin-containing selection medium. In future studies, the plants regenerated from these calli will be subjected to molecular analyses to confirm their transgenic nature and if confirmed to contain the desired transgene, they will be evaluated for enhanced disease resistance using *in planta* antimicrobial assays.

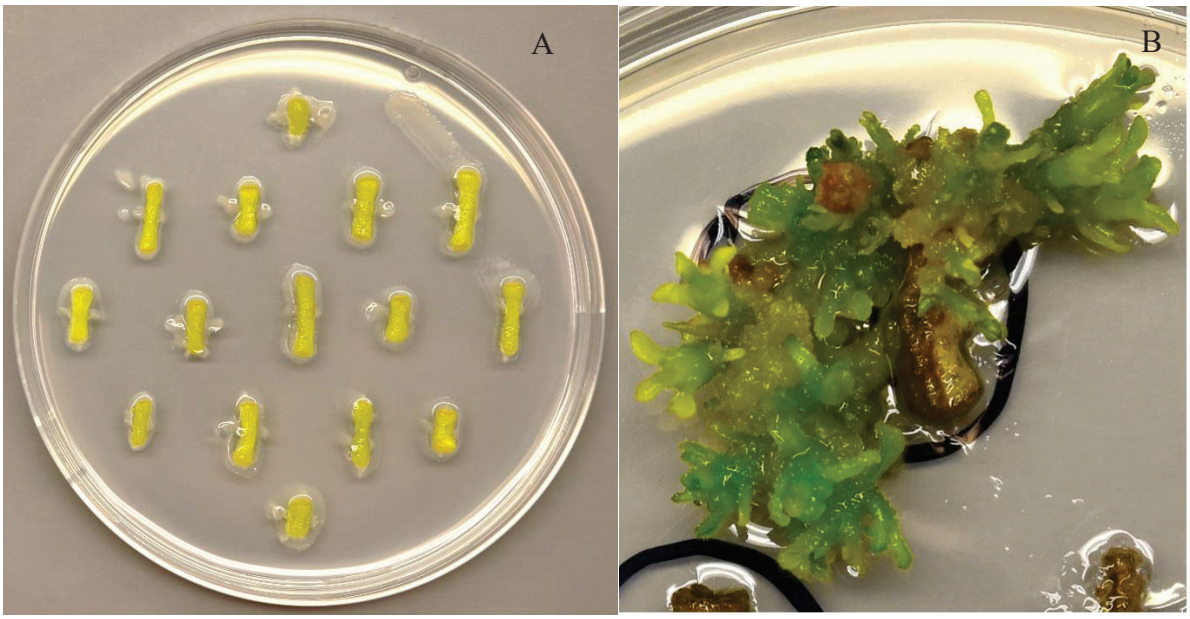

Figure 27 A**.** *Solanum tuberosum* L. cv. Desiree internodal stem segments after 5 days of co-cultivation with *Agrobacterium* cells containing *CaMV 35S/Shepherin2* vector; non-selective media. B. Callus forming on a *CaMV35S/Shepherin2* petiole explant after 53 days on selective PetM media.

4. Discussion

During this study, the antimicrobial activities of four HDPs of plant origin: Shepherin 2, Skh-AMP1, Cn-AMP1, and Cr-ACP1 were evaluated against major potato pathogens *in vitro*. These peptides were also tested in combinations to determine if there were any synergistic or antagonistic interactions occurring between the peptides during the antimicrobial assays. The result of this experiment indicates that Shepherin 2, derived from the roots of shepard's purse, has significant levels of antimicrobial activity *in vitro* against both bacterium *P. carotovorum* and fungus *F. culmorum* while exhibiting low cytotoxicity towards potato protoplasts and mammalian cells, making it a promising candidate for expression *in planta* and development of disease-resistant plants.

4.1 Antimicrobial assays

Of the four peptides evaluated for this study, Shepherin 2 achieved the overall greatest inhibition, both individually and when combined with other peptides. In fact, it was the only peptide to reach over 50% growth inhibition when tested alone and almost every peptide combination, which produced significant levels of inhibition, included Shepherin 2. Every HDP combination, which reached over 50% inhibition, included this peptide.

4.1.1 Single peptides. Park et al. (2000) conducted antimicrobial assays with Shepherin 2 against gram-positive bacteria, gram-negative bacteria, and fungi, including yeast and filamentous fungi. Specifically, they tested *A. alternata* and were unable to achieve 50% inhibition (they tested up to 30 μM), this is comparable to the results with *A. solani* and Shepherin 2 in this experiment. Significant inhibition was not achieved at any tested concentration (up to 100 μM) with any of the tested peptides. Park et al. (2000) also assayed Shepherin 2 against *F. culmorum*, they achieved 50% inhibition at 20 μM, lower inhibition than

the results of this study which found that 8 μM of Shepherin 2 was sufficient to induce 87% inhibition. The discrepancy can probably be explained by the difference in antifungal assay methods because the Park et al. (2000) experiment used absorbance (OD_{600}) to determine the level of fungal inhibition instead of the method employed in this experiment which involved counting germinated and ungerminated conidia, and using those data to calculate growth inhibition. The difference in levels of resistance of the specific fungal culture to Shepherin 2 may have caused some of the discrepancy because natural resistance may vary between laboratory cultures (isolates) of the same species, or it may be the fact that they isolated Shepherin 2 directly from the roots of shepherd's purse which may have introduced some contamination to the peptides, whereas the Shepherin 2 used in our study was chemically synthesized and verified to be pure. Regarding gram-negative bacteria, 56% inhibition was achieved using Shepherin 2 against *P. carotovorum* at 8 μM, which increased to 84% inhibition at 64 μM, the highest concentration tested in the present study. This agreed very closely with the results for *Erwinia herbicola*, a gram-negative pathogenic bacterium that attacks flowering plants: it had 50% inhibition at 7.7 μM (Park et al., 2000).

When the peptides were tested against *A. solani,* none of the peptides alone caused significant inhibition and appeared, in the case of Cn-AMP1 and Skh-AMP1, to promote fungal growth, although not to a significant level. If further experiments are conducted with these two peptides, such as expressing them in crop plants, then further testing will be necessary to make sure that they do not aid some pathogens while destroying others. Although, given that these two HDPs offered little antimicrobial inhibition during the assays carried out, I would not consider them to be very promising for plant protection, especially given the plethora of options currently being discovered. Regarding the results of the *P. atrosepticum* assays, no significant levels of

inhibition were observed with any of the peptides. The highest level of inhibition attained was 32% at 4 μM using Skh-AMP1.

The peptides appeared to be non-toxic to mammalian cells because no significant levels of toxicity to the HEK293 human kidney cells was detected during the cytotoxicity assays. This is supported by studies conducted on Skh-AMP1 and Cr-ACP1 which found negligible levels of toxicity towards red blood cells (Khani et al., 2019; Mandal et al., 2012). To my knowledge, no further studies, aside from the Park et al. (2000) study, have been conducted with Shepherin 2; however, in an experiment by Remuzgo et al. (2014), Shepherin I, a very similar peptide which is part of the Shepherin precursor protein, displayed no hemolytic activity during experiments. On the other hand, the toxicity assays conducted with Shepherin 2 against potato mesophyll protoplasts are more concerning because when the protoplasts were stained with Evan's blue dye the estimated toxicity to the protoplasts was considered statistically significant at all tested concentrations (1 μM to 100 μM). However, the protoplasts stained with neutral red were affected to a significant degree only at 100 μM. The discrepancy seems to be mainly caused by the differences in the dye-cell interactions; the blue dye stains dead cells, which means that all the cellular debris present in the sample were very visible. When the red dye is used, all those debris are far less visible, which causes a higher estimation of protoplast viability relative to the no peptide control. For this reason, I consider the assays in which the Evan's blue dye is used to be a more reliable visual indicator of peptide phytotoxicity than neutral red. Nonetheless, at 16 μM, Shepherin 2 affected viability of only about 20% of potato mesophyll protoplasts, whereas the same peptide concentration almost completely stopped germination of fungal *F. culmorum* conidia (98%). At 8 μM, Shepherin 2 phytotoxicity was less than 20%, whereas bacterium growth of *P. carotovorum* was inhibited by 56%. Because conditions of *in vitro* are different

from *in vivo*, it is possible that when expressed ectopically *in planta,* Shepherin 2 will cause negligible deleterious effects on the host plant because whole plants, tissues, and organs are usually better able to withstand the effects of HDPs than the supremely sensitive protoplasts (Yevtushenko & Misra, 2007). Also, Shepherin 2 is naturally present in the roots of the shepherd's purse plant. That being said, any transgenic plants expressing Shepherin 2 would still need to be monitored closely for any deleterious effects on plant development, growth, and yield. The use of an inducible promoter to eliminate high, continuous levels of expression should also be considered to reduce the chance of toxic effects. Skh-AMP1 and Cr-ACP1 also displayed some significant levels of phytotoxicity at concentrations above 60 μM towards the protoplasts. However, because they showed quite low levels of inhibitory activity when tested alone, not even reaching 50% inhibition at any tested concentration, I do not think that testing their expression in plants would be worthwhile at this time.

4.1.2 Peptide combinations. All the peptide combinations tested, which resulted in significant levels of inhibition, included Shepherin 2. The sole exception was that of Cn-AMP1 combined with Cr-ACP1 which when tested against *P. carotovorum,* inhibited bacterial growth by 29% at 4 μM. When all the combinations were tested against *F. culmorum,* every combination which resulted in significant levels of inhibition appears to have had interacted in an antagonistic manner. This result was unusual: synergistic interactions, or at least additive interactions, have much more commonly been observed when antimicrobial peptides have been tested together (Rahnamaeian et al., 2015; Yan & Hancock, 2001; Yu et al., 2016); that was not the case for the peptides tested in the present study. Because antagonism is less commonly reported, not much is known about the mechanisms or the pathogen responses which lead to antagonistic interactions between HDPs (Yu et al., 2016). It may be that results of antagonism are rarely reported because

they are not seen as an experimental success; if that is not the case then I would hypothesize that because the assays used were conducted *in vitro*, some other factor(s) which allow the peptides to interact in beneficial ways, were absent. The results may be different in a living plant, where the other components of the immune system are present and functional. There is also the possibility that the presence of additional peptides, or one specific peptide, may trigger a microbial defence response in some pathogens, such as the release of bacterial proteases, which in turn can degrade the HDPs before the peptides kill the pathogen. Clearly, more study is needed if we are to understand the mechanisms involved in antagonistic interactions of combined HDPs. The antagonism which has been found with *F. culmorum* may also be partly due to my choice of using the Abbott approach (Abbott, 1925) to calculate the peptide interactions. Kosman & Cohen (1996) have reported that the Abbott method is less reliable in cases when one of the antimicrobial agents is relatively effective, i.e., reaching an inhibition of nearly 100%, compared to the other antimicrobial agent(s). An observed rate of inhibition at nearly 100% skews the expected inhibition rate towards 100% as well.

The combinations of peptides offered far greater, compared with single peptides, inhibition when they were tested against *A. solani*, particularly the triple peptide combinations. Shepherin 2, combined with Cn-AMP1, caused 53% inhibition at only 0.5 μM: inhibition peaked at that level indicating a very narrow range of activity. Several of the triple peptide combinations offered even higher levels of inhibition, also in a relatively narrow range from 1 to 4 μM. Shepherin 2, combined with Skh-AMP1 and Cn-AMP1, peaked at 4 μM with an inhibition of 57%, and Shepherin 2 combined with Cn-AMP1 and Cr-ACP1 peaked at 2 μM with an inhibition of 55%. In each case the interactions were synergistic. When Shepherin 2 is combined with Skh-AMP1 or Cn-AMP1, the synergistic results observed when tested against *A. solani*

could be explained by the different antimicrobial mechanisms of action employed by each peptide. The different mechanisms may complement each other, resulting in an increase in activity which is higher than otherwise may be expected. Shepherin 2, and its co-occurring HDP, Shepherin I, are considered to be unique antimicrobial peptides due to their repeating Gly-Gly-His motifs, lack of cysteine residues, and the absence of any α-helices present in the secondary structure. It is suspected that Shepherin 2 acts on intracellular targets, without disrupting the cell membrane (Park et al., 2000). One method for cell entry suggested for this type of HDP is that cell entry is initiated via electrostatic interactions between the highly cationic HDP and the anionic microbial cell surface. The peptide aggregates in small groups at the cell surface and then induces endocytosis after which the peptides pass through the cell membrane in the endocytotic vesicle before being released into the cytoplasm via some mechanism. At that point the peptide is free to bind to its intracellular targets and disrupt cell function (Nunes et al., 2021). An example of this type of interaction has been observed with human α-defensin 1, which enters bacterial and fungal cells using endocytosis, without damaging the cell membrane, and then targets bacterial DNA causing double strand breaks (Nunes et al., 2021). Since Skh-AMP1 is thought to act via membrane permeabilization and increased ROS production (Khani et al., 2020), and Cn-AMP1 is also thought to act by permeabilizing the cell membrane (Silva et al., 2012); it would make sense that these two peptides could open pores in the microbial membrane, thus allowing Shepherin 2 an additional route to enter the cell and reach its targets more quickly, hastening cell disruption and death (Yu et al., 2016). Another theory suggests that the HDPs may conjugate and form larger molecules capable of opening larger or more stable pores in the cell membrane (Yu et al., 2016).The same may be said of either Skh-AMP1 or Cn-AMP1 when they are combined with Cr-ACP1 because Cr-ACP1 is thought to act upon the microbial cell by entering the cell

through ABC transporters, then once in the cell it binds to the DNA and prevents replication (Mandal et al., 2012). The creation of pores by Skh-AMP1 or Cn-AMP1 would once again speed up the process of Cr-ACP's entry into the cell, speeding up its ability to disrupt microbial DNA replication.

In the combination assays involving *P. carotovorum*, it was once again the combinations containing Shepherin 2 that inhibited pathogen growth to the greatest extent. Each of these combinations displayed peak inhibition at 16 μM, indicating a narrow range of activity for these combinations. This narrow effective concentration range may occur because once the concentration of the peptides reaches a high enough concentration to kill the bacterial cells in greater numbers, the microbial defense system may also be able to detect them at a slightly higher concentration. At that point the bacterial defense system may release enough bacterial proteases to neutralize the peptides. Surprisingly, the combination of Shepherin 2 and Cr-ACP1 performed the best, achieving an inhibition of 89% at 16 μM, a value greater than that achieved by Shepherin 2 alone. This was the only significant result which indicated that a synergistic interaction had taken place, except for Cn-AMP1 and Cr-ACP1, which showed 29% inhibition at 4 μM, and because the expected inhibition was 19%, was also synergistic. Given that Cn-AMP1 and Shepherin 2 are both thought to target intracellular processes, the synergy may be the result of some initial electrostatic interaction between the negatively charged Cr-ACP1 and the highly cationic Shepherin 2 molecule, which would also be attracted to the negatively charged bacterial cell surface. Perhaps the uptake of Cr-ACP1 is increased by accompanying Shepherin 2 via endocytotic vesicle through the membrane. This would not explain why some of the interactions between these two peptides, when acting on *P. carotovorum*, were antagonistic. All other combinations which resulted in significant levels of inhibition of *P. carotovorum* were either

additive or antagonistic. Host defence peptide combinations tested against *P. atrosepticum* all failed to produce any significant level of inhibition. The highest result was achieved with Skh-AMP1 with Cn-AMP1 at 16 μM with an inhibition of 36%.

The phytotoxicity assays conducted with the double peptide combinations raise some concerns. The combinations of Shepherin 2 with Skh-AMP1, and Shepherin 2 with Cn-AMP1 proved to be highly toxic to protoplasts at the higher tested concentrations, but it is important to note that the most effective double peptide concentrations for inhibition of pathogenic microorganisms ranged from 0.5 μM to 16 μM which is well below the concentrations produced notable phytotoxic effects (40 μM for Shepherin 2 combined with Cn-AMP1, and 70 μM for Shepherin 2 combined with Skh-AMP1). The results for the triple peptide combinations indicate far lower levels of toxicity to the protoplasts; possibly because the amount of each individual peptide is reduced, lowering overall toxicity (Yu et al., 2016). In fact, only Shepherin 2 combined with Skh-AMP1 and Cr-ACP1 was estimated to have a significant phytotoxic effect on protoplasts, and that was only at a level above the peptide concentrations used for the antimicrobial assays.

4.2 Transformation of potato

Taking all these results into account, it was decided that Shepherin 2 was the best candidate for further experimentation. Therefore, I generated transgenic potato plants containing the *Shepherin 2* gene under control of one of the following promoters: the inducible *PmBiPPro1-3* promoter and the constitutive *CaMV35S* promoter. This will allow comparisons between the promoter's effects on plant health, growth and development, yield, and pathogen resistance. The transformed explants have formed several green calli for each DNA construct, under selective pressure on the callus-inducing and plant regeneration PetM medium. The regenerating shoots

will soon be excised from the calli and transferred to hormone-free MS media for rooting. A future study will confirm whether the regenerated lines contain stably integrated *Shepherin 2* transgene, its transcription, and translation into bioactive peptide. Any antimicrobial assays conducted on the plants may produce quite different results than were achieved with the *in vitro* bioassays because many HDPs are promiscuous peptides; playing several roles in plant immunity as well as in growth and development. It has been found that HDPs are not only directly toxic to pathogens, but they may also play a role in immunomodulation in plants or in various stages of growth and development, such as seed development (Goyal & Mattoo, 2014). Assays conducted in living plants may allow Shepherin 2 to fulfill such additional roles and further enhance overall potato plant growth and defence.

An additional transformation experiment was conducted during this study. Potato plants were transformed with the green fluorescent protein (gfp) reporter gene under the control of the inducible *PmBiPPro1-3* promoter. The intent was to visualize the spatio-temporal, *PmBiPPro1-3*-driven expression pattern of gfp throughout the living plant organs and tissues. The potato explants were transformed, regenerated into plants, and PCR was used to verify the presence of the gfp gene in the plants. However, we were unable to detect any fluorescence in these plants using an Olympus BX41 fluorescence microscope: the background fluorescence was high enough to mask the gfp fluorescence if the latter was not very strong, or the transgene may have been present only in non-expressing regions of the genome. Transgene-induced gene silencing may also occur when multiple repeats of transgenes are inserted into the plant genome (Vaucheret et al., 1998).

Because we were unable to detect fluorescence in the transgenic potato plants, transient transformation of tobacco was utilized. The *Agrobacterium* culture containing the *PmBiPPro1-*

3/m-GFP5-ER construct was used to carry out transient transformation of mature tobacco leaves. Transient transformation allowed us to quickly assess whether the *gfp* gene was being expressed under the control of the Douglas-fir promoter and that the gene was functional. Tobacco was chosen because it is fast growing and is a commonly used model in transient transformation experiments (Salazar-González et al., 2023). As a result, gfp fluorescence was observed in all tobacco leaves tested in this experiment, confirming the activity of *PmBiPPro1-3* promoter and the proper promoter-transgene fusion (Fig. 25) which indicates that the truncated promoter from Douglas-fir may be a good candidate for controlling the expression of Shepherin 2 in potato plants.

5. Conclusion

During this study, antimicrobial assays were conducted using four linear, plant-derived HDPs, alone or in combinations with each other, against two fungal and two bacterial plant-pathogenic species. Human cells and leaf protoplasts were also evaluated for any cytotoxic effects caused by the HDPs. The results of the present study suggest that an HDP from shepard's purse, Shepherin 2, is a good candidate for further experimentation for pathogen resistance in potato or other plant species due to its high level of activity towards *F. culmorum* and *P. carotovorum,* as well as its low level of cytotoxicity at concentrations relevant to its antimicrobial activity. Transgenic potato plants, containing the *Shepherin 2* gene under two different promoters are currently being developed and will be used for future evaluation of Shepherin 2-contaning plants for enhanced disease resistance. Further experiments with Shepherin 2 should include *in planta* antimicrobial assays against a wider range of important potato pathogens, as well as monitoring the two promoters for differences in spatio-temporal activities and their effects on antimicrobial resistance, plant growth and development, tuber

yield, and overall plant health. This will help to determine the most appropriate promoter and will also aid in the detection of any possible deleterious effects that may result from the expression of Shepherin 2 in the plants. The results of this study may also contribute to further research projects, such as the elucidation of subcellular localization and the mechanisms of action of Shepherin 2, a unique HDP, as well as contributing to our overall understanding of plant host immunity.

References

Abbott, W. S. (1925). A method of computing effectiveness of an insecticide. *Journal of Economic Entomology, 18*, 265-267.

Agrobacterium tumefaciens LBA4404 electro-cells: Product manual. (n.d.). TaKaRa Bio Inc. http://www.TaKaRa-bio.com

Ali, G. S., & Reddy, A. S. N. (2000). Inhibition of fungal and bacterial plant pathogens by synthetic peptides: In vitro growth inhibition, interaction between peptides and inhibition of disease progression. *Molecular Plant-Microbe Interactions, 13*(8), 847-859. https://doi.org/10.1094/MPMI.2000.13.8.847

Anjanappa, R. B., & Gruissem, W. (2021). Current progress and challenges in crop genetic transformation. *Journal of Plant Physiology, 261*, 153411. https://doi.org/10.1016/j.jplph.2021.153411

Bakhsh, A. (2020). Development of efficient, reproducible, and stable *Agrobacterium*-mediated genetic transformation of five potato cultivars. *Food Technology and Biotechnology, 58*(1), 57-63. https://doi.org/10.17113/ftb.58.01.20.6187

Bauske, M. J., Robinson, A. P., & Gudmestad, N. C. (2018). *Early blight in potato.* North Dakota State University. https://www.ndsu.edu/agriculture/sites/default/files/2022-07/pp1892.pdf

Broekaert, W. F., Mariën, W., Terras, F. R. G., De Bolle, M. F. C., Proost, P., Van Damme, J., Dillen, L., Claeys, M., Rees, S. B., Vanderleyden, J, & Cammue, B. P. A. (1992). Antimicrobial peptides from *Amaranthus caudatus* seeds with sequence homology to the cysteine/glycine-rich domain of chitin-binding proteins. *Biochemistry, 31*(17), 4308-4314. HTTPS://DOI.ORG/10.1021/BI00132A023

Büyükkiraz, M. E., & Kesmen, Z. (2022). Antimicrobial peptides (AMPs): A promising class of antimicrobial compounds. *Journal of Applied Microbiology, 132*(2), 1573-1596. https://doi.org/10.1111/jam.15314

Campos, M. L., De Souza, C. M., De Oliveira, K. B. S., Dias, S. C., & Franco, O. L. (2018). The role of antimicrobial peptides in plant immunity. *Journal of Experimental Botany, 69*(21), 4997-5011. https://doi.org/10.1093/jxb/ery294

Dolničar, P. (2021). Importance of potato as a crop and practical approaches to potato breeding. *Methods in Molecular Biology, 2354*, 3. https://doi.org/10.1007/978-1-0716-1609-3_1

FAO. (2009). *How to feed the world in 2050*. Rome. https://www.fao.org/fileadmin/templates/wsfs/docs/expert_paper/How_to_Feed_the_World_in_2050.pdf

Goyal, R. K., & Mattoo, A. K. (2014). Multitasking antimicrobial peptides in plant development and host defense against biotic/abiotic stress. *Plant Science (Limerick), 228*, 135-149. https://doi.org/10.1016/j.plantsci.2014.05.012

Goyal, R. K., & Mattoo, A. K. (2016). Plant antimicrobial peptides. In R. M. Epand (Eds.), *Host defense peptides and their potential as therapeutic agents* (pp. 111-136). Switzerland: Springer International Publishing. https://doi.org/10.1007/978-3-319-32949-9_5

Graser, G., Walters, F. S., Burns, A., Sauve, A., & Raybould, A. (2017). A general approach to test for interaction among mixtures of insecticidal proteins which target different orders of insect pests. *Journal of Insect Science (Tucson, Ariz.), 17*(2), 39, 1-12. https://doi.org/10.1093/jisesa/iex003

Huang, X., Xie, W., & Gong, Z. (2000). Characteristics and antifungal activity of a chitin binding protein from ginkgo biloba. *FEBS Letters, 478*(1), 123-126. https://doi.org/10.1016/S0014-5793(00)01834-2

Haney, E. F., Mansour, S. C., & Hancock, R. E. W. (2017). Antimicrobial peptides: An introduction. *Methods in Molecular Biology (Clifton, N.J.), 1548*, 3. https://doi.org/10.1007/978-1-4939-6737-7-1

Howard, R. J., Garland, J. A., Seaman, W. L., Canadian Phytopathological Society, & Entomological Society of Canada (1951-). (1994). *Diseases and pests of vegetable crops in Canada: An illustrated compendium.* Canadian Pathological Society.

Iqbal, A., Khan, R. S., Shehryar, K., Imran, A., Ali, F., Attia, S., Shah, S., & Mii, M. (2019). Antimicrobial peptides as effective tools for enhanced disease resistance in plants. *Plant Cell, Tissue and Organ Culture, 139*(1), 1-15. https://doi.org/10.1007/s11240-019-01668-6

Jacobi, V., Plourde, A., Charest, P. J., & Hamelin, R. C. (2000). In vitro toxicity of natural and designed peptides to tree pathogens and pollen. *Canadian Journal of Botany, 78*(4), 455-461.

Keshavareddy, G., Kumar, A. R. V., & Rama, V. S. (2018). Methods of plant transformation – A review. *Int. J. Current. Microbiol. App. Sci. 7*(7), 2656-2668. https://doi.org/10.20546/ijcmas.2018.707.312

Khani, S., Seyedjavadi, S. S., Zare-Zardini, H., Hosseini, H. M., Goudarzi, M., Khatami, S., Amani, J., Imani Fooladi, A. A., & Razzaghi-Abyaneh, M. (2019). Isolation and functional characterization of an antifungal hydrophilic peptide, skh-AMP1, derived from satureja khuzistanica leaves. *Phytochemistry (Oxford), 164*, 136-143. https://doi.org/10.1016/j.phytochem.2019.05.011

Khani, S., Seyedjavadi, S. S., Hosseini, H. M., Goudarzi, M., Valadbeigi, S., Khatami, S., Ajdary, S., Eslamifar, A., Amani, J., Imani Fooladi, A. A., & Razzaghi-Abyaneh, M. (2020). Effects of the antifungal peptide skh-AMP1 derived from satureja khuzistanica on cell membrane permeability, ROS production, and cell morphology of conidia and

hyphae of aspergillus fumigatus. *Peptides, 123*, 170195. https://doi.org/10.1016/j.peptides.2019.170195

Kluge, J., Terfehr, D., & Kück, U. (2018). Inducible promoters and functional genomic approaches for the genetic engineering of filamentous fungi. *Applied Microbiology and Biotechnology, 102*(15), 6357-6372. https://doi.org/10.1007/s00253-018-9115-1

Kosman, E., & Cohen, Y. (1996). Procedures for calculating and differentiating synergism and antagonism in action of fungicide mixtures. *The American Phytopathological Society, 86*(11), 1263-1272.

Kumar, M., Yusuf, M. A., Yadav, P., Narayan, S., & Kumar, M. (2019). Overexpression of chickpea defensin gene confers tolerance to water-deficit stress in *Arabidopsis thaliana*. *Frontiers in plant science*, *10*, 290-290. https://doi.org/10.3389/fpls.2019.00290

Lacerda, A. F., Vasconcelos, E. A. R., Pelegrini, P. B., & Grossi de Sa, M. F. (2014). Antifungal defensins and their role in plant defense. *Frontiers in Microbiology, 5*, 116-116. https://doi.org/10.3389/fmicb.2014.00116

Li, J., Hu, S., Jian, W., Xie, C., & Yang, X. (2021). Plant antimicrobial peptides: structures, functions, and applications. *Botanical Studies, 62*(5), 1-15. https://doi.org/10.1186/s40529-021-00312-x

Mandal, S. M., Dey, S., Mandal, M., Sarkar, S., Maria-Neto, S., & Franco, O. L. (2009). Identification and structural insights of three novel antimicrobial peptides isolated from green coconut water. *Peptides (New York, N.Y.: 1980), 30*(4), 633-637. https://doi.org/10.1016/j.peptides.2008.12.001

Mandal, S. M., Migliolo, L., Das, S., Mandal, M., Franco, O. L., & Hazra, T. K. (2012). Identification and characterization of a bactericidal and proapoptotic peptide from cycas revoluta seeds with DNA binding properties. *Journal of Cellular Biochemistry, 113*(1), 184-193. https://doi.org/10.1002/jcb.23343

Medgyesy, P., Menczel, L., Maliga, P., FAO, Rome (Italy). Plant Production and Protection Div. International Board for Plant Genetic Resources, Rome (Italy), & Biological Research Centre, Szeged (Hungary). Inst. of Plant Physiology. (1980). The use of cytoplasmic streptomycin resistance: Chloroplast transfer from nicotiana tabacum into nicotiana sylvestris and isolation of their somatic hybrids. *Molecular & General Genetics, 179*(3), 693-698. https://doi.org/10.1007/BF00271759

Nawrot, R., Barylski, J., Nowicki, G., Broniarczyk, J., Buchwald, W., & Gozdzicka-Jòzefiak, A. (2014). Plant antimicrobial peptides. *Folia Microbiol, 59*, 181-196. https://doi.org/10.1007/s12223-013-0280-4

Nicolas, P. (2009). Multifunctional host defence peptides: Intracellular-targeting antimicrobial peptides. *The FEBS Journal, 276*(22), 6483-6496. https://doi.org/10.1111/j.1742-4658.2009.07359.x

Nunes, L. G. P., Reichert, T., & Machini, M. T. (2021). His-rich peptides, gly- and his-rich peptides: Functionally versatile compounds with potential multi-purpose applications. *International Journal of Peptide Research and Therapeutics, 27*(4), 2945-2963. https://doi.org/10.1007/s10989-021-10302-z

Oliveira-Lima, M., Benko-Iseppon, A. M., Neto, J. R. C. F., Rodriguez-Decuadro, S., Kido, E. A., Crovella, S., & Pandolfi, V. (2017). Snakin: Structure, roles and applications of a plant antimicrobial peptide. *Current Protein & Peptide Science, 18*(4), 368. https://doi.org/10.2174/1389203717666160619183140

Ortiz, O., & Mares, V. (2017). The historical, social, and economic importance of the potato crop. In S. Chakrabarti, C. Xie & J. Tiwari (Eds.), *The potato genome* (pp. 1-10). Springer International Publishing. https://doi.org/10.1007/978-3-319-66135-3_1

Park, C. J., Park, C. B., Hong, S. S., Lee, H. S., Lee, S. Y., & Kim, S. C. (2000). Characterization and cDNA cloning of two glycine- and histidine-rich antimicrobial peptides from the roots of shepherd's purse, capsella bursa-pastoris. *Plant Molecular Biology, 44*(2), 187-197. https://doi.org/10.1023/A:1006431320677

Potenza, C., Aleman, L., & Senguta-gopalan, C. (2004). invited review: Targeting transgene expression in research, agricultural, and environmental applications: Promoters used in plant transformation. *In Vitro Cellular & Developmental Biology. Plant, 40*(1), 1-22. https://doi.org/10.1079/IVP2003477

Rahnamaeian, M., Cytryńska, M., Zbybicka-Barabas, A., Dobslaff, K., Wiesner, J., Twyman, R. M., Zuchner, T., Sadd, B. M., Regeos, R. R., Shmid-Hempel, P., & Vilcinskas, A. (2015). Insect antimicrobial peptides show potentiating functional interactions against gram-negative bacteria. *Proceedings of the Royal Society. B, Biological Sciences, 282*(1806), 20150293-20150293. http://doi.org/10.1098/rspb.2015.0293

Rahnamaeian, M., Cytryńska, M., Zbybicka-Barabas, A., & Vilcinskas, A. (2016). The functional interaction between abaecin and pore-forming peptides indicates a general mechanism of antibacterial potentiation. *Peptides (New York, N.Y.: 1980), 78*, 17-23. https://doi.org/10.1016/j.peptides.2016.01.016

Remuzgo, C., Oewel, T. S., Daffre, S., Lopes, T. R. S., Dyszy, F. H., Schreier, S., Machado-Santelli, G. M., & Machini, M. T. (2014). Chemical synthesis, structure-activity relationship, and properties of Shepherin I: a fungicidal peptide enriched in glycine-glycine-histidine motifs. *Amino Acids, 46*(11), 2573-2586. https://doi.org/10.1007/s00726-014-1811-2

Rivera, A. L., Gómez-Lim, M., Fernández, F., & Loske, A. M. (2012). Physical methods for genetic plant transformation. *Physics of Life Reviews, 9*(3), 308-345. https://doi.org/10.1016/j.plrev.2012.06.002

Rodrigues, T. T., Maffia, L. A., Dhingra, O. D., & Mizubuti, E. S. (2010). In vitro production of conidia of Alternaria solani. *Tropical Plant Pathology*, *35*(4), 203-212. https://doi.org/10.1590/S1982-56762010000400001

Romero, J. B. (1954) *The Botanical Lore of the California Indians*. New York: Vantage Press, Inc.

Rongai, D., Pulcini, P., Pesce, B., & Milano, F. (2015). Antifungal activity of some botanical extracts on *Fusarium oxysporum*. *Open Life Sciences, 10,* 409-416. https://doi.org/10.1515/biol-2015-0040

Salazar-González, J. A., Castro-Medina, M., Bernardino-Rivera, L.E., Martínez-Terrazas, E., Cason, S. A., & Urrea-López, R. (2023). *In-planta* transient transformation of avocado (*Persea americana*) by vacuum agroinfiltration of aerial plant parts. *Plant Cell, Tissue and Organ Culture 152*(3), 635-646. https://doi.org/10.1007/s11240-022-02436-9

Santana, M. J., de Oliveira, A. L., Queiroz Júnior, L. H. K., Mandal, S. M., Matos, C. O., Dias, R. d. O., Franco, O. L., & Lião, L. M. (2015). Structural insights into cn-AMP1, a short disulfide-free multifunctional peptide from green coconut water. *FEBS Letters, 589*(5), 639-644. https://doi.org/10.1016/j.febslet.2015.01.029

Sathoff, A. E., & Samac, D. A. (2019). Antibacterial activity of plant defensins. *Molecular Plant-Microbe Interactions, 32*(5), 507-514. https://doi.org/10.1094/MPMI-08-18-0229-CR

Scherm, B., Balmas, V., Spanu, F., Pani, G., Delogu, G., Pasquali, M., & Migheli, Q. (2013). *Fusarium culmorum*: Causal agent of foot and root rot and head blight on wheat: The wheat pathogen *Fusarium culmorum*. *Molecular Plant Pathology, 14*(4), 323-341. https://doi.org/10.1111/mpp.12011

Sidorov, V.A., Zubko, M.K., Kuchko, A.A., Komarnitsky, I.K., Gleba, Y.Y. (1987). Somatic hybridization in potato: use of γ-irradiated protoplasts of *Solanum pinnatisectum* in genetic reconstruction. *Theoretical and Applied Genetics, 74*, 364-368

Silva, O. N., Porto, W. F., Migliolo, L., Mandal, S. M., Gomes, D. G., Holanda, H. H. S., Silva, R. S. P., Dias, S. C., Costa, M. P., Costa, C. R., Silva, M. R., Rezende, T. M. B., & Franco, O. L. (2012). Cn-AMP1: A new promiscuous peptide with potential for microbial infections treatment. *Biopolymers, 98*(4), 322-331. https://doi.org/10.1002/bip.22071

Sood, S., Bhardwaj, V., Pandey, S. K., & Chakrabarti, S. K. (2017). History of potato breeding: Improvement, diversification, and diversity. In S. Chakrabarti, C. Xie & J. Tiwari (Eds.), *The potato genome* (pp. 31-72). Springer International Publishing. https://doi.org/10.1007/978-3-319-66135-3_3

Stotz, H. U., Spence, B., & Wang, Y. (2009). Defensin from tomato with dual function in defense and development. *Plant Molecular Biology, 71*(1-2), 131-143. https://doi.org/10.1007/s11103-009-9512-z

Tilman, D., Balzer, C., Hill, J., & Befort, B. L. (2011). Global food demand and the sustainable intensification of agriculture. *PNAS, 108*(50), 20260-20264. www.pnas.org/cgi/doi/10.1073/pnas.1116437108

Tiwari, R. K., Kumar, R., Sharma, S., Sagar, V., Aggarwal, R., Naga, K. C., Lal, M. K., Chourasia, K. N., Kumar, D., & Kumar, M. (2020). Potato dry rot disease: Current status, pathogenomics and management. *3 Biotech, 10*(11), 503-503. https://doi.org/10.1007/s13205-020-02496-8

Vaucheret, H., Béclin, C., Elmayan, T., Feuerbach, F., Godon, C., Morel, J. -B., Mourrain, P., Paluqui, J. -C., & Vernhettes, S. (1998). Transgene-induced gene silencing in plants. *The Plant Journal : For Cell and Molecular Biology*, *16*(6), 651-659. https://doi.org/10.1046/j.1365-313x.1998.00337.x

Yan, H., & Hancock, R. E. W. (2001). Synergistic interactions between mammalian antimicrobial defence peptides. *Antimicrobial Agents and Chemotherapy, 45*(5), 1558-1560. https://do.doi.org/10.1128/AAC.45.5.1558-1560.2001

Yevtushenko, D. P., Sidorov, V. A., Romero, R., Kay, W. W., & Misra, S. (2004). Wound-inducible promoter from poplar is responsive to fungal infection in transgenic potato. *Plant Science (Limerick), 167*(4), 715-724. https://doi.org/10.1016/j.plantsci.2004.04.023

Yevtushenko, D. P., Romero, R., Forward, B. S., Hancock, R. E., Kay, W. W., & Misra, S. (2005). Pathogen-induced expression of a cecropin A-melittin antimicrobial peptide gene confers antifungal resistance in transgenic tobacco. *Journal of Experimental Botany, 56*(416), 1685-1695. https://doi.org/10.1093/jxb/eri165

Yevtushenko, D. P., & Misra, S. (2007). Comparison of pathogen-induced expression and efficacy of two amphibian antimicrobial peptides, MsrA2 and temporin A, for engineering wide-spectrum disease resistance in tobacco. *Plant Biotechnology Journal, 5*(6), 720-734. https://doi.org/10.1111/j.1467-7652.2007.00277.x

Yevtushenko, D. P., & Misra, S. (2012). Transgenic expression of antimicrobial peptides in plants: Strategies for enhanced disease resistance, improved productivity, and production of therapeutics. In Rajasekaran, K., et al., *In Small Wonders: Peptides for Disease Control* (pp. 445-458). Washington, DC: ACS Symposium Series; American Chemical Society. https://pubs.acs.org/doi/10.1021/bk-2012-1095.ch021

Yevtushenko, D. P., & Misra, S. (2018). Spatiotemporal activities of douglas-fir BiP Pro1 promoter in transgenic potato. *Planta, 248*(6), 1569-1579. https://doi.org/10.1007/s00425-018-3013-8

Yoshida, K., & Shinmyo, A. (2000). Transgene expression systems in plant, a natural bioreactor. *Journal of Bioscience and Bioengineering,* 90(4), 353-362. https://doi.org/10.1016/S1389-1723(01)80001-3

Yu, G., Baeder, D. Y., Regoes, R. R., & Rolff, J. (2016). Combination effects of antimicrobial peptides. *Antimicrobial Agents and Chemotherapy, 60*(3), 1717-1724. https://doi.org/10.1128/AAC.02434-15

Appendix A

Modified SW medium for culture of potato protoplasts*
For 1000 ml

Macronutrients:

NH_4Cl…….....133.8 mg
KNO_3…….……...…950 mg
$CaCl_2$……....185 mg (or $CaCl_2 \cdot 2H_2O$…220 mg)
$MgSO_4 \cdot 7H_2O$…….....185 mg
KH_2PO_4……..…85 mg

Micronutrients (MS micronutrients):

Boric Acid…….6.2 mg
Cobalt chloride•$6H_2O$……...0.025 mg
Cupric sulfate•$5H_2O$……..0.025 mg
$Na_2EDTA \cdot 2H_2O$……..…..37.26 mg
Ferrous sulfate•$7H_2O$……27.8 mg
Manganese sulfate•H_2O……...…16.9 mg
Molybdic acid (sodium salt)• $2H_2O$…….....0.25 mg
Potassium iodide……..……0.83 mg
Zinc sulfate•$7H_2O$……..8.6 mg

Vitamins (Gamborg vitamins):

myo-Inositol…….……..…100 mg
Nicotinic acid……..……..1 mg
Thiamine•HCl (Vitamin B1)……10 mg
Pyridoxine•HCl (Vitamin B6)……..1 mg

Others:

L-Glutamine…….…….100 mg
D(+)-Xylose……..250 mg
Casein, enzymatic hydrolysate…….…….100 mg

Growth regulators:

α-Naphthaleneacetic acid (NAA)……..…….2 mg
6-Benzylaminopurine (BA)…….……0.5 mg
2,4-Dichlorophenoxyacetic acid (2,4-D)…….0.2 mg

Carbohydrate:

D-Glucose (0.4 M)…….……72 g

Buffering agent:

2-(N-morpholino)ethanesulfonic acid (MES)……90 mg

Solidifying agent:

Agarose…….…..3.8 g

pH 5.7 (adjusted with 1N KOH)

*The medium was filter-sterilized.